HUNGARIAN UNIVERSITY OF AGRICULTURE AND LIFE SCIENCES

MATHEMATICAL MODELLING OF FOOD QUALITY PARAMETERS BASED ON MULTIVARIATE AND SPECTRAL DATA

ISTVÁN KERTÉSZ

BUDAPEST

2021

A doktori iskola megnevezése: Élelmiszertudományi Doktori Iskola

Tudományága: Élelmiszertudományok

vezetője: Simonné Prof. Dr. Sarkadi Livia
Egyetemi tanár, DSc
Magyar Agrár- és Élettudományi Egyetem
Élelmiszertudományi Intézet
Élelmiszerkémiai és Táplálkozástudományi Tanszék

Témavezetők: Dr. Felföldi József
Egyetemi tanár, PhD
Magyar Agrár- és Élettudományi Egyetem
Élelmiszertudományi Intézet
Élelmiszerpari Méréstechnika és Automatizálás Tanszék

Dr. Baranyai László
Egyetemi tanár, PhD
Magyar Agrár- és Élettudományi Egyetem
Élelmiszertudományi Intézet
Élelmiszerpari Méréstechnika és Automatizálás Tanszék

....

Az iskolavezető jóváhagyása A témavezetők jóváhagyása

Table of contents

List of abbreviations

Abbreviation	English meaning
ANN	Artificial Neural Network
AR-AIC	AR-Akaike Information Criterion picker algorithm
CF	Characteristic Function
CV	Cross-validation
CWD	Continuous Wavelet Decomposition
EW	East-West (laid down) position
FFT	Fast Fourier Transformation
GOF	Goodness of Fit
KNN	K-Nearest Neighbors classification
RLS	Recursive Least Squares
LDA	Linear Discriminant Analysis
LV	Latent Variables
MSE	Mean Squared Error
NDT	Non-Destructive Testing
NS	North-South (upright) position
PCA	Principal Component Analysis
PLS	Partial Least Squares Regression
QDA	Quadratic Discriminant Analysis
R^2_{adj}	Adjusted Coefficient of Determination.
RMSEC	Root Mean Squared Error of Calibration

RMSEP	Root Mean Squared Error of Prediction
RPD	Residual Prediction Deviation
SD	Standard Deviation
SNR	Signal-to-Noise Ratio
SRD	Sum of Ranking Differences
STA/LTA	Short Time Average / Long Time Average algorithm
SVM	Support Vector Machine
TOF	Time-of-Flight
XC	Cross-correlation algorithm

1. Introduction

The quality of edible products has been an important factor since the beginning of human history, but the means of quality inspection have since evolved tremendously. Key drivers for these changes were specialized agricultural (primary) production, the appearance of civilized societies, and therefore the necessity to establish logistics to support such complex systems. This includes storage at different, product-specific conditions, transportation and –more recently– changes in modes of merchandise and the demand for elevated levels of quality. These factors have led to a necessary overproduction because they increase the probability of depreciation and hence the likelihood of rejection of lower quality products of the same type.

Of course this increased rejection rate is disadvantageous for all members of the food chain: the producer receives less money per produced product for the same amount of products sold, the total amount of spoiled products to be handled is higher. Also, the supplier has to increase storage and transportation capacity, the trader has to lower prices because of the higher supply, and the consumer is more likely to discard the purchased product.

As the above-mentioned dynamics throughout the food chain took effect progressively, so did the measures to counter them, leading to the emergence of novel quality control solutions. One of the key aspects of such methods is objectivity, making sure that standardized comparisons are possible irrespective of time and location. But what is another factor, gaining importance in recent years is the minimization of the effect on the inspected product itself. This has been achieved by different sampling methods with the advancements of statistical quality control in recent decades, and in the meantime, the technological revolution supported the creation of more sophisticated measurement tools. The latter, coupled with the need to monetize as many unspoiled products as possible inevitably led to the rise of non-destructive testing techniques, or NDT for short. These methods provide details of the tested sample rapidly and reliably, without the expense of the tested item, which consequently means the possibility to sell the said product, and to test more of them, diminishing or complete elimination of sampling restrictions.

An important factor for the utilization of NDT methods is the possibility of automation and financial viability. The most prevalent techniques capitalize on either electromagnetic properties (mainly visible or infrared light) or mechanical oscillatory properties. Both are interpretable as energy-carrying oscillation or waveform feedback to a controllable excitation, therefore –as it is

generally understood for oscillations– they have certain features inherent to waves, such as amplitude, or frequency et cetera. Scientists throughout the centuries have developed methods to understand the nature of such waves through mathematical analysis, even for complex superimposed signals, but we have lacked the computational capacity to effectively untangle them until recent decades. As such signals are composed of sinusoids of changing frequency and amplitude, they can be understood and processed as spectra, opening a myriad of possibilities for characterization of complex materials, exploited through multivariate statistical analysis.

Objectives

The primary goal was to find a mathematical procedure for estimation of different quality attributes of complex materials, such as food products, based on non-destructive testing data. There are some methods in existence for this at the moment, but a critical problem arises with data reduction, meaning the systematic decrease in explanatory variables. This reduction is necessitated by the fact that multivariate estimations gathered from spectral data (or other test results with high number of variables) has information content regarding food quality features shared among several variables, but present procedures are calculation-heavy and would not be able to reveal these correspondences in a reasonable amount of time (in the realms of hours, sometimes days).

Clearly, any such procedure which does not utilize all available data will suffer from a certain level of increase in uncertainty, and thus the goal should be to choose the extracted explanatory variables with the highest possible information retained.

In my thesis, I focus on the application of various multivariate analysis methods to extract information on the attributes of different food products corresponding to quality properties. I do this with the intention of finding algorithms that can be implemented in an industrial setting or quality assurance protocols, meaning they are required to be rapid enough for practical, possibly on-line use. At the same time, they need to be flexible in terms of applicability to other quality parameters and possibly other products, not discussed in the present thesis.

My doctoral thesis, therefore, focuses more on the methodology, rather than analysis of the results of experiments, the proportions of the document are reflecting this.

The experiments presented in the following thesis were conducted with the following objectives:

1. Developing a signal analysis process for efficient extraction of the most amount of information from spectral data, primarily ultrasound signals. This process should be fast and applicable in a food industry setting.
2. Finding an apt experimental setup as well as calibration and estimation protocols for indirect viscosity measurement of enzymatic curdling of milk, measured with ultrasound.
3. Developing an experimental setup for eggshell crack detection based on acoustic response signals, and development of a procedure for accurate classification from an industrial perspective.

4. Evaluation of the developed signal analysis protocol with a multiclass differentiation problem with a food product.

2. Literature review

2.1. Acoustic testing

2.1.1. Basics of acoustic measurements

Acoustic testing has been conducted for thousands in not millions of years one way or another, for example, woodpeckers are searching for their prey under the bark of trees based on the sound response. But as a more relatable example, knocking of melons inducing a voice response to assess ripeness is a way of non-destructive testing, because customers do not want to cause damage to the fruit if they are not sure they will purchase it. The use of the acoustic technique is related to the internal structure of the tested sample (*e.g.* testing of train wheels for internal errors) because the vibration of the tested material is highly correlated with the internal forces working against the mechanical waves induced upon agitation (Kinsler et al. 2000),.

However, acoustic testing was not a mature technique for analysis until the middle of the 20th century. Clark and Mikelson (1942) in their patent (filed in 1940) described an instrument to test ripeness of different fruits, pineapple as an example used in their patent, based on their natural mechanical vibration frequency (figure 1.) induced with an electromagnetic oscillator.

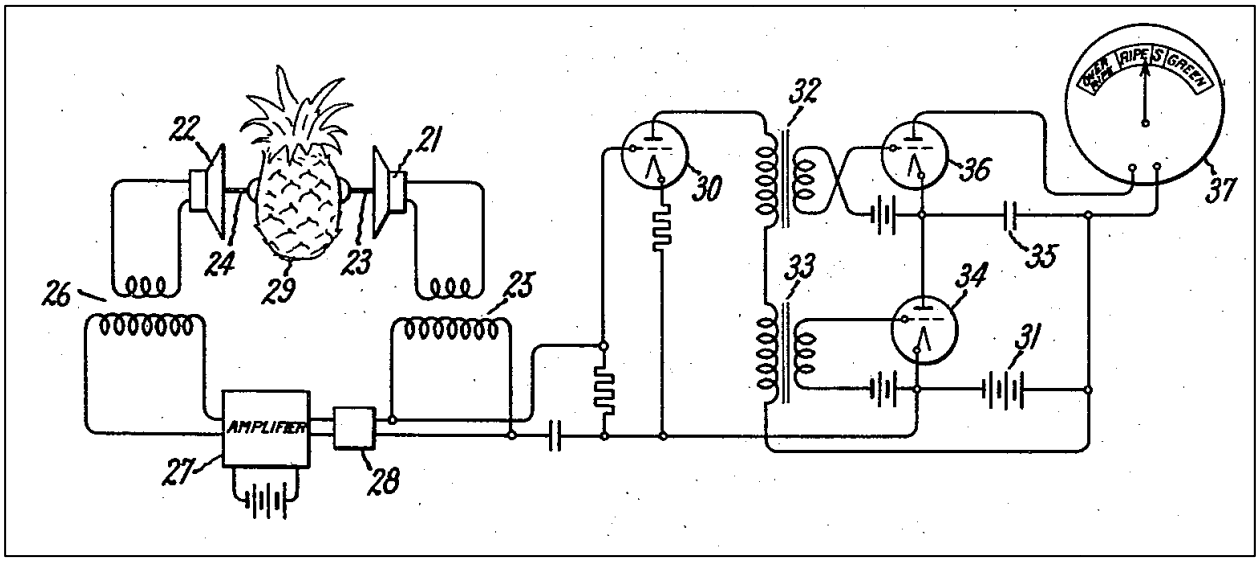

Figure 1. Original drawing of the oscillator for testing of fruit ripeness from the patent of Clark and Mikelson (1942)

They theorized the difference throughout storage was detectable because the ripening caused a change in the texture going from semi-solid to semi-liquid. They stated that the frequency changed from 100 Hz to 200 Hz during ripening of pineapple.

The nature of the vibration being longitudinal (along the length of the produce or across) or torsional might play an important role in the way the excitation, *i.e.* knocking of the product is carried out, which is a key factor when testing a product with highly differing dimensions. Istella in his doctoral thesis (2008) and Zsom-Muha and Felföldi (2007) showed the suitability of the method to test products with an elongated shape during storage. Istella et al. (2006) in an article described the experimental approach and setup, with the sample resting on a soft foam pad for stability and sound insulation (as shown in figure 2.).

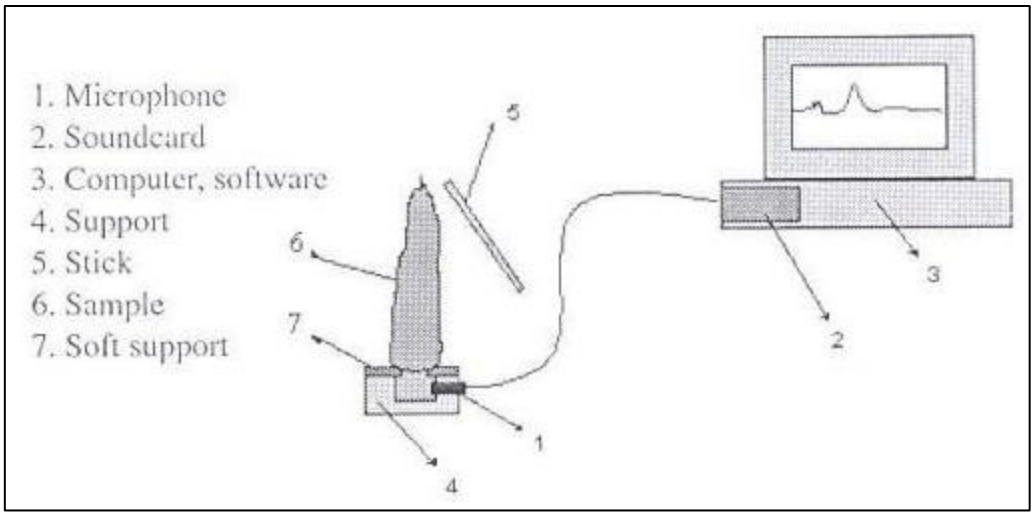

Figure 2. Experimental setup by Istella et al. (2006)

This arrangement was earlier suggested by Felföldi & Ignát (1999), they carried out the excitation on four different locations (based on Istella & Felföldi, 2003), and found the shoulder of the root to be the best spot for testing. This was in accord with the findings of Schotte et al. (1999) stating that the best location for the excitation is either 0° or 180° relative to the microphone. For calculation of the acoustic firmness coefficient (*S*, Nmm), Istella and his colleagues used the following formula, suggested by Felföldi (1996):

$$S = f^2 \cdot m \tag{1}$$

, where f is the resonant frequency in Hz, m is the mass in kg. This is a widely used formula (Campanella et al., 2011, Felföldi, 1996), for many different produces, another formula for the same metric is

$$S = f^2 \cdot m^{\frac{2}{3}} \quad (2)$$

, which results in a very uncommon unit, $kg^{2/3} \cdot s^{-2}$, and it is also difficult to comprehend, therefore is not preferred although being a better estimator in many cases (Gómez et al., 2005), if the difference between the mass is caused by a difference in size and not in density (Zsom-Muha, 2008). The formula (in equation 1.) was published by Cooke (1972) as a modification of the original equation proposed by Abbott et al. (1968): $S = f_2 \cdot m$, which used the second resonant frequency instead of the first as in Cooke's formula. De Belie et al. (2000a) used Cooke's formula to predict the ripening of Doyenné pears on trees and found a 0.82 correlation coefficient with the destructive penetrometer firmness, and therefore deemed it a good technique for non-destructive estimation of harvesting time. Taniwaki et al. (2009) also measured firmness, although using the second resonant frequency in the modified formula and applied it to two persimmon cultivars to predict the optimum eating ripeness during the post-harvest storage period.

As Felföldi and Zsom-Muha (2010) showed with the support of finite element modeling that the acoustic method was suitable to follow the softening of apple, pear, and cucumber during ripening in the field. Nerya et al. (2001) found evidence that the change in acoustic response in European pear is not only caused by softening, but also by transpiration caused weight loss, and theorized that other factors, like harvest maturity, storage conditions, *etc.* (Róth et al., 2008) are systematically affecting the acoustic characteristics of other fruits. This was a confirmation of the findings of a small-scale preliminary study by De Belie et al. (1999), which found that the acoustic firmness coefficient of Jonagold apples is dependent on mass loss, but they also state that they did not find a connection between firmness and the rate of the loss of mass. This seems to be contradictory because mass during storage usually approaches a finite value (Zsom et al., 2016) and therefore can be described with a negative exponential equation, linking the mass, mass loss and firmness together. Zsom et al. also add in their short communication that a full-scale study is required to verify their findings. A great advantage of the method is its high reproducibility, which was demonstrated by Felföldi & Fekete in their 2003 study, finding it suitable to determine firmness changes of fruit on the scale of 0.1%.

Another interesting approach (although not being a non-destructive method) was described in the study of De Belie et al. (2000b) which tried to predict the ripeness of Cox's Orange Pippin apples based on their sound during biting. The difference in texture was caused by different storage conditions, and the samples were therefore classified as mealy or crispy. They managed to classify the two groups correctly, but the main issue with the study is a rather common one: they used the

storage condition as a categorical variable and not the actual texture as a continuous dependent variable.

2.1.2. Non-destructive eggshell crack detection assays

Non-destructive testing for eggshell and internal egg faults is highly important for the industry because of two reasons.

1. As opposed to other foodstuff, destructive testing of a batch sample cannot be extrapolated to critical faults of individual pieces, which account for about 3% of total production (Coutts et al., 2007).
2. Quasi-non-destructive testing would completely null the value of the product for customers.

These two factors created an ideal circumstance for researching NDT solutions for the industry. At the same time, the most commonly used method at the present, candling, requires human labor, and workers tend to get tired. Candling means the emission of an intense light through the egg, which can reveal cracks and spoilage (Jindal & Sritham, 2003, Bell & Weaver, 2002) (figure 3.).

Figure 3. Traditional candling of eggs at an industrial scale (internet 1.)

There are several attempts for automation of this process with the aid of computer vision systems, but these are very costly, and their reliability is questionable, as shown from analysis of the literature in the following paragraphs. Nevertheless, the pressure of the industry leads to creative solutions, such as the one described in a patent (Lawrence et al. 2009), which is able to detect microcracks (figure 4.), but also requires a pressurized chamber of alternating pressure, and therefore is expensive and difficult to implement. This shows the difficulties faced when high precision is a factor to consider.

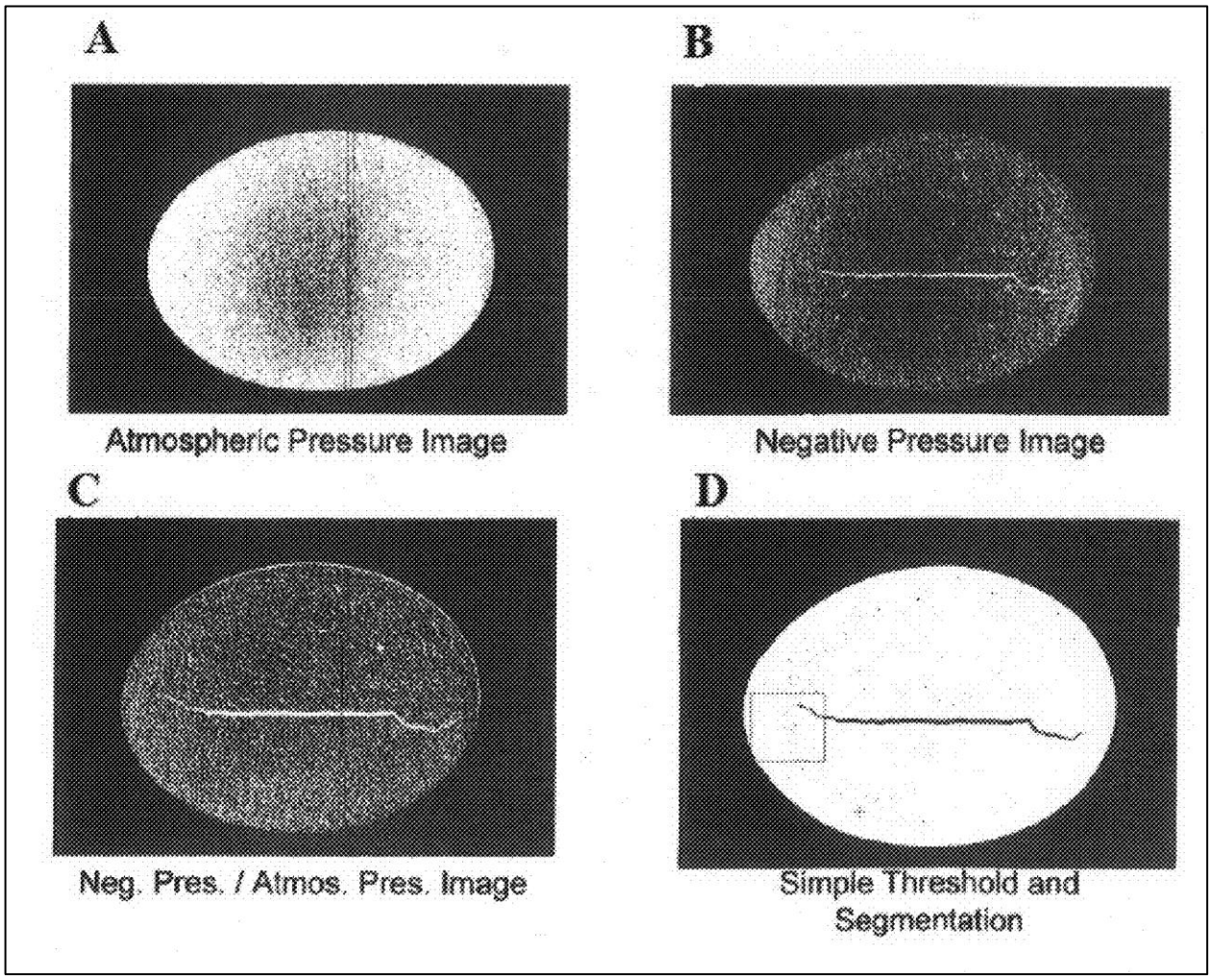

Figure 4. Microcrack detection with alternating pressures and computer vision (Lawrence et al. 2009)

Classification of cracked eggs with such systems is challenging. Wu et al. (2018) managed to achieve a 93% cross-validated correct classification using soft-margin Support Vector Machine (SVM) classification (figure 5.). This might be due to the fact that they were able to separate pronounced defects, on pictures, but not hair cracks.

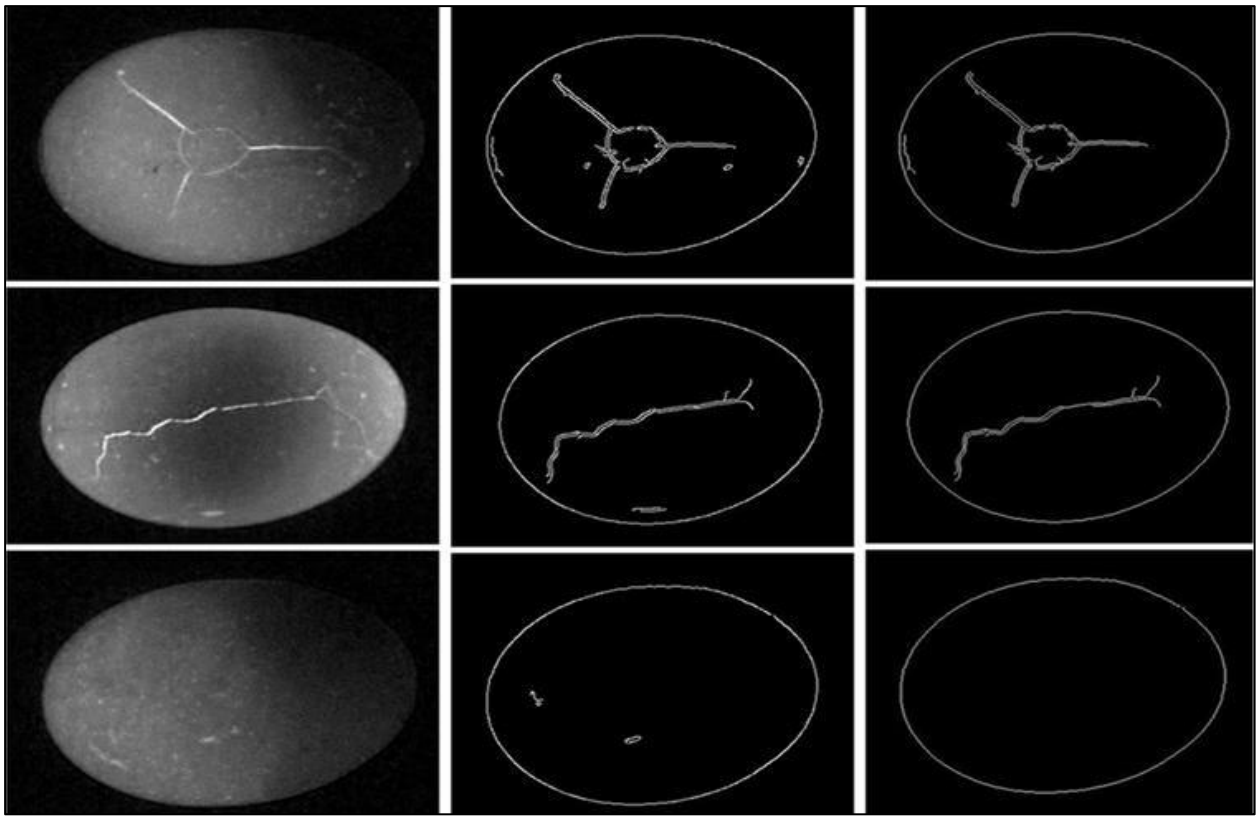

Figure 5.: Detection of shell defects by Support Vector Machine classification (original figure from Wu et al., 2018)

As it is obvious, it is a difficult task to determine the presence of eggshell cracks based on visual cues, and I see this to be due to two main reasons. Firstly, computer vision systems can only see the samples in two dimensions, which means it is required to move the eggs in a calculable manner (direction and speed wise), and detection of surface faults on constantly moving ovoid bodies with a high variance in spatial dimensions is an immensely complex task. The other problem is that there ought to be no lower threshold on the size of the fault, it is a matter of presence or absence. This means that the tiniest cracks, in some cases width measured in microns, need to be detected (Arivazhagan et al., 2013). These two issues create an obstacle very difficult to overcome, and therefore a property must be looked for that is not size-dependent and is an attribute of the shell as a whole to avoid the need of revolution of the egg. However, a huge benefit of visual techniques is that they bear the possibility of applying spectroscopic analysis to measure internal qualities (De Ketelaere, 2004a), which is difficult, but not impossible. Estimation of density and mass in Wang et al. (2004) 0.62-0.68 with acoustic measurement was achieved. Zhang et al. (2015) found a combination of hyperspectral imaging and SVM applicable for estimation of air cell and yolk quality (being intact) with 90% and 96.3% respectively and 4% root mean squared error for prediction of freshness.

The acoustic response is a feature that is fast to gather and analyze, requires less precision in an on-line industrial setting and last but not least, significantly less data to be processed as opposed to multiple high-resolution pictures. These factors made it a prevalent technology in the industry, although not perfect.

Coucke et al. published a study in 1997 about successful testing for fertility of eggs based on acoustic signals but pointed out in their later study and doctoral thesis (Coucke, 1998, Coucke et al., 1999) that the acoustic response of the egg is mostly characterized by the mechanical properties of the shell. In 2014, Attar & Fathi found a strong correlation (0.97) between resonance frequency and shell strength, verifying his findings. From this point, the number of publications in the topic increased rapidly, with a wide variety of methods tested. This is probably also a result of the boom in computer science and technology, which allowed researchers to use multivariate statistical techniques comfortably (the number of which also inflated in the past decades) and test many of them in a short period of time. Just a few decades ago, consistent use of methods of higher statistics was only available for those who deeply understood them and put in the effort to write their own code for analysis in basic programming environments.

Coucke's footsteps were followed, and his method used and further developed by De Ketelaere (2000 and 2003) and Cho et al. (2000) at the same time for crack detection. The latter team, using discriminant analysis, achieved 4% and 6% misclassification error for intact and cracked eggs respectively. A Chinese team achieved 87% correct classification in a laid down position in 2005 (Pan et al. 2005), and the same team in 2011 achieved 98% correct classification with joint acoustic and computer vision using Artificial Neural Network (ANN) (Pan et al., 2011). A similar value was reached by Zhu et al. in 2012 (87.5%), who applied the Bayesian classifier for their prediction. Li et al. in the same year (2012) also applied the Bayesian probabilistic classifier on wavelet transforms of acoustic responses for detection of cracks, reaching a higher correct classification rate, but they did not report their results in detail, only stated that their results were above 95%, which sounds dubious. Jindal and Sirtham (2003) reported identification of 99% of all cracked eggs, but their false rejection rate was 10%, compared to Coucke's method based on the dynamics stiffness (K_{dyn}) calculated from the spectrum, which gave until 2010 the best results of 1%, used in later research by De Ketelaere (2002) and Bain et al. (2006) (Bamelis 2006). Deng et al. in 2010 applied a wavelet transformation-based technique, reaching a maximum of 98.9% detection rate with SVM and 0.8% false rejection rate.

One of the most interesting configurations was proposed by Jin et al. in their 2015 study. They put an emphasis on industrial applicability, and their principle later showed up in grading machines. They arranged a seven-step setup, where the eggs rolled down hitting the surface of all steps with equal force, generating a sound response at each step, providing seven repetitions of the same measurement for each sample although they only reached a 90% total correct classification, the simplicity and elegance of such a passive excitation method should be noted. A 2018 study used basic principle in a modified setup along with a classic impulse-response method, using ANN (Lashgari & Mohammadigol, 2018) (figure 6.). They achieved a validated 92.3% and 94.6% correct detection accuracy for the two methods respectively.

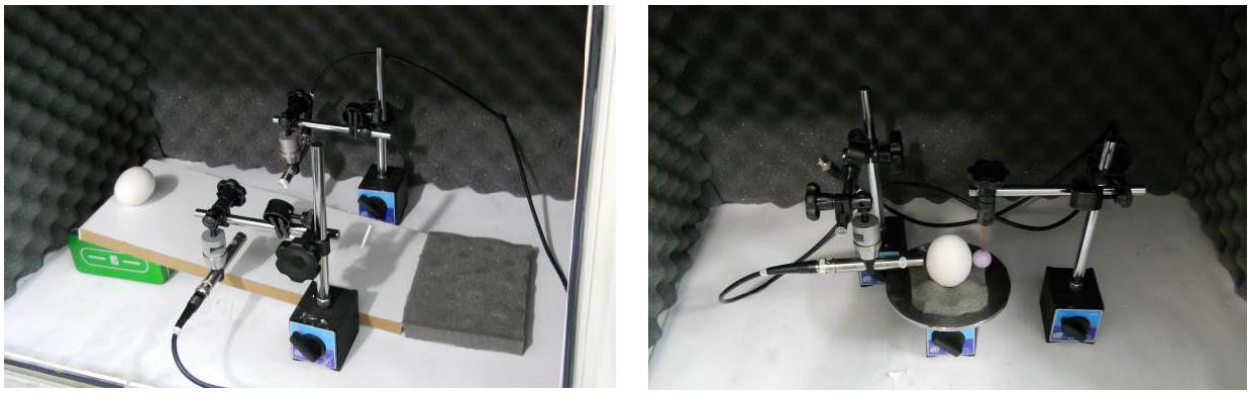

Figure 6. Experimental setup with incline roller and impact-response setups (Lashgari & Mohammadigol, 2018)

One study should be discussed in detail because it provides several lessons to learn when read with a healthy amount of criticism, and also resembles my conducted assay. Lin et al. (2009) developed a method for testing which used a variety of multivariate methods to predict crack presence. They tested 260 eggs, 170 used for calibration and 90 for testing, both groups had a fault rate of 50% (85 and 45 pieces respectively). They evaluated the spectra of the sound signals (acquired with 512-point Fast Fourier Transform) with non-linear methods, such as SVM and Back Propagation Artificial Neural Networks (BP-ANN), suggested by Jindal & Sritham (2003) and one linear classifier, the K-Nearest Neighbor (KNN) method. They also enhanced the signals with Recursive Least Squares (RLS) in order to minimize the means square error of the individual signals, after applying a bandpass filter between 1000 Hz and 8000 Hz (I need to note that this seems counterintuitive because lower frequencies might contain valuable information). Without RLS correction they had found peak frequencies of intact eggs in the 3500-5000 Hz but observed no distinct peaks for the cracked samples but also found a peak after using the said correction (figures 7. and 8.).

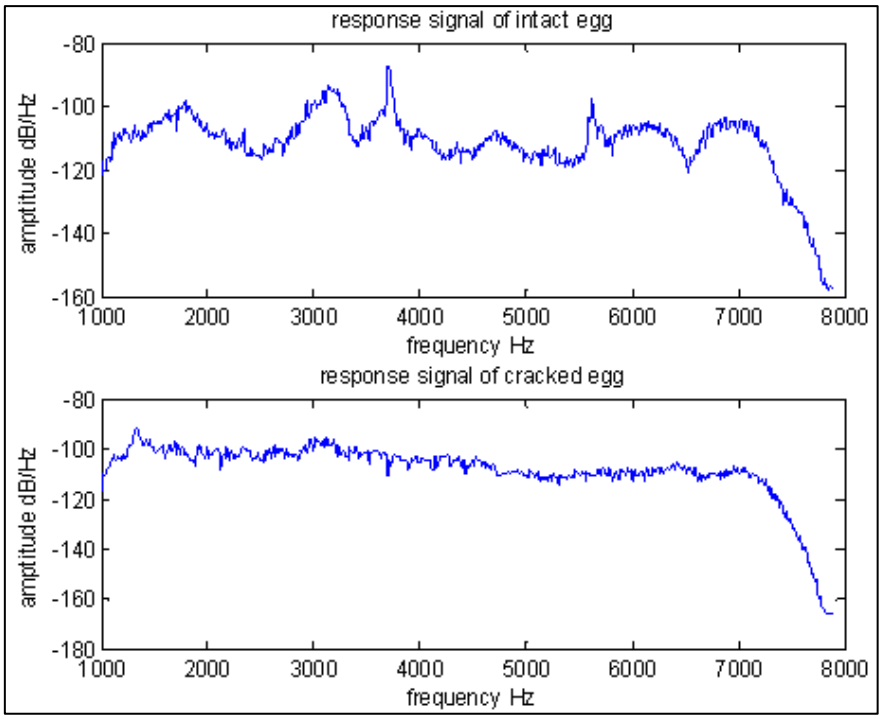

Figure 7. Acoustic responses of intact and cracked eggs without Recursive Least Squares correction (Lin et al., 2009)

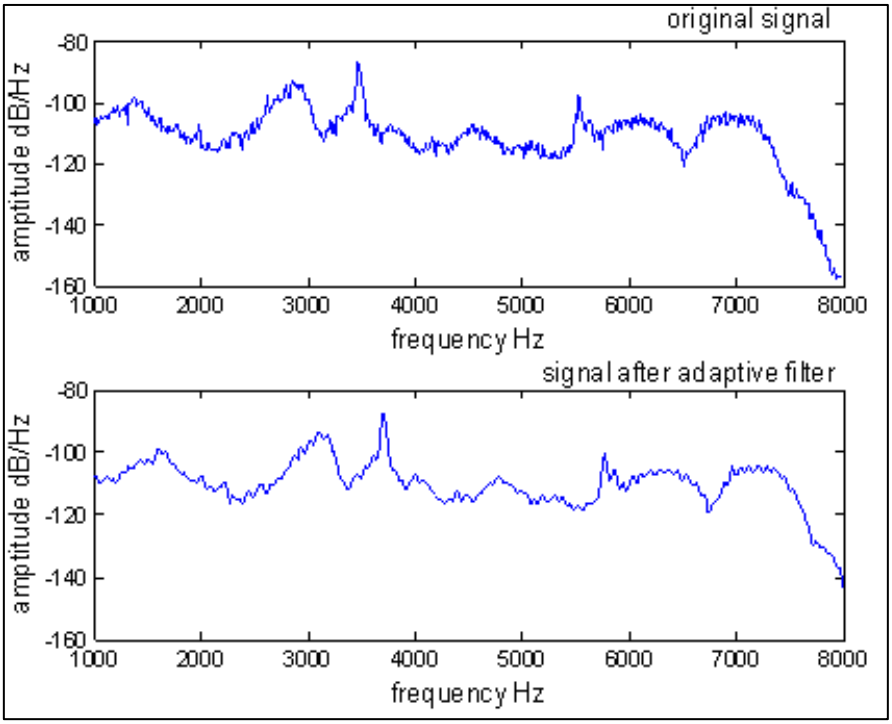

Figure 8. Acoustic responses of intact and cracked eggs with Recursive Least Squares correction (Lin et al., 2009)

They have achieved a correct classification of 97.1% for prediction (and 95.1% on the training set) with the SVM method, concluding that “the acoustic resonance system combined with the supervised pattern recognition has a significant potential for the cracked eggs detection”.

There are a few important things to address with this study: the comparison of different statistical methods is highly appreciated, also the pre-processing phase is noteworthy. Problems emerge when we take a closer look at methods used. There was only one linear method, whereas there are other, more common and simpler methods, and the principle of parsimony suggests gravitating towards these. Another point of criticism is the use of ANN, which requires much higher sample numbers to be reliable, preferably several ten thousands to millions. Even then, the models are non-transferable for other setups, because of lack of rigor and adaptability, and needs to be trained on new sites every time. From a statistical standpoint, a troubling point is the training set having a lower correct classification than the prediction, and not only for SVM but KNN as well (86.1% vs 88.9%), the probability of which is very low.

There are two common problems devouring most research articles on the topic. One is the fact that most of them do not report whether the results are validated or not, and therefore need to be treated as non-validated. The second is that they report an overall classification accuracy, as a common way to present results for estimation of categories, but for eggs it is much more important to disclose the composition of misclassified samples: on an industrial scale, most of the time cracked, but fresh and clean eggs can be used for the manufacturing of other processed products, such as pasta, but it is a worse situation when a cracked egg is missed and is sold raw for customers because of food safety and customer loyalty issues (Lin et al., 2011).

An important drawback of the acoustic technique is the presence of noise in processing facilities, for which, again De Ketelaere et al. (2004b) tried to address in on-line operations. They tested adaptive noise-canceling and Independent Component Analysis, which is used in image and sound processing to recover independent signals, but they have found the latter to be a slow and unreliable process for such environments, and noise-canceling did not bring truly reliable results either. This concludes that a truly robust method still needs to be developed.

Despite these issues, still, the most reliable method for crack detection on an industrial scale is the acoustic response method, illustrated in figure 9. taken from a public video of a Sanovo grading machine using multiple exciters. Even though it is the prevalent technique, as it was discussed in this section, there is still room for improvement, as the producers tend to heavily underestimate the ratio of defected eggs, by approximately half (Bain et al., 2006).

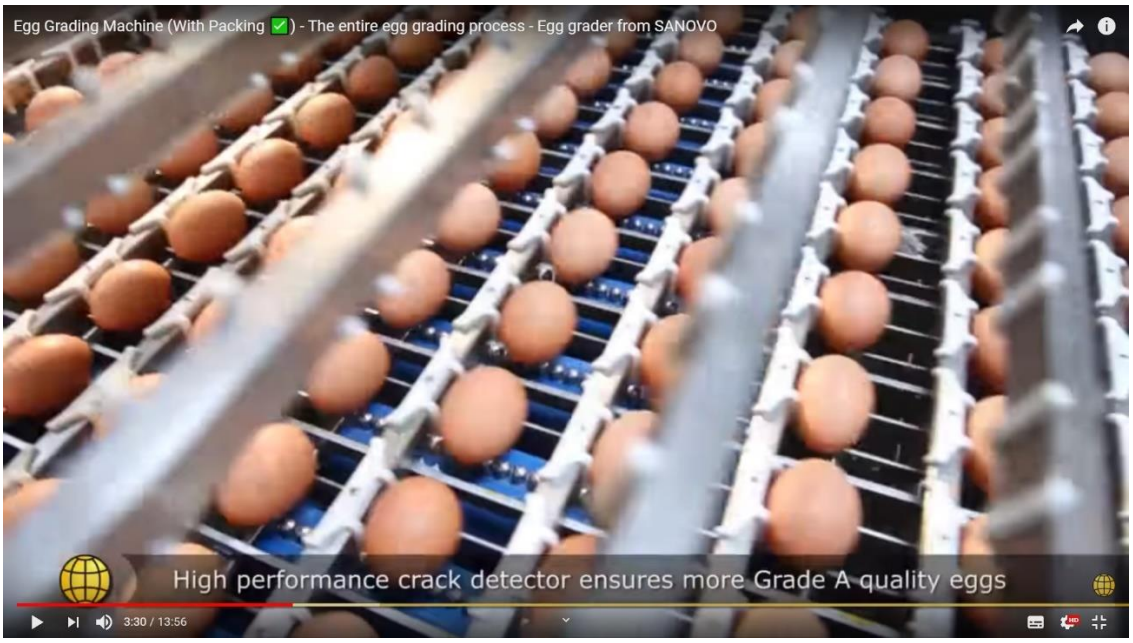

Figure 9. Industrial crack detector with multiple exciters in a grading system for eggs (internet 2.)

2.2. Passive ultrasound

2.2.1. Basics of ultrasonic measurements

Ultrasounds are mechanical oscillations propagating through elastic media above the audible frequency range, the upper threshold of this range is generally considered >20 kHz (or $2 \cdot 10^4$ oscillations per second). Upper threshold for ultrasounds in terms of frequency is not defined, but rather is limited by technical capabilities, as physical limitations of the source of the oscillating signal (mostly called a pulser or transducer) and sampling rate, putting a limit of approximately 50 MHz on the applicable frequencies, but food research and quality control applications above 10 MHz are scarce. These oscillations have several features, which can be measured precisely to gather information on their changes in assays. Some of these are collected in table 1.

Table 1. Properties of ultrasonic waves, their usual notations units and calculations

	Annotation	Unit	Formula
Period time	T	s, µs	-
Frequency	f	s^{-1} = Hz	$\frac{1}{T}$
Phase velocity	v_p	$m \cdot s^{-1}$	$\frac{s}{T}$
Wavelength	λ	m	$\frac{v_p}{f}$
Amplitude	A	mV, Pa, dB, *etc.*	Depends on interpretation
Sound pressure	p	Pa	P_{total}-P_{static}
Sound velocity	c	$m \cdot s^{-1}$	Gases: $\sqrt{\frac{K}{\rho}}$ Solids: $\sqrt{\frac{K+\frac{4}{3}G}{\rho}}$
Sound intensity	I	$W \cdot m^{-2}$	$p \cdot v_p$
Attenuation	α	dB	$P \cdot e^{-\alpha \Delta x}$

note: *s* denotes distance in m, *K* is the bulk modulus in Pa, G is the shear modulus also in Pa, *e* is the Euler number, *α* is the frequency-dependent attenuation coefficient in m^{-1}, *Δx* is the distance between the two points for which the attenuation is calculated (Szabo, 1994).

Frequency is the number of waves that pass a given point per second. The inverse of frequency is proportional to the distance over which shape of the wave repeats, the wave period. Phase velocity, the rate at which the phase of the wave propagates in space, divided by the wavelength is frequency. Amplitude is the maximum displacement of a periodic wave, also the strength of the vibrating wave of sound. It is the height of a wave, describing the instantaneous value of a varying waveform as well. Sound pressure, caused by a sound wave, is the local pressure deviation at a given point in the medium either from atmospheric or average pressure. The product of sound pressure and the acoustic particle velocity is the local instantaneous sound intensity. The speed of sound is the distance traveled during a unit of time through an elastic medium, referring to how fast the disturbance is passed on from paticle to particle. Attenuation of the sound is the decrease in intensity over a given distance (Kinsler et al., 2000).

For ultrasonic measurements passive ultrasound is used, which is defined by practical considerations: the sound wave must not interact with the tested material in a way that it induces changes in the sample, therefore, the relative energy is used for distinction between passive and active ultrasounds: under 10 $kW \cdot m^{-2}$ we consider them passive, or testing ultrasounds (Friedrich 2008). Over this level (depending on the type of material), cavitation can occur, which is an effect caused by rapidly changing pressure values in and the collapsing bubbles can cause structural damage to the material the wave encounters.

Different types of measurement techniques are used in terms of technical implementation and theory of the phenomenon exploited for the investigation. In terms of implementation A-scan (single point scan, stationary measurement), B-scan (moving a line scanner over the measured area) and C-scan (scanning consecutive points in successive lines) are applied. My measurements focus on A-scans, which are mostly used in one of the following configurations:

1. Through-transmission: The transducer and the receiver are spatially separated, and the tested material is located between them. The configuration allows the investigator to measure the inner structure or textural parameters of the sample as factors during interactions with the wave.
2. Pulse-echo configuration: The transducer and the receiver are built in one instrument, or more often the transducer acts as the receiver at the same time. The principle of operation is the measurement of the travel distance of waves calculated from echoes reflecting off phase surfaces.
3. Pitch-catch configuration: the transducer and the receiver are located close to the surface in a certain distance, angled toward each other. This setup allows for measuring the propagation of waves on the surface of the sample.

Technology development in the last decades was focusing on creating clearer images, higher resolutions (Rao et al, 1995, Tobocman et al., 2002, Amirmazlaghani & Amindavar, 2012) and increase of signal-to-noise ratios (Rao, 1994, Gan et al., 2001, 2002, Izuka, 1998), or combinations with other non-ultrasonic techniques (Moreau et al., 2002, Potter et al., 2006), for material testing and medical ultrasound tests.

As the relevance and possibilities of application became evident in food production and quality control for foreign bodies (Hæggstrom & Luukkala, 2001, Leemans & Destain, 2009), the research became focused rather on the applicability for different materials and different food matrices

(Létang et al., 2001) and non-destructive measurement of processes including maturation (Benedito et al. 2000a, 2000b, 2006, Cho & Irudayaraj, 2003, Vanevenhoven, 2012,).

2.2.2. Testing ultrasound in food research

A very broad topic for ultrasonic testing is the ability to test various structures built by organic tissue, and the most evident range of products for these are fruits and vegetables. Prof. Amos Mizrach contributed to this field with many studies and publications with exploring relationship between tissue structures, shelf-life and physicochemical attributes in relation to ultrasonic parameters in such produces (Mizrach et al., 1989, 1994, 1996, 1999, Mizrach, 2000, 2004, 2008).

Gan et al. (2002) used ultrasonic pulse compression (UPC) technique for sensitivity amplification of non-contact transducer with a chirp signal which according to Izuka (1998) has a very high signal-to-noise ratio (Häupler et al., 2014). They also determined the natural spectral sensitivity of their instruments (Gan et al., 2001) using the UPC technique.

El Kadi et al. in 2013 published a study for estimation of optimal thawing time of frozen fish, for which they measured the acoustic parameters, using a 0.5 MHz pulser-receiver couple in a pulse-echo configuration. This study deals with phase change in time, using peak-to-peak maximum amplitude and acoustic impedance (the ability of a medium to exert attenuation on the signal), which indicates some useful features to test during phase change: liquids generally dampen the signal more than solids, and they also conduct sound waves slightly worse than solids, therefore significant changes are probable in these measures. This effect was also exploited by Aparicio et al. (2008), who reported that crystallization of water can be reliably measured indirectly by the sound velocity near the freezing point, Gülseren & Coupland (2007) determined the correspondence between the solution concentration and speed of sound, which might also contribute to the change in sound velocity in thawing products.

Another phase change experiment was conducted by Santacatalina et al. in 2011, measuring the crystallization of lard at different temperatures. They applied modified Gompertz and Avrami models to describe phase change, as these are offering good estimates, and they found, in general, a better fit for the latter, but it also seems from the high explained variances (94.78%-99.99%) and high root mean squared error values (5-10%) that the models are either overfitted or not as well-fitting as expected, also no goodness of fit statistics were reported, therefore the article is only useful for methodology considerations.

Benguigui et al. (1994) showed that clotting can be effectively measured by ultrasonic techniques, and even could distinguish acidic and enzymic coagulation as they theorized, based on the micelle formation mechanism. This was the study that sparked interest and was the motivation to replicate the experiment with some modifications. They have found characteristic curves typical for enzymatic and acidic gelation while following the process with 60MHz ultrasonic sine wave in through-transmission configuration. They measured viscosity with a rotational viscometer at 1 s^{-1} shear rate, a value at which they observed competition dynamics between aggregate formation and disintegration.

3. Materials and methods

3.1. Fast Fourier Transform

Fourier transformation, developed by the famous French mathematician, Jean-Baptiste Joseph Fourier, is an algorithm that interprets a signal on the frequency domain instead of the time domain which is the conventional representation of sinusoidal signals (Fourier, 1807). The spectrum of a signal, *i.e.* the magnitude of the sound at given frequencies is the product of the Fourier algorithm, which has been substantially simplified by a calculation method, that produces the same values faster, known as the Fast Fourier Transform or FFT for short (Cooley & Tukey, 1965). The process treats signals as a collection of sinusoids with varying frequency, amplitude and phase, not changing abruptly. The resolution of the frequency domain is determined by the sampling frequency, according to the Nyquist-Shannon criterion, the highest frequency represented is that of half the sampling frequency, because digital processing can interpret consecutive points as a (part of a continuous) wave of that frequency. FFT of a signal is prone to produce unwanted lobes (shown in figure 10.), and therefore most of the time a multiplier function, called an envelope, or window function is applied that reduces the prominence of the artifacts whilst retaining the characteristics of the transformed signal.

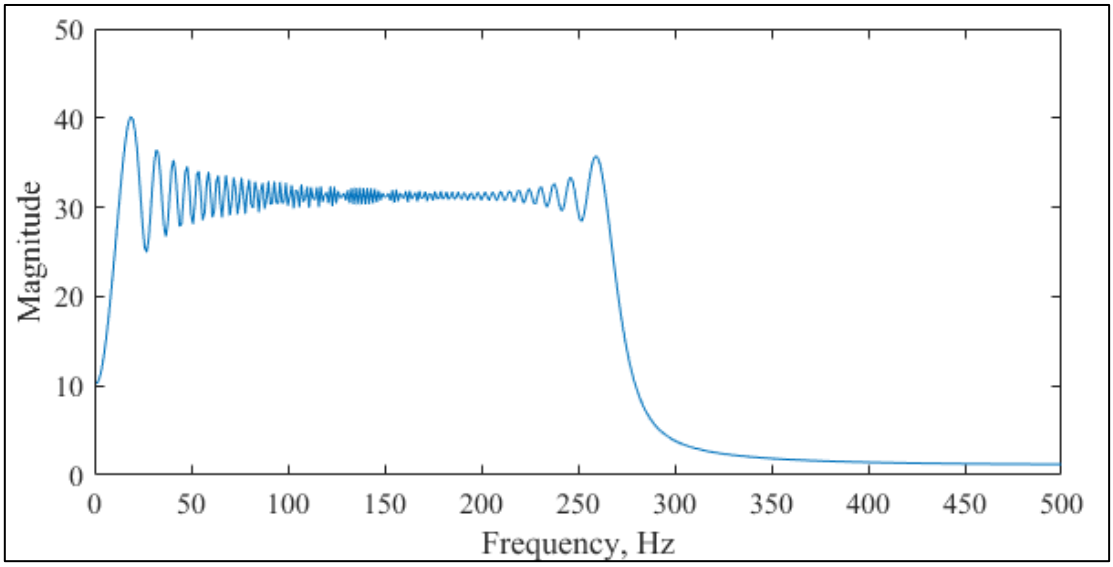

Figure 10. Artifacts created by the Fast Fourier Transform algorithm on a 20-250 Hz sweep signal

Certain applications require different characteristics, and therefore different windowing functions have been developed, such as Hanning, Hamming, Blackmann, Triangular, *etc.* The size of the window, *i.e.* the number of consecutive data points transformed is limited by FFT to 2^n, and has a

profound effect on the output spectra: the lower the window size, the more responsive the algorithm is to changes in time (in case of a continuously changing signal), the higher the window size, the better resolution, but lower responsiveness we can observe. This suggest that resolution can be manipulated by padding a signal with zeros to achieve a longer total signal with a number of data points that equals a power of two, but this –as with Continuous Wavelet Transformation (CWT) –, over a certain value does not provide real added information through increased number of data points.

FFT of signals can be as well calculated with a running window, which means that a window size lower than that of the signal is run throughout the extent of the signal, either overlapping or not overlapping, and the spectrum is then generated for the interval being transformed, the output is a matrix with coefficient values as a function of frequency and time. The two parameters to set are the window size, and number of overlapping points, which define resolution. When overlapping is present, weighted average of the two spectra is calculated, affecting the actual, or perceived resolution of the output matrix, but not affecting the apparent resolution in time, since the number of columns is still dictated by the number of points in the signal, therefore might be misleading. The spectral resolution is a function of the window size as described in the previous paragraph, and it is evident, that window size has an important role in balancing the total number of coefficients to be used as variables: too high is detrimental to calculation speed, and is therefore inapt for industrial use, too low produces insufficient resolution to analyze signal patterns. There is a clear tradeoff in resolution increase for both FFT and CWT algorithms, which has to be balanced for every measurement for an optimal customized solution.

3.2. Wavelet analysis

Wavelet analysis is a powerful, but calculation-heavy tool for analysis of acoustic signals, based on the wavelet decomposition algorithm. When executed on a presumably continuous (sound, or other spectral) signal, CWT is used, which shows the change of the spectrum over time. The output of the process is a two-dimensional matrix, containing the so-called wavelet coefficients, with time and scale factor corresponding to the columns and rows of the matrix respectively. A single coefficient captures the amount of the energy compared to the total energy content of the signal at a certain time point and at a given scale factor. The resolution of time is determined by the sampling frequency, the scaling factor can be adjusted and affects the resolution of the spectrum produced. The algorithm takes a so-called mother wavelet, a short, well-defined signal form with a mean amplitude of zero, and a predetermined central frequency (C_f, Hz) and cross-correlates it with a short part of the signal, the sampling interval (δt, expressed in the number of data points

and not in Hz), the output is a correlation coefficient. This process is carried out again at the next point of the signal, and so forth, the cross-correlation is calculated throughout the entire signal with the original mother wavelet traveled along the signal. This gives the examiner the correlation coefficients for all the points of the original signal, giving an n-by-1 array, where n is the number of points in the original signal. The mother wavelet is then scaled up (or down) by a scaling factor (*s*, dimensionless), and the previous process is repeated, resulting in the next line of coefficients. This is then cross-correlated again in the same manner as before, and the process is repeated to an arbitrary value of the scaling factor, or until it produces the mother wavelet with the size of the original signal or the signal sampling frequency matches the sampling interval. The scale factor, therefore, is corresponding to a given frequency, F_s (Hz) which can be calculated with the following equation:

$$F_s = \frac{C_f}{s \cdot \delta t} \tag{3}$$

In a more comprehensible way, an octave in music is defined as two tones with one being of double the frequency as the other. This can be interpreted as a scaling factor of two. Fractional scaling factors are possible, but after a certain value, added resolution does not contribute better use of the gained extra coefficient, albeit increases the required computational power.

3.3. Statistical methods

3.3.1. Principal Component Analysis (PCA)

PCA is a dimension-reduction method also used for exploratory data analysis. Principal components of a multivariate dataset are calculated based on their variances in all possible dimensions (the number of which is predicated on the number of variables), starting with the direction of the highest variance. This direction will define the first principal component. The consecutive perpendicularly defined dimension is similarly elected based on the direction of the highest variance in the remaining dimensions, and this process is repeated to successively define the new dimensions up to the total number of original variables. This will in essence serve us with a set of new dimensions, in which all original variables have some level of contribution, characterized by the loading (or coefficient) values. The new dimensions, also called principal components, are created in order of the explained variance, which allows selection of only a few variables to describe most of the variance in the dataset. This inherently means a loss of information regarding the original data, but allows the analysis of covarying factors, and is useful

to lower the number of variables for further analysis. Also, these principal factors can reveal groups formed by, or tendencies encapsulated in the data (Seber, 1984).

3.3.2. Partial Least Squares Regression (PLS)

PLS is a popular linear model building process for estimation, and is very similar to PCA in terms of calculation of new variables based on variances within the dataset. However, the goal is not to find components for maximizing information-content within new variables, but to find components, from which a response variable can be estimated with the highest accuracy. Essentially, we are not looking for tendencies within the dataset, but tendencies between a multivariate predictor dataset and another single-variate dataset that is to be predicted (Wold et al., 2001, Rosipal & Kramer, 2006). In the present thesis, this is a very useful tool, as the goal for every estimation is to predict as reliably as possible from spectral data, which are inherently multivariate

3.3.3. Linear and Quadratic Discriminant Analyses (LDA, QDA)

Discriminant analyses are linear classification methods, where the highest distances between groups are classified by new axes (or dimensions) generated for maximum separation. The new dimensions are generated to maximize the ratio of the compound group mean distances to their variances. LDA and QDA are generally fast algorithms, but they assume normal distribution of observations within the classes. The difference between linear and quadratic discriminants is that for the latter, an identical covariance matrix is not assumed, resulting in a boundary between groups that can be quadratic (Seber, 1984).

3.3.4. Support Vector Machine (SVM)

SVM is a discrimination method for separation of to groups by vectors an the multivariate space for finding the largest distance, also called the margin of separation between groups. With real-life data, especially multiclass datasets, this can become very difficult, but SVM allows for non-linear transformation of the data for better group separation. Also, several distance calculation, transformation, dimension extension methods are possible, which makes SVM a versatile tool. However, these adjustments can be very taxing in terms of calculation and memory efficiency, and speed as well (Christianini & Shawe-Taylor, 2000).

3.3.5. K-Nearest Neighbor (KNN)

The basic concept of this method is to calculate the distance between each data point and their closest neighbors, the number of which is set by the user. The group membership of the observation

is dictated by the membership of the nearby training points, the distance from which can be calculated with different metrics and weighting functions. The algorithm has a balanced speed and memory use, but might be difficult to interpret and prone to lose predicting accuracy with a high number of variables (Coomans & Massart, 1982).

3.3.6. Decision Trees

The underlying principle of decision trees is finding simple, binary-output rules to attribute data points to the different classes based on their score for the different variables. Once a distinction has been made, a new rule is given to further refine the decision, which is called a branching, and this process is continued in a cascading manner. The split criterion and the depth *i.e.* the number of branches can be set, increasing the depth results in increased training accuracy, but lower prediction accuracy and robustness and *vice versa.* Although a the Decision Tree classifier is oftentimes not very reliable for prediction, it is a fast method with low memory usage, which can be beneficial for industrial use (Breiman et al., 1984).

3.3.7. Ensemble Methods

Ensemble classifiers attempt to increase prediction quality by merging models with different classifier settings for a given classification method. This results in a wide range of settings, speed, and memory usage for the different methods, but they always offer more complex models and therefore the results are more difficult to interpret (Rokach, 2009).

3.3.8. Sum of Ranking Differences (SRD)

For the selection of the best classification or estimation method, validation of the prediction might not be sufficient in some cases, therefore a comparison between the classifiers for fairness is advised if ranking by the dependent variable is possible. The algorithm compares the composite rankings by the exploratory variables to the rankings by the output variable and finally assigns a value and an order to the methods by fairness of prediction (Héberger & Kollár-Hunek, 2011, 2019).

3.3.9. Goodness of Fit (GOF) and prediction accuracy statistics

Regarding PLS regression in general, the Mean Squared Error (MSE) is calculated for both the calibration (MSEC) and the prediction set (MSEP), and in cross-validation is calculated as the mean of the multiple validation models' average MSEP. The above statistics, for clarity, are most of the time converted to the original unit of measurement by taking the square root, resulting in the root mean squared errors, RMSEC and RMSEP (sometimes reported as RMSECV)

respectively. The lower the value the more accurate the estimate is, but it is important to emphasize that it is not a measure of goodness of fit. For that purpose, the adjusted coefficient of determination, also called the adjusted r-square statistic, R^2_{adj}, with corrected degrees of freedom due to the number of explanatory variables in the model and the number of samples is commonly used and is reported as one of the main metrics of estimation performance. The R^2 value calculated for the test set for a regression model is often called the Q^2, in the reported results of this thesis henceforth the R^2_{adj} value will be reported for the cross-validated results. This value is fallible however, and is prone to show higher values for overfitted models using an excessive number of latent variables (LV), therefore RMSEP values should be supplied along with the R^2_{adj}. As for the precision of the prediction, the similarity in results of repeated measurements is best described by the Standard Error of Prediction (SEP), which contributes to the RMSEP through $RMSEP^2 = Bias^2+SEP^2$, with the bias being the sum of all errors of prediction. The value of the Bias is most of the time a negligibly small value (in the realms of 10^{-20} and 10^{-30}) if the fit is reasonably good, RMSEP and SEP values are essentially numerically the same and practically interchangeable, suggesting model accuracy and precision are very similar (van der Laar, 1998).

For evaluation of overfitting, the Residual Prediction Deviation (RPD, sometimes also called the Ratio of Performance to Deviation) statistic was used, which is the ratio between the standard deviation of the original data and the SEP. This metric lowers when overfitting occurs, and is commonly used in near-infrared spectroscopy for testing the true prediction power of models. The values generally used in near-infrared spectroscopy, although arbitrary, widely accepted in scientific research: >10: excellent and equivalent, or better than the reference method, 5-10: adequate for quality control, 2.5-5: satisfactory for screening (Williams & Sobering, 1993).

3.3.10. Cross-validation (CV)

When validation of a prediction model with independent samples is not possible, cross-validation is a useful tool using the original dataset for classification and estimation purposes as well. This requires the observations to be divided into blocks, the number of which will be determined by the folds of the cross-validation: *e.g.* a 5-fold cross-validation will divide it into five blocks, of approximately equal size regarding the number of observations. This process is called partitioning, in this instance a k-fold cross-validation with k=5. A model will be built for four blocks and tested on the remaining one, then this process is repeated until all permutations for building and testing are carried out to evaluate the average error of these models. Generally speaking, the higher the number of folds are, the more reliable the validation becomes, as the models tend to become more

similar. However, if the number of observations is much smaller (by at least an order of magnitude), cross-validation will not give an accurate estimate of the error (Hastie et al., 2001).

3.4. Milk clotting measurements

Altogether, 13 measurements were conducted, at three different milk fat contents, 1.5%, 2.8%, and 3.5%. Samples were purchased from the same manufacturer, and the three different types were identical in every other feature including heat treatment. 100 ml of the samples were fortified with a small grain (app. 0.1 g) of crystalline $CaCl_2$ to ensure no limitation of clotting due to low calcium content. A transducer-receiver couple was submerged in the beaker containing the milk sample, using a stand made of rigid foam to ensure a constant distance of four millimeters. The sample was heated to 38°C, measured with a pt100 thermometer connected to a digital multimeter, and kept at a constant temperature in a thermostat until the end of the clotting process, which took 120 minutes. Once the sample reached the desired temperature, the ultrasonic measurement was started using the instruments and methods discussed in Chapter 3.3.1. Before the addition of 1000 µl rennet (Présure simple Brun calf stomach enzyme, Alpha-Vet Kft.), a number of initial measurements ($3<n<10$) were saved for reference, and for posterior determination of the time of addition of the enzyme. After addition, which was executed with simultaneous agitation, five ml of the inoculated sample was transferred to the tempered viscometer beforehand, and the viscosity measurement was started immediately.

3.4.1. Ultrasonic measurements

Experiments were carried out with a piezoelectric ultrasonic transducer-receiver couple with a nominal frequency of 250 kHz (The Ultran Group, USA), meaning the peak sensitivity frequency, but the actual range for measurement can be extended, and the instrument can be used at a wide bandwidth. Preliminary tests were done with probes of higher nominal frequency, but the change in the response signals were barely detectable. In theory, high variation in the response signal would be expected at wavelengths corresponding with the average size of casein micelles (which converts to approximately 7.5-8 MHz testing frequency), but this could not have been tested because a suitable ultrasonic probe couple was not available. Therefore, only the effect on the texture properties was the subject of the investigation. To capture the input and response signals, a Velleman PCSGU250 Oscilloscope (Velleman NV, Belgium) was used and connected to a PC via USB port. The transducer was connected to the signal generator output with a coaxial cable and branched off to channel 1 on the oscilloscope for signal acquisition with a signal splitting piece, the receiver probe was connected to channel 2. The commanding program, PcLab2000LT

v1.12 (Velleman NV, Belgium) was used to adjust signal generation and acquisition parameters: signal form and frequency, amplification and offset, signal gain, range, sampling frequency and trigger level for ensuring temporally stationary signals. The received signals were saved into ASCII format .txt files for further processing in Matlab 2017a (The Mathworks Inc., USA). The generated files included 4096 data points in three columns: the serial number of the measurement data point, channel 1 (input) and channel 2 (return) signal values in one volt per 32 samples and ten millivolts per 32 samples ($3.125 \cdot 10^{-2}$ V per quantum and $3.125 \cdot 10^{-1}$ mV per quantum) resolution respectively (resolution also specified in the generated file). Files were automatically generated once a minute, resulting in 120 measurement files in a span of two hours.

During the measurements, a so-called “chirp” signal was utilized. This is a double-modulated test signal, with increasing frequency, enveloped by a filter. In the case of the present experiment, the applied signal had a linearly increasing frequency sweep from 50 kHz to 450 kHz, and was modulated by a Hanning filter; this signal form is widely used in ultrasonic material testing. Example input and output signals (centered to zero, denoised, not normalized) from the present analysis are shown in figure 11. Amplitudes are shown in digital units, calculated as explained in the previous paragraph, therefore the order of magnitude of the amplitudes are not matching.

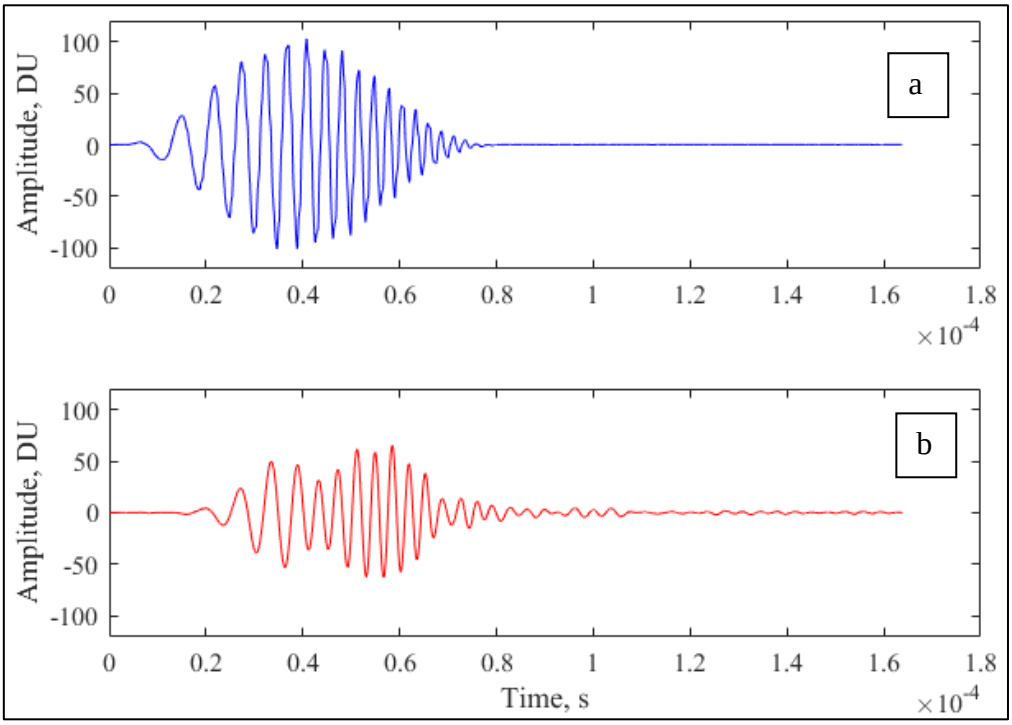

Figure 11. Input (a) and response (b) signals

The sampling frequency was set to 125 samples per 10 μs in the driver program of the instrument, yielding 1.25 10^7 s^{-1} (12.5 MHz) final sampling frequency, which is more than enough to ensure the spectral resolution required to analyze the generated signals.

3.4.2. Viscosity measurement

Measurements for the milk clotting experiments were carried out with a HAAKE RotoVisco 1 (Haake Technik GmbH, Germany) rotational viscometer, tempered at 38°C (± 0.1°C), to match the conditions with the ultrasonic measurement setup. The cylindrical probe revolves in a sleeve, between the two, the resistance force of the viscous sample is measured which exerts force on the probe through a given contact surface area. This allows us to calculate the apparent shear stress (Pa) and since the shear rate (s^{-1}) is adjusted in the controlling program of the device, division of the two grants is the numerical value of the viscosity in Pa·s. The measurement program was based on the experiences of earlier experiments with sol-gel transition investigations: following a short, ten seconds long high speed (500 s^{-1}) agitation period (ten seconds ramp up and ten seconds slowing time), throughout the rest of the 7200 seconds long measurement, the shear rate was set to 2 s^{-1}, with data acquired every ten seconds.

A specific problem emerging during measuring samples with sol-gel transformation of the matrix is the formation of particles through connection of micelles, the disintegration of which requires extra energy, which shows up as peaks on the rheogram (figure 12.). In the case of curdling, the shape –extent and height– and distribution of such peaks depend on the fat content of the milk sample. These peaks also appear overlaid on the viscosity curve, which was recorded over a two hours span, and show a steady negative exponential increase in this timeframe after an initial lag phase (measuring very low viscosity). As the probability distribution of occurrence of the spikes as a function of time is a much more complex task to estimate (and requires a very high number of experiments), I focus on the base viscosity curve estimation, and in case this results in a highly explanatory fit, henceforth I estimated the predicted viscosity values from the ultrasound signals processed with wavelet-decomposition.

The trend in the viscosity curves seem to follow an inverse negative exponential equation:

$$\eta = A \cdot e^{-\frac{B}{t}} + C \tag{4}$$

A (Pa·s), *B* (s) and *C* (Pa·s) are the model parameters, *t* (s) is the time. This assumption is backed by the notion of the viscosity of the medium approaching a maximum value of conversion through an enzymatic reaction; therefore, the model I deem conclusive. The major problem of fitting is to

find an algorithm that offers a generic solution for any such curve, meaning virtually random, non-noise induced peaks, superimposed with data following a curve of mathematically definable change.

The following procedure is proposed: minima of the curve is calculated for consecutive, overlapping intervals of a size that ensures the absence of positive extremes caused by peaks of an observed width. This width in the case of the present measurements is between 2-5 data points (with a sampling frequency of 0.1 Hz). Unfortunately, in some cases the frequency of the peaks was high enough to merge consecutive spikes, which created a longer skip in the reliable data, these resulted in a series of outlier points, and such curves could not be used as a reliable dataset for fitting, and therefore were left out of the analysis. To ensure reliability, the minimum of ten data points was collected per interval, resulting in the original number of points. To enable the estimating model to handle corresponding input and output variables, every sixth data point was extracted, yielding one datum for each minute, meaning 1/60 s^{-1} final sampling frequency, matching the sampling frequency of the ultrasonic measurements.

Although this method, by principle, slightly underestimates the true value of the viscosity, it estimates the baseline viscosity well (including the lag phase). An example is shown in figure 12. and the results are very similar to the curves seen in the study of Benguigui et al. (1994). The R^2_{adj} values are between 0.7251 and 0.9985 (mean = 0.9618), as shown in table 2.

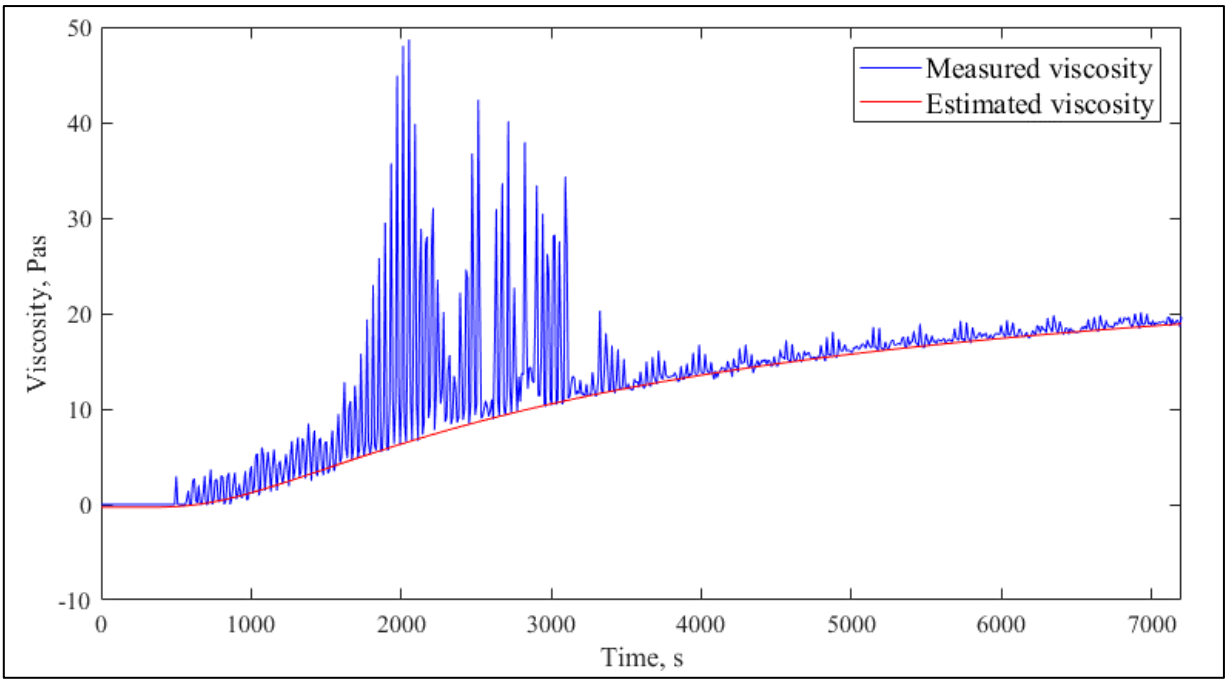

Figure 12. Example for measured and estimated viscosity (R^2_{adj} = 0.9973)

Table 2. R^2_{adj} values for viscosity estimations

fat content (m/m%)	R^2_{adj}
1.5	0.9985
	0.9948
	0.9980
	0.9792
	0.9984
2.8	0.9862
	0.9510
	0.9973
	0.9858
3.5	0.9869
	0.7251
	0.9101
	0.9917

The goodness of fit statistics imply that the models gained for individual measurements are apt to substitute the original measurement values which were technically impossible to base a prediction on. One exception is the second measurement with an R^2_{adj} of 0.7251, which is due to the high number of outliers because of merged peaks, but as figure 13. shows, the estimate itself is close to the baseline viscosity.

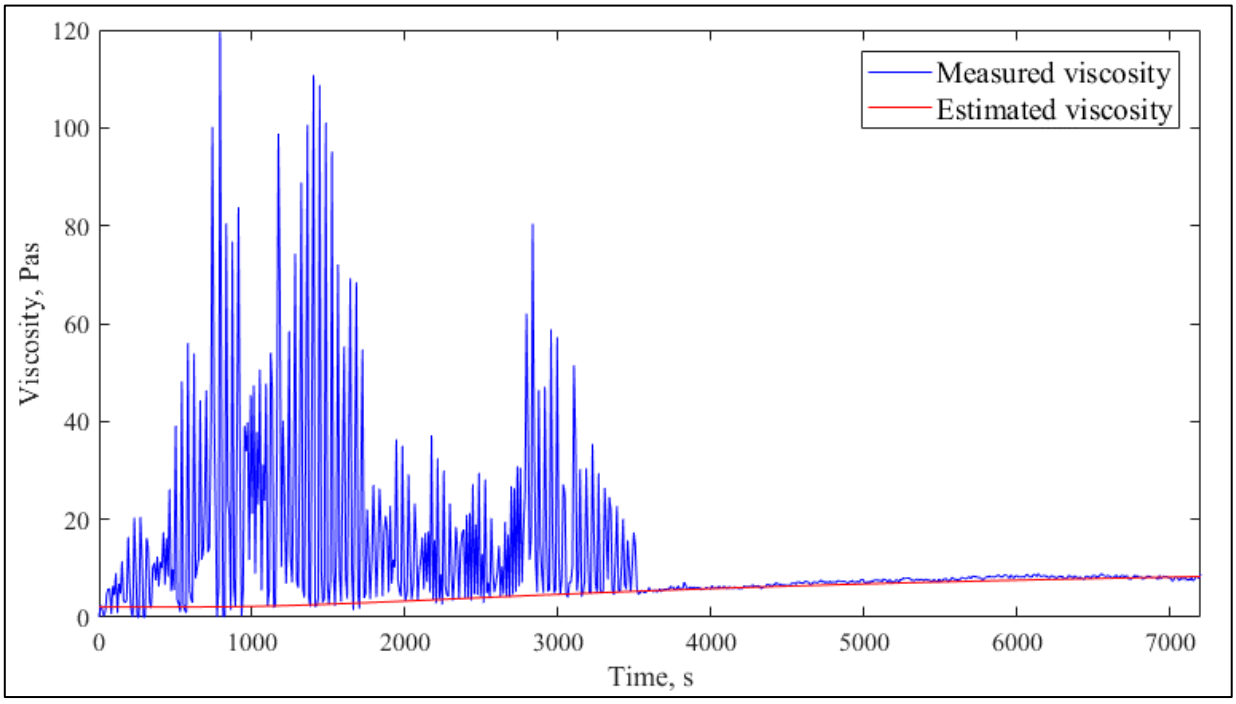

Figure 13. Measured viscosity and the fitted negative exponential model with the lowest goodness of fit result.

3.5. Cheese classification

3.5.1. Ultrasonic measurements

Time-of-Flight (TOF), measured in μs or s, is a commonly used estimator in material science, in through-transmission mode investigation, being an important measure of the amount of material with a certain sound conductance expressed in the speed of sound. An essential question raised was how important is it to measure the TOF at all? This feature is informative on the overall structure and composition of the sample, but for complex materials, as foodstuff usually are, it might be useful to measure the TOF not only at one single frequency but multiple frequencies, in other words for a spectrum. I elaborate on this question further in Chapter 3.6.1. further, but the conclusion was that it might be useful to test the sample with a chirp signal described in 3.3.1. in detail for the ability to test spectral information, and therefore new methods for signal processing. The thickness of the layer of material determines how fast the sound wave travels through the sample, and the sound velocity (for primary waves) is affected by material properties:

$$c_p = \sqrt{\frac{K+\frac{4}{3}G}{\rho}} \tag{5}$$

, where c_p is the sound velocity of the primary wave in $m \cdot s^{-1}$ K is the bulk modulus in Pa, G is the shear modulus in Pa, ρ is the density in $kg \cdot m^{-3}$ (Kinsler et al., 2000). Also, in some cases with samples with curvature, secondary waves travel on the surface of the sample similar to earthquakes (Kinsler et al., 2000):

$$c_s = \sqrt{\frac{G}{\rho}} \tag{6}$$

The importance of precise calculation of the TOF parameter is obvious, it is not a simple task due to acoustic dispersion (described in 3.6.1.), which affect the shape and spectrum of the response signal greatly, as the denomination suggests, the signal arrives dispersed greatly as displayed for the present investigations in figure 14. with a 250 kHz single impulse signal.

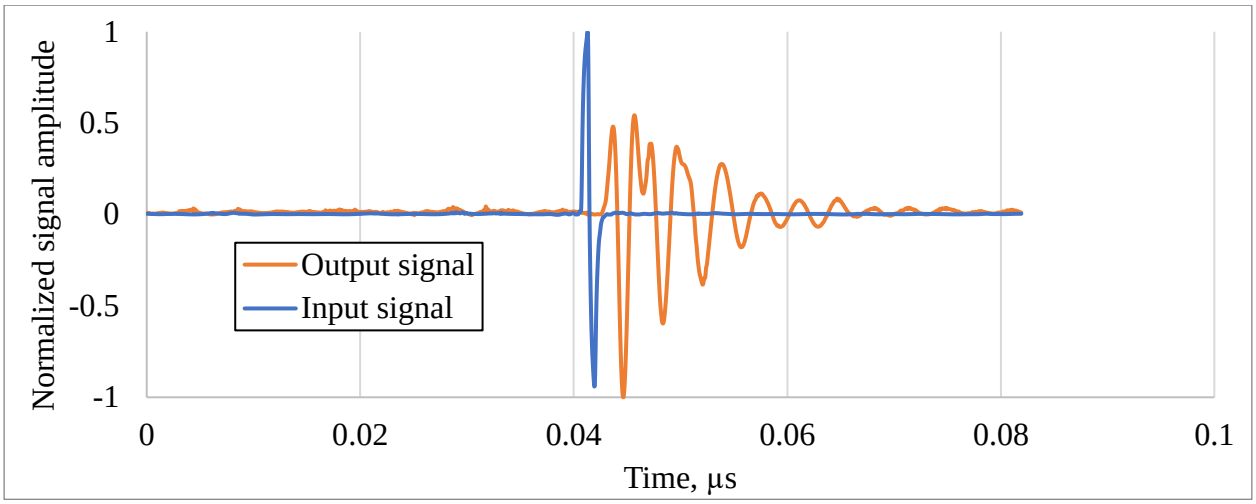

Figure 14. Impulse signal and the effect of acoustic dispersion on the response signal in a pulse-echo configuration

60 samples of sliced mozzarella cheese (from Szarvasi Mozzarella Kft. Hungary) were compared in order to test new methods for calculation of the TOF parameter. Two types of these cheese were considered: 20 of the samples were smoked, the rest (40 slices) were normal, untreated cheese. They were matching exactly in composition, meaning if the difference between the two is detectable, it is not caused by chemical variation, which is verified by the datasheet supplied by the manufacturer (confidential data). This is an important constraint because in general, fatty solids and liquids conduct sound better and the speed of sound changes accordingly. The other factor affecting the TOF is the distance (L, m) traveled in the material, because of:

$$TOF = \frac{L}{c_p} \tag{7}$$

This had to be investigated before experimenting, Analysis of variances showed no significant difference between the two groups at p = 0.062, shown on the boxplot in figure 15.

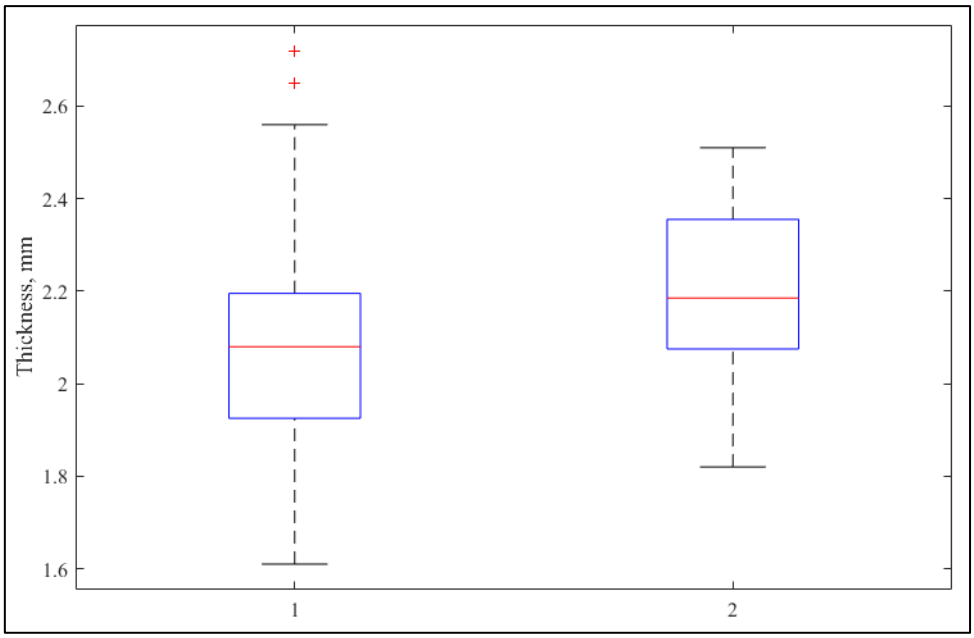

Figure 15. Boxplot of the sample thicknesses of cheese slices of untreated (left) and smoked (right) types.

The experimental setup (figure 16.) consisted of the same instruments as in the case of the milk clotting measurements as described in 3.3.1., The difference in the setup is the use of an ultrasonic gel to avoid highly insulating air pockets to form between the probes and the sample. This was a necessary modification because of the low amplitude of the signal.

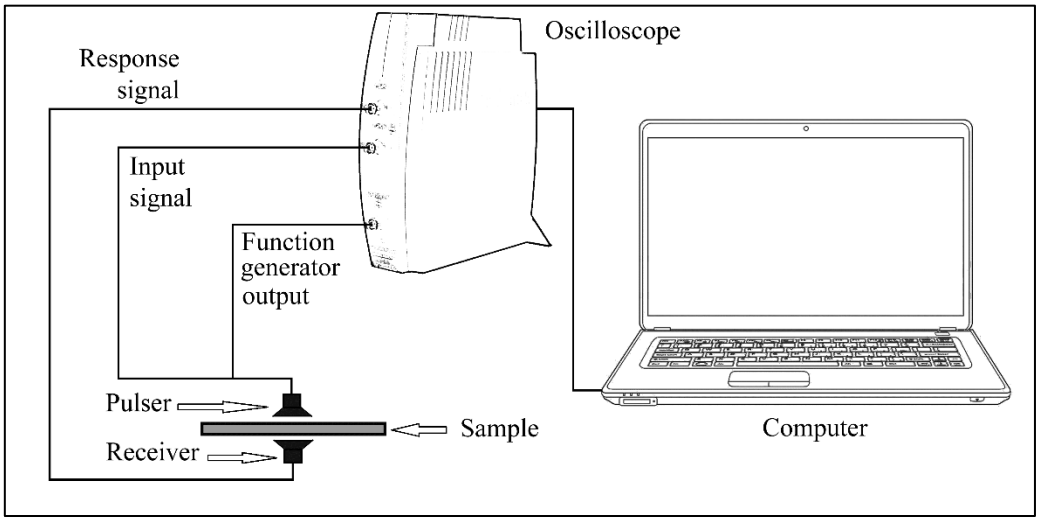

Figure 16. Experimental setup for investigation of cheese slices.

The experiment was revisited in 2019, after collection of a few years of experience and signal processing technique, and (except the one TOF estimation method) the same set of investigations were carried out with adjustment of processing algorithm parameters.

In this instance, three different types of samples from the same manufacturer (Szarvasi Mozzarella Kft.) were used, normal untreated (annotated with N), smoked (F), and lactose-free (L), 30 samples of each type. The composition was the same for types N and F, the nutrition facts for group L showed the same values, but as the name suggests, the carbohydrate profile and therefore –through affecting fermentation– the structure must be different as well. Also, the total fats in solids ratio was >35% whereas for the other two it was >40%, which is an important piece of information because fats conduct sound waves better. From a classification standpoint this leads to an expected higher confusion of the other two groups due to better distinction between compositionally matching and differing samples. Thicknesses were essentially the same in low variability (<5% as SD/range), their means were compared by Kruskall-Wallis test, and was found to be different ($p = 4.5 \cdot 10^{-5}$) as shown in the boxplot (figure 17.).

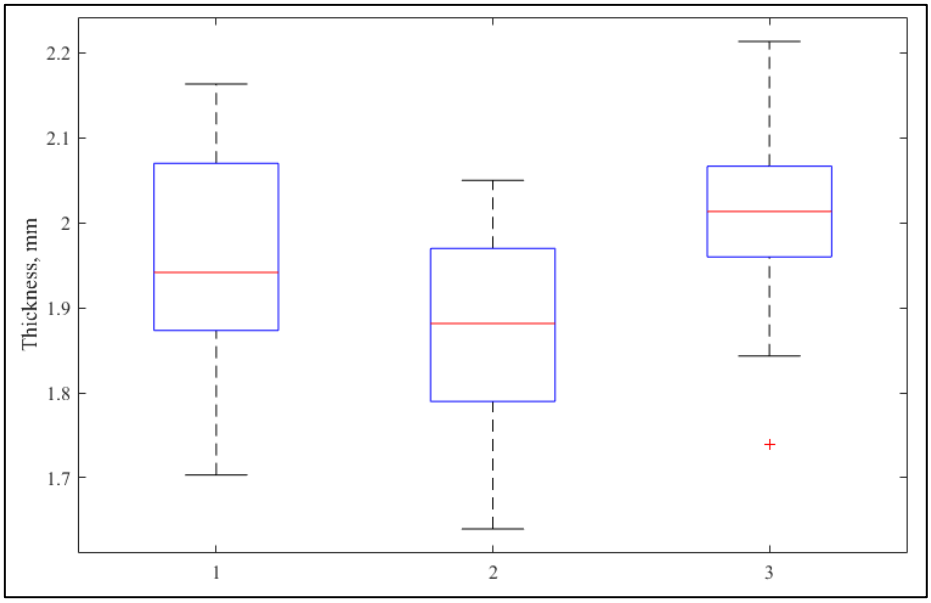

Figure 17. Boxplot of the sample thicknesses by groups: smoked (left), untreated (middle), lactose-free (right)

This concludes that separation of the groups with only wavelets should be difficult in theory if the Time-of-Flight does not show an apparent difference by the groups. This effect was taken into consideration during the design of the processing algorithm. The exact same experimental setup and acquisition parameters were used, and the measurements were conducted at room temperature as in the earlier experiment.

3.6. Eggshell crack detection

Acoustic measurements were conducted through a course of six weeks on medium-sized eggs, the distribution of sample masses is shown in figure 18.

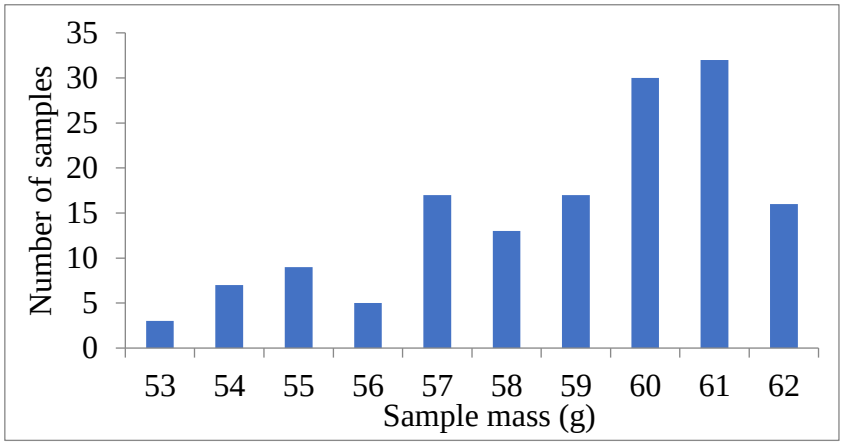

Figure 18. Histogram of the masses of the egg samples

Eggs were stored at 22 °C (± 1°C), between 50-70% relative humidity. The storage experiment was set up in order to follow mass loss and other structural and chemical changes, but this part of the experiment was unsuccessful, because of this, the measurements described hereby do not discuss the storage effect. Before starting the experiment, all eggs were tested for cracks by candling (a bright light was shone through the eggs) to reveal hair cracks (see figure 19.).

Figure 19. Seemingly intact egg (left), and cracks revealed on the same egg by a bright light shining through (right)

All eggs were measured on the zeroth day, 20 eggs were weekly tested for constituents, which meant cracking them open in the process, therefore these samples were removed from the set. Before opening them completely, first a very small, most of the time invisibly thin microcrack was inflicted on the pointy tip (opposite of the air chamber) of the eggs, and acoustic testing was done before and after this destructive action, totaling in 705 measurements in six weeks. The test itself was done by excitation with a hollow metal rod, meaning a single light knock on the shell. This knock was done in an upright (North-South, NS) and a laid down (East-West, EW) position as well, on the uppermost part, meaning the pointy tip in NS and along the equatorial circumference in EW arrangement. For stabilization and noise reduction, in both positions, the samples were placed on a foam pad (as suggested by Felföldi & Ignát, 1999), hollowed out for insertion of a microphone.

For recording a very sensitive microphone was used with a practically flat spectrum sensitivity. This instrument was connected to a Hewlett-Packard 53670A (Hewlett-Packard Inc., USA) signal analyzer, from which the sound signal was sent to a laptop for recording with 96000 Hz sampling frequency in lossless .wav format. The experimental setup is shown in figure 20. The sound files were processed with a program compiled in Matlab 2017a environment.

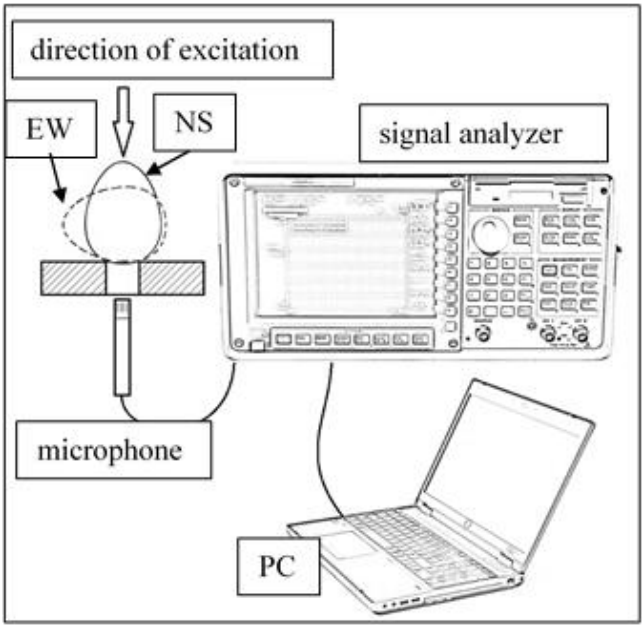

Figure 20. Experimental setup, for the acoustic measurement of eggs in two positions (Kertész et al., 2019)

Estimations were done for mass, weight loss, ovality, shell thickness, shell mass, yolk mass, albumen mass, albumen dry matter and yolk/albumen ratio, but none of these variables showed a

reliable prediction. Although in NS position, many of these yielded acceptable R^2_{adj} values (0.86-0.87), and RMSEP% (relative to the range of measurement values) between 3.6% and 5.0%, these values became double-digit with validation, therefore will not be discussed in the Results and discussion Chapter.

3.7. Signal processing and analysis

3.7.1. Theoretical considerations

It is important to emphasize that the ultimate goal was to work out a procedure for signal processing that is applicable in most circumstances, thus not very specific to the individual measurement, is highly reliable, and requires minimal or no adjustments and corrections. Earlier studies mainly focus on the Time-of-Flight, or the acoustic attenuation parameters (Friedrich, 2008, Espinoza, 2018, Kertész & Felföldi, 2016).

TOF being the time required for the signal to travel through the material is a single value extracted by various algorithms, which need to account for signal form. In most cases, corrections are not necessary if the measurement setup is consistent throughout measurements. As a counterexample, a chirp signal might show different peaks at different frequencies if the signal form is not corrected for the sensitivity spectrum (most of the time not being completely uniform) of the specific experimental setup. This can be solved by choosing a signal form that is not prone to produce such problems upon processing, *e.g.* a short burst of constant frequency, but on the other hand, different signal forms were developed, because of the different analytical features, which might be lost due to the aforementioned considerations.

Acoustic attenuation is the effect of an acoustic signal losing energy whilst traveling through media, thus the received signal has a much lower amplitude than the input signal, in effect it describes the acoustic resistance. This descriptor has been studied extensively (Friedrich, 2008), since it is correspondent to the rheological properties of the material. Highly elastic media being a better acoustic conductor than plastic media, allows scientists to draw quantitative conclusions of the rheology of a material. Acoustic attenuation is frequency-specific for a given material, meaning the testing frequency needs to be determined a priori. This is usually done by trial and error, searching for the highest correlation between attenuation and the property desired to estimate. Also, undisturbed conduction of the signal to the tested sample has to be ensured, or such interferences with the measured values need to be resolved.

The issue with these two parameters lies in them being a single value. This is beneficial if we want to compare a highly descriptive feature between samples, but in many cases for highly complex materials, such as food, they do not capture a lot of the extractable information, and –from a statistics viewpoint– account for a small amount of the physical variance of the samples. It is quite understandable therefore, why they are good descriptors for changes in less complex materials (Benedito et al., 2002, Gülseren & Coupland, 2007, Aparicio et al., 2008, Santacatalina et al., 2011). *Nota bene*, the goal here is not to overcomplicate processing of experimental results, but to achieve the best estimation or classification using the data at hand with the lowest chance of misinterpretation of gathered information, and therefore less complex methods should be favored. With that being said, conventional single descriptors were used during processing measurement data for estimation and classification (also in experiments not presented in this doctoral thesis), but in most cases, to no avail.

Another phenomenon of high importance is the effect of acoustic dispersion, which creates a range of complications with signal analysis, but at the same time, can provide various information on the tested material. This is witnessed daily, for example when hearing a conversation through a wall, we can often not comprehend what has been said, although we can identify the speakers, voices are mingled. The reason for this is quite prosaic but reflects very well on the mechanism of acoustic dispersion. Different materials conduct sounds differently, meaning a difference in sound wave velocity, phase shifting, and attenuation, moreover, some properties are affected differently at different frequencies. A wall is composed of various materials in particles of different sizes and in a diverse arrangement of layers, and every phase boundary of differing materials is a location of acoustic refraction, the deflection of a wave. In such greatly compound materials, such refractions take place steadily, creating echoes, and profoundly affect the sound perceived by the listener. The result is a voice with more or less preserved timbre, the collection of attributes of the human voice our brain is most sensitive for in identification of the speaker, but not the content of the speech. The same effect takes place in tested materials, although the aim is different: the intent is not to identify the original signal (because it is given and well-characterized) but gaining insight on the sample in view of the known signals, or the change in the material affecting the response signal.

Milk coagulation studies generally focused on measuring either the attenuation or the TOF (for sound velocity calculation) parameters at one given frequency or with impulse signals to estimate certain characteristics of coagulation. This approach has the limitation of not examining the response in a spectrum, and this requires the assumption that all relevant information can be extracted from the response of one single frequency. Although in some cases this might be true, it

is certain that testing a wide spectrum will inherently serve us with more information on the material (Bakkali et al., 2001, Yang et al., 2021, Nassar et al. 2004, Ay & Gunasekaran, 2003). As Budelli et al. (2017) pointed out, measurements of only attenuation or the TOF parameter have their own specific limitations. Few studies investigated the spectral response of clotting milk, and these only focused on a very limited number of testing frequencies or bandwidths, hence the same issue persists, although slightly mitigated (Jiménez et al., 2017, Corredig et al., 2004).

In this experiment, I was aiming to develop, and on a complex material, test an algorithm that can alleviate these issues, which emerge from the necessity to compare the output and the input signal. The great benefit of such an algorithm is that there is no need to determine the instrumental spectral sensitivity, distance between probes, or even exact amplitude, as long as the source signal is unchanged. Such processing can be done only in a fashion that analyzes the intrinsic features of the response signal and compares the description of these internal variances to the changes in the test material's specific properties. Consequently, this requires a minimum of two features with matching dimensions to be extracted from the response, and this –on a more philosophical note– is just as big a difference statistically compared to single-feature methods as between none and one in good deeds done. The implication is that if a method needs to be developed to handle two explanatory variables, it is not too big a difference to handle ten or a hundred, because we must then rely on multivariate analysis. This principle can be carried on to other measurement methods yielding spectra or other data with a very high number of variables (such as acoustic measurements), although needs to be customized depending on the specific technique. Complications start to manifest when there are an enormous number of variables to handle, and it is not known which will carry meaningful information. The standard procedure is to extract latent variables and base estimations or classification on these, unfortunately, this necessitates calculation of covariance matrices, which even with today's vast computational power is not achievable for several thousands of variables (sometimes millions depending on resolution). What makes the case even worse, peaks in spectral data might not be the most information-rich points when comparing amplitudes, they only tend to retain variance in carried information better due to the higher signal to noise ratio.

If simple algorithms do not yield satisfying results, and the number of explanatory variables is very high, methods like Principal Component Analysis (PCA) and other statistical methods calculating covariance matrices might not be an option. Nevertheless, the fundamental principle underlying them can be utilized, namely the calculation of variable variances but instead of assigning new LV based on their covariance matrices, variance across single variables is a less

computation demanding procedure. For calculation of covariance, the following equation should be considered (Zhang et al., 2012):

$$Cov(X,Y) = \frac{1}{n^2}\sum_{i=1}^{n}\sum_{j=1}^{n}\frac{1}{2}\left(x_i - x_j\right)\left(y_i - y_j\right) \quad (8)$$

Where n is the number of observations, x_i, x_j, y_i, y_j are the *i*-th and *j*-th observed values for variable *x* and *y* respectively. Clearly, the required number of calculations increases dramatically with the number of observations and variables introduced, since the formula needs to be calculated for each pair of data points of each pair of variables. On the contrary, more efficiently, the variance across individual variables is calculated as follows:

$$Var(X) = \frac{1}{n}\sum_{i=1}^{n}(x_i - \mu)^2 \quad (9)$$

, where μ is the mean of the dataset. The difference in information content is not quantitative but qualitative and requires a procedure to be found in order to avoid the necessity of LV. The reason to calculate LV, to begin with, is to lower the number of estimators needed to carry out a statistical procedure more effectively and to ensure the independence (or quasi-independence) of the variables when necessary (for example in discriminant analysis). The latter might cause concerns with spectral data: depending on resolution, consecutive values in fact do vary together (produce high covariation) in most cases, and have overlapping information content, therefore are not to be considered independent. Choosing frequency values as explanatory variables relatively distant from each other spectrally (or temporally) can to some extent mitigate this problem. Described in 3.6.1., acoustic dispersion, and therefore the extension of peaks due to echoes and delays makes the descriptors of these effects an important set of metrics, although explicit numerical representation is not necessary if these characteristics are implicitly present in the extracted variables

3.7.2. Evaluation of milk clotting measurements

The acquired signals were processed with a program compiled in Matlab 2017a. After reading the raw data was centered to zero (the mean of the input and output signals were separately shifted by their specific means). A normalization was applied to match the absolute maximum of the signals with a value of one. This has two very important implications: the unit of the measurement values is canceled out, because of the division as

$$A_i = \frac{U_i}{|U|_{max}} \quad (10)$$

, where A_i (dimensionless) is the normalized amplitude of the *i*-th value of the signal, U_i (V) is the amplitude of the *i*-th value of the signal, and U_{max} (V) is the maximum amplitude. As with processing of other measurement data, this makes the original units irrelevant as long as the different measurements are conducted in a way that the dimensions are constant. The other, possibly even more remarkable feature of this transformation is the fact that it makes further comparison of attenuation impossible (cf. 3.6.1.). The motivation behind this choice was to support the comparison of the changes within the response signals themselves and not the changes between the input and output signals, and normalization helps greatly because of the preprocessed signals having identical amplitudes.

This was followed by a denoising process with a built-in function based on wavelet analysis and parameterized for the signals processed. For correction, the input signals were aligned in time, because they were more reliably adjusted being essentially identical, and then the output signals were arranged accordingly. This correction was necessary because otherwise, a shift in time between the response signals would be present, which defeats the purpose of comparison of differences within the signals. As a next step the measurement following the addition of the rennet was identified, and the previous signals were removed from the investigation, only the next 120 measurements were considered.

CWT using a Morse wavelet and running short-time FFT were calculated for each ultrasonic measurement file. The FFT uses a window size relatively small (512) compared to the extent of the sound signal (4096 point) and is run through the signal overlapping each other with a predetermined number of points (511). This resulted in a high enough spectral and temporal resolution for further calculations. An important difference between the two methods is that FFT provides a linear resolution curve, whilst CWT yields a hyperbolic resolution curve, meaning that there are more values associated with lower frequencies. Parameters for both algorithms were chosen to supply values of comparable and sufficiently high resolution in the bandwidth of interest, *i.e.* 50-450 kHz. The colored surface plots (for CWT called a scalogram, for FFT a spectrogram) in figure 21., aligned to show coefficient values along the frequency (*f*, Hz) and time (*t*, μs) axes, display the similarity of the gathered coefficient values in the addressed region. Color differences correspond to the energy content of individual points, or coefficients, yellow being higher, blue being lower.

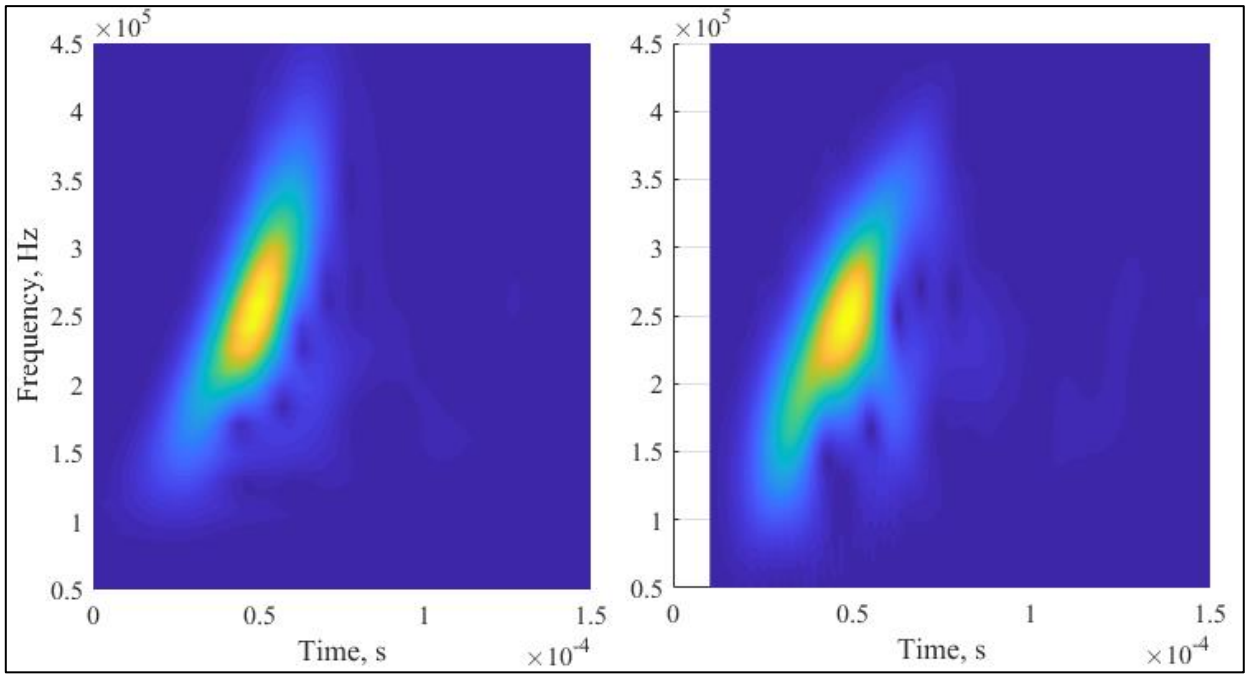

Figure 21. Scalogram (left) and the spectrogram (right) of the same response signal in the range of interest

Although not being entirely identical, the same internal patterns are clearly visible. In general, the wavelet transforms seem to carry less distortion, which is a burden of the FFT algorithm. In later analysis, spectrogram coefficients produced subpar estimation performance and therefore were omitted from the evaluation.

The standard deviation of the sample (SD, applying Bessel's correction), as a good descriptor of variance is calculated for the panel data (meaning across wavelet coefficients of consecutive measurements). This describes the change of individual coefficients over time; hypothesizing that the frequencies corresponding the most to the changes in viscosity are the ones most likely to change, it is reasonable to assume that the peaks appearing in the matrix containing the SD values of coefficients are describing these changes well.

The peaks of the resulting matrix were identified by calculation of the gradient through time and frequency, considering the matrix a scalar field:

$$grad(F) = \nabla F = \frac{\partial F}{\partial t}\vec{e}_t + \frac{\partial F}{\partial f}\vec{e}_f \tag{11}$$

, where F (dimensionless) is the coefficient standard deviation field, and $\vec{e}$ is the vector field along the respective variable, t or f. A contour plot of the resulting field (or rather the surface defined by it) is shown in figure 22.

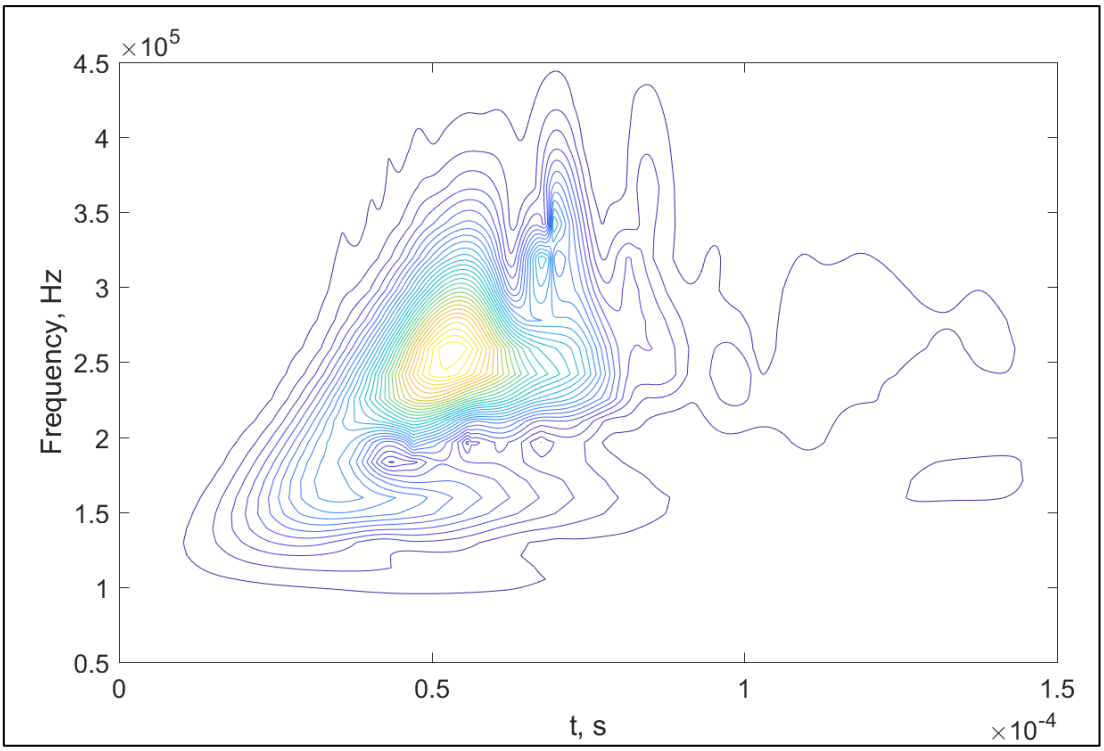

Figure 22. Contour plot of the gradient vector field.

This shows similar, but not identical patterns of the gradient compared to the original signals, with the highest peak at the nominal frequency of the transducer, and the frequency of the highest amplitude in the input signal.

After finding the peaks, the corresponding values of that certain location in time and frequency was extracted from F, an example is shown in figure 23.

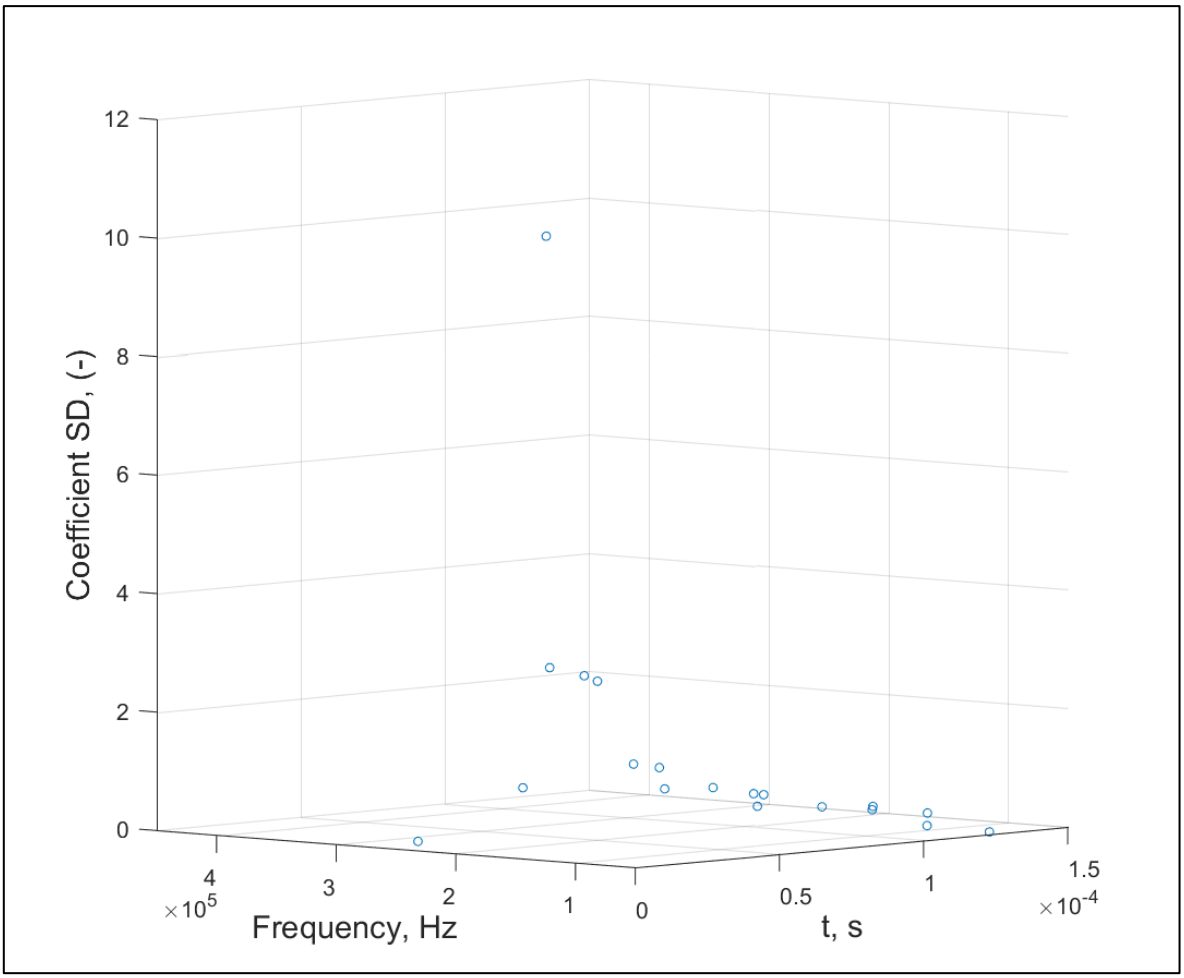

Figure 23. Example of a 3D scatter plot of the located local maxima in the range of interest

Many local maxima form near the highest peak, reflecting on the effect of the earlier described acoustic dispersion.

It needs to be addressed that it was assumed that the variance in the amplitude of noise is lower than the variance in the amplitude of the peaks induced by physical change in the material. I also assumed that the distribution of peaks associated with noise are random, which is essentially the definition of noise itself. This assumption was verified by calculation of the change of variance of individual coefficients throughout the timespan of measurements (henceforth called T, s) in successive cycles. It is calculated for the *i*-th measurement as

$$\Delta F_i = F_{T+i} - F_{T0} \tag{12}$$

If ΔF is gradually changing and is not constant over several instances, the change is not random and is considered a factor. This might be important because some of the values of explanatory variables were smaller by two orders of magnitude than others and were closer to the variance of noise than that of high variance variables. All of the extracted variables have been used for the

estimation of individual measurements, their number varying between 7 and 32 (mean = 22.5). Using Partial Least Squares regression, one of the outputs of the PLS regression function is the Means Square Error (MSE) of prediction, and the number of LV was adjusted in a two-step loop, in which the minimum value of MSE was marking the optimal number of LV for the second run.

3.7.3. Evaluation of cheese classification experiments

TOF was calculated with three different approaches: cross-correlation (XC) method, the Short-Time Average/Long-Time Average (STA/LTA) (Trnkoczy, 2012) and the Autoregressive Akaike Information Criterion Picker (AR-AIC) methods, the latter two are used in earthquake detection (Takanami & Kitagawa, 1991), where early response is very important. The program to calculate these three metrics was developed in Matlab 2012a.

The XC method relies on detection of the prominence of similarity of the input and output signals as the name suggest, calculated by the cross-correlation of the two signals as in

$$\hat{R}_{xy}(m) = \sum_{n=0}^{N-m-1} x_{n+m} \cdot y_n^* \tag{13}$$

, where $\hat{R}_{xy}(m)$ is the estimated correlation at the $n+m$-th point of dataset x, y_n^* denotes the complex conjugate of dataset y at the n-th value (or the original value of y_n if it is not a complex number), and N is the length of the signals (Buck et al., 2002, Stoica & Moses, 2005). The final cross-correlate is given as the vector

$$XC(m) = \hat{R}_{xy}(N - m) \tag{14}$$

, having 2N-1 elements and therefore the timescale needs to be resized accordingly.

An example of the XC curve is shown in figure 24.

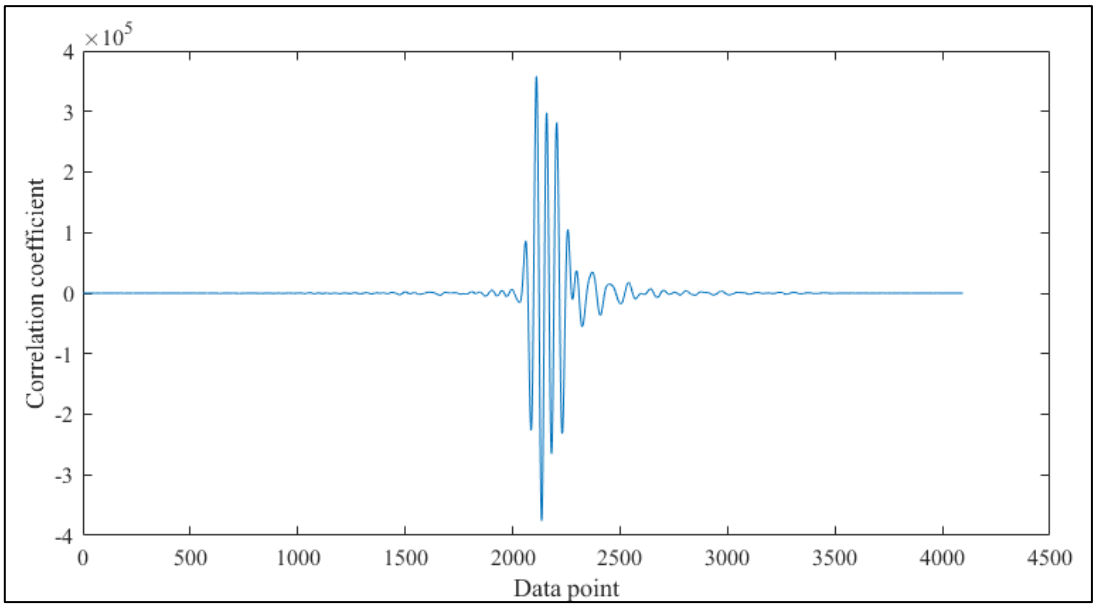

Figure 24. Cross-correlation curve of the input and output signals

The curve does not show the maximum value at the delay between the two signals, but it is at a location relative to the first instance of signal *x*, in this case, the output signal, figure 24. shows the original scale in time as the number of data points of XC and not had been resized. For TOF calculation, the location of the maximum was used and translated into time units. Not the maximum of the absolute was calculated, as it is most commonly used in the processing of random signals, because in case of a response guided by a well-defined exciting signal inversion of the displacement does not occur in theory (and the similarity of the response signals verifies this assumption).

The STA/LTA method is used in seismology and is an algorithm that can be tuned in several ways. It compares a short interval window average and a long interval window of a signal (Kertész & Felföldi, 2016):

$$a_j = \frac{\frac{\sum_{i=j-s}^{j} x_j}{s}}{\frac{\sum_{i=j}^{j+l} x_j}{l}} \tag{15}$$

, where a_j is the ratio of the means of the two windows, x_j is the j-th element of the signal x, j is the time index, s and l are the length of the short and long windows respectively. The length of the windows, their relative delay, their trigger threshold and their weight can be varied (Trnkoczy, 2012), actually this is one of the drawbacks of the method: it does require a very precise tuning to work reliably.

The AR-AIC picker is an autonomous but more complicated algorithm, the original version was published by Kurz et al. (2005), which has been modified to a two-step method, preceded by the computation of a characteristic function (CF) which increases the certainty of the estimation dramatically (Sedlak et al. 2008). This function takes the form of either

$$CF_i = y_i^2 + K(y_i - y_{i-1})^2 \tag{16}$$

, as suggested by Allen (1982), where *K* is an empirical amplifier value (in processing of the data set to 1, y_i is the *i*-th element of the original signal y. Another alternative for computation proposed by Sedlak et al. (2008) is by taking the absolute values of the elements instead of the squares, which supposedly enhances the differences in spectrum coefficients, but this was not observed in the signals of this experiment, therefore the original calculation method was applied according to Allen.

After calculation of the CF, the AR-AIC was computed as follows:

$$AIC_k = k \cdot \ln\left(\sigma^2(CF_{1..k})\right) + (N-k) \cdot \ln\left(\sigma^2(CF_{k+1..N})\right) \tag{17}$$

, where *k* is the serial number of the data point in CF, *N* is the number of elements of the CF *var* signifies variance and log signifies the natural logarithm (Espinoza et al. 2018). The minimum of the resulting data signifies the arrival of the signal, and the difference between the AIC of the response and the input signal yields the TOF (figure 25.):

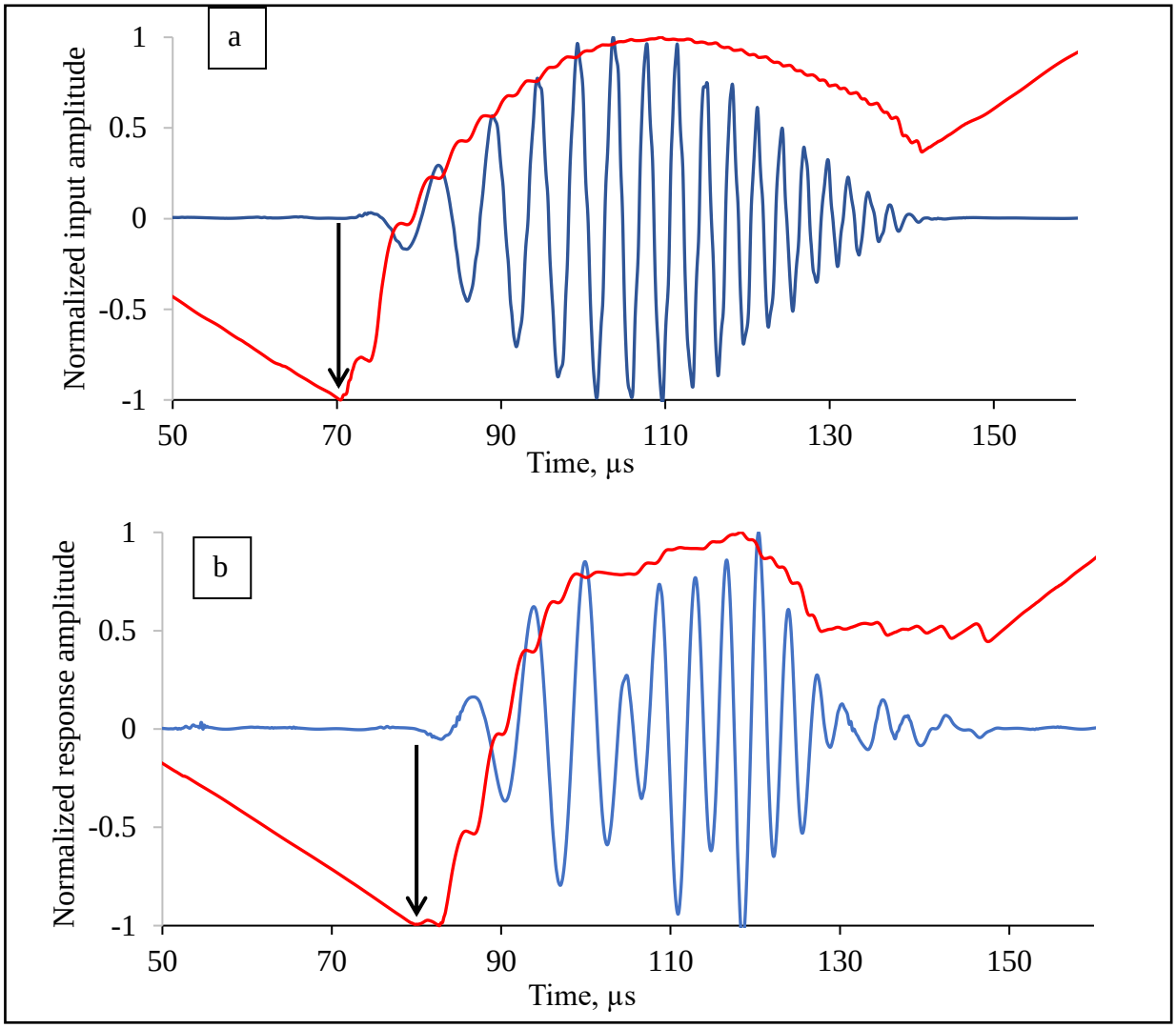

Figure 25. Normalized input (a) and output (b) signals with blue lines, and their corresponding AR-AIC function with red lines with their minima marked with arrows

The signals were also introduced to a classification assay for the prediction of the group membership of untreated and smoked cheese samples. The classifiers tested included an array of linear and non-linear methods: Decision trees, Linear Discriminant Analysis (LDA), Quadratic Discriminant Analysis (QDA), Support Vector Machine (SVM), K-Nearest Neighbors Classifier (KNN), and different ensemble methods. Only the LDA method showed reasonable results in terms of prediction power, therefore the rest of the classifiers, –yielding subpar classification results– are not discussed further for this experiment. Since no other methods gave acceptable results, and these were the only models applicable in Matlab 2012a, therefore eligibility of LDA was not tested further.

For the classification, explanatory variables used were the TOF acquired with the AR-AIC picker, FFT coefficients, and wavelet coefficients. Using a limited number of estimators was a defined

goal, therefore only 66 coefficients were used for FFT and 65 for CWT. CWT was carried out on the cross-correlated signals in the hope, that this captures the most detail on how the sample material modifies the original signal. The decomposition itself was achieved with a Daubechies mother wavelet at refinement level 8 (db8) (Daubechies, 1994). This wavelet granted the maximum characteristics retainment of the original signal meaning the true frequencies and the difference between the minima and maxima of the waves. The CWT yields a matrix with wavelet coefficients corresponding to the energy levels of the signal at a given time at a certain frequency. For every extracted frequency (represented by a scale factor), one maximum was delivered only, hence the 65 collected coefficient value for the 65 frequencies of a narrower range of interest instead of a total of approximately 166 thousand variables, and double of this for XC.

The recordings of the second experiment conducted in 2019 were pre-processed the same way as in the previous experiment: denoising and normalization were done, but no modifications were performed in terms of time localization and amplitude comparison of the input and the output signals. The XC and the XC TOF estimates of the two signals were calculated, alongside the CFs and the TOF estimated by the local minima of the AR-AIC curves of the two signals. Since the signals did not show any difference in shape and other meaningful characteristics, they are not illustrated again.

For classification, yet again the same methods were utilized, this time the difference was in the signal post-processing algorithm, and of course, the number of classes to predict was increased from two to three. This introduction of a new class has two effects: 1. the decrease of correct prediction rate due to random chance to 1/3 instead of 1/2, pointing towards the verification of a more reliable algorithm. 2. Since one of the groups had a different composition than the other two, it is expected to be more likely to be correctly classified, and therefore the other two to be more prone to be misclassified: the bigger the difference between clusters, the more likely it will affect the outcome. First, the explanatory variables for comparison of effect were the reciprocal of TOF calculated with AR-AIC and the sample thickness. The reason for this was that (after critical examination of the original experiment), it was apparent that with linear classifiers, the TOF is of not much use, and the resulting correct classifications for two groups being above the levels of mere chance is only explained by the thickness (although not very well): the sound velocity, a highly explanatory feature of material structure is composed of their ratio, in the form of L/TOF, hence the reciprocal of TOF should be used in the process.

3.7.4. Evaluation of eggshell crack detection experiments

After removing erroneous measurement files, the total number of processed measurements was 693. The signals were first cropped to a reasonable length (4096 points), which includes the entirety of the response signal and grouped according to the position of testing, examples for the two signals (without denoising) are shown in figure 26.

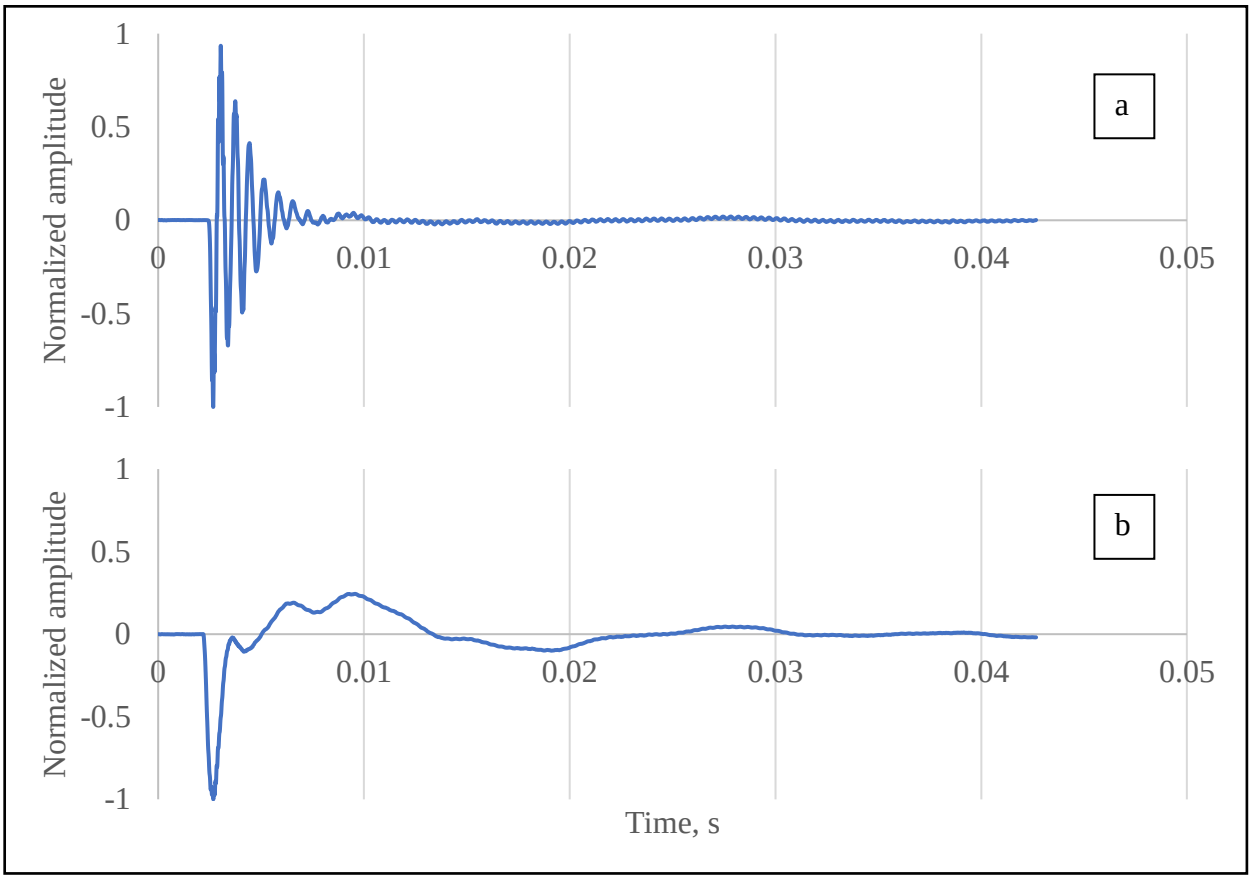

Figure 26. Normalized response signals of the eggs in NS (a) and EW (b) positions

Then the procedure, described at the processing of the ultrasonic measurements was followed, including denoising and normalization. FFT of the signals were calculated with different window sizes, to assess the effect of increasing resolution. Examples of the spectra of the response signals in two positions are shown in figure 27.

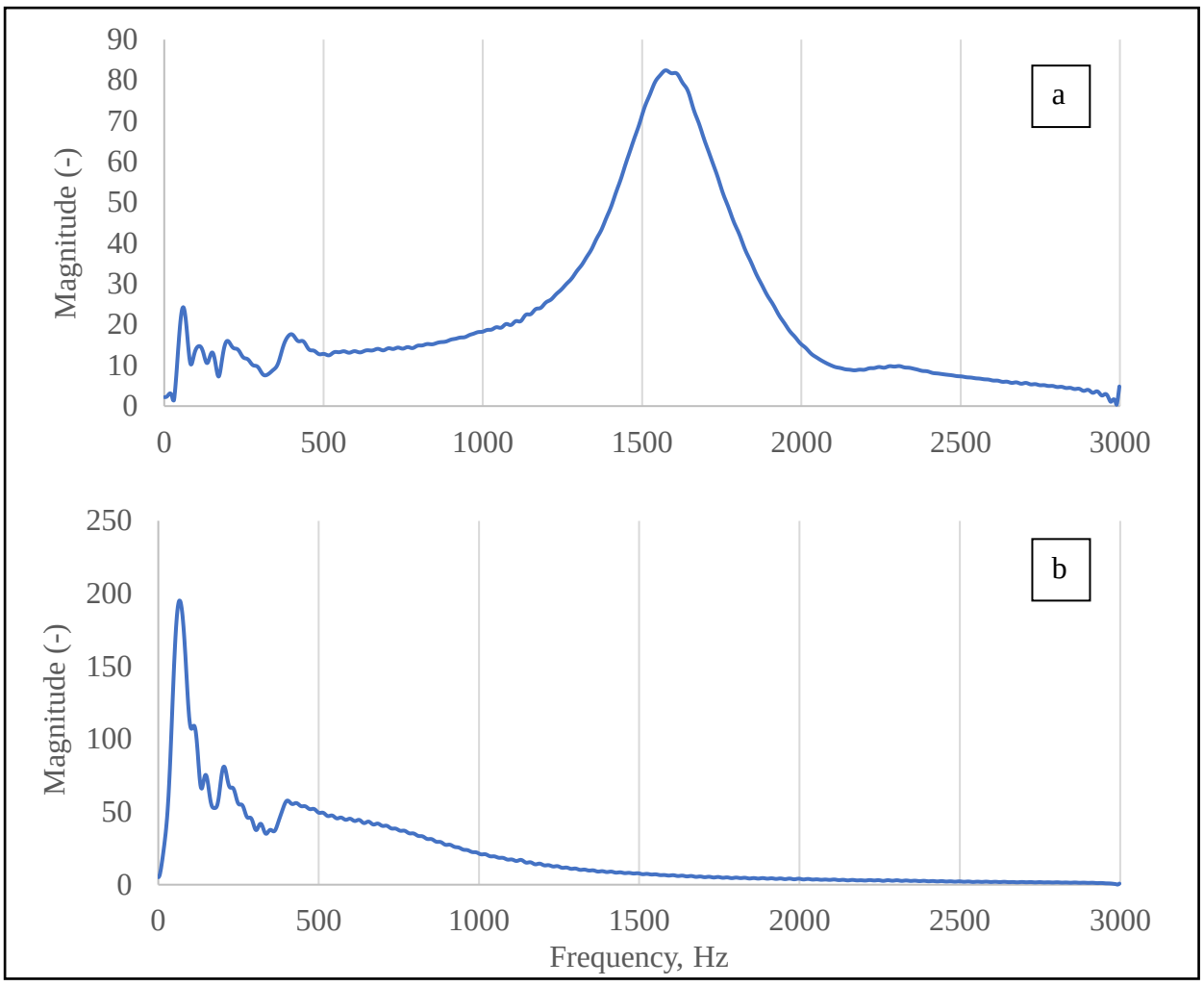

Figure 27. Spectra of the signals in NS (a) and EW (b) positions

As an extra step, padding with zeros was also carried out, functioning as a basis to use multipliers for further increase of the resolution, by the effect described in Chapter 3.1. The number of padding zeros was calculated as

$$N \cdot (M - 1) \tag{18}$$

, where *N* is the number of data points in the signal, *M* is the value of the multiplier. These multipliers take the form of the powers of two because the FFT algorithm window sizes are also restricted to 2^n points. The lowest number used as the multiplier was 2, meaning the total length of the transformed signal was double of the original, but window sizes used were not necessarily matched, resulting in the original resolution, with a running window, theoretically capturing more of the variation in time. Different window lengths and the corresponding minimum multiplier values used are shown in table 3.

Table 3. Window sizes and corresponding minimum resolution multipliers

window length (-)	resolution multiplier (-)
4096	2
8192	4
16384	8

This manipulation of the resolution in such a manner was done to verify the hypothesis that there is more meaningful information in the spectrum than what can be extracted using the idle window sizes. This is a useful technique when the precise location of moving peaks (searching for resonant frequencies) are to be identified, but it might also have an effect on using the magnitude values as variables, because with relocation of resonant frequency peaks the magnitude change in their original location occurs. This effect can also stack along neighboring frequencies and can be exploited if the entire spectrum is used as a series of explanatory variables.

Spectra were considered as $0\ \text{Hz} < f < 3000\ \text{Hz}$, because there was no apparent change apart from the noise in the higher frequencies, the lowest frequency was determined by the resolution. The magnitudes of all frequencies were used for classification, but for NS and EW positions separately because on an industrial scale it is not realistic to expect that sorting machines can move around eggs and handle both positions in a reasonable timeframe.

4. Results and discussion

4.1. Milk clotting measurements

PLS regression estimations were carried out in three arrangements of data:

1. Estimation of viscosity for individual experimental runs
2. Estimation of viscosity for different fat contents with joint measurement datasets
3. Estimation of viscosity for all measurements at once

In all cases, the predicted parameter was the modeled viscosity values described in Chapter 3.3.2.

The order of the three estimations is based on the robustness and therefore the degree of universal applicability of the models, not their industrial importance or relevance. The first set is generally useful to prove the generic applicability of the method and to prove the assumption of the algorithm being able to reliably estimate viscosity and therefore the progress of fermentation. This is the most important step because if the evidence suggests that the algorithm is based on a valid general idea, it suggests that by making adjustments it is appropriate for use.

The second set could verify that the fermentation of independent samples that are chemically and physically uniform can be reliably followed. This means a new tool to continuously monitor the curdling process and have precise information and control of the product without having to rely on the more or less subjective experience of workers.

The third set would prove that the method is applicable for estimation of viscosity change during fermentation of samples of different chemical compositions. This would prove that it is possible to develop a commonly suitable means to monitor curdling of cheese, and possibly other processes causing change in viscosity of milk.

The results of the evaluation of the first set (all samples modeled individually) are shown in table 4. with R^2_{adj} and Residual Prediction Deviation values included.

Table 4. Coefficients of determination and Residual Prediction Deviation values of the models

Fat content (m/m%)	R^2_{adj}	RPD
1.5	0.9944	5.07
	0.9697	4.49
	0.9876	6.96
	0.9966	10.88
2.8	0.9688	5.20
	0.9758	4.53
	0.9983	14.22
	0.9877	6.23
3.5	0.9632	4.38
	0.9943	10.09
	0.9973	13.99
	0.9684	4.71
	0.9910	8.27

GOF is in most cases outstanding, R^2_{adj} averaging at 0.9841, and model accuracies are excellent as well, in many cases extremely high, therefore it can be asserted with confidence that the estimation performance is not due to overfitting. This clearly displays the applicability of the algorithm for viscosity estimation. It needs to be mentioned that the values of RPD slightly vary with the random data partitioning of the cross-validation. It might be interesting to note that there is no apparent connection between the fat content and estimation performance. Graphs of the lowest and highest estimates are shown in figure 28. and 29.

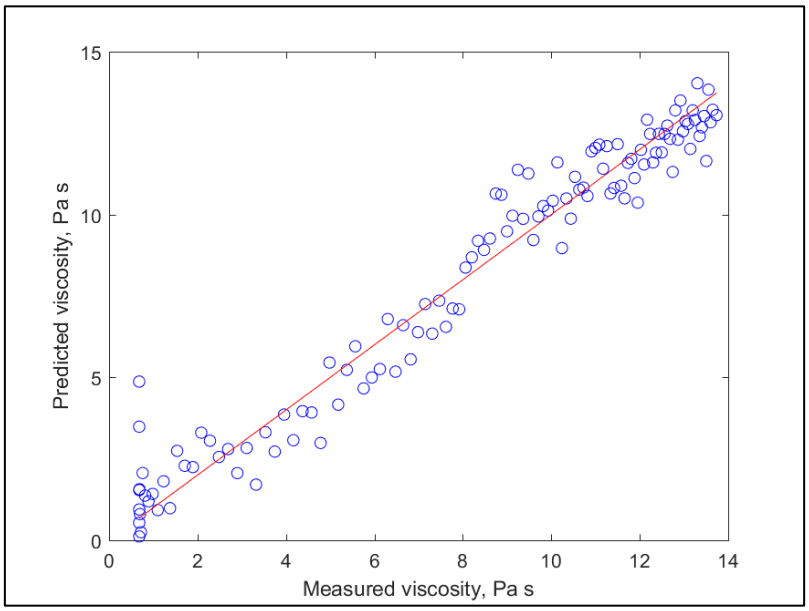

Figure 28. The worst prediction for individual modelling (R^2_{adj} = 0.9632 RPD = 4.38)

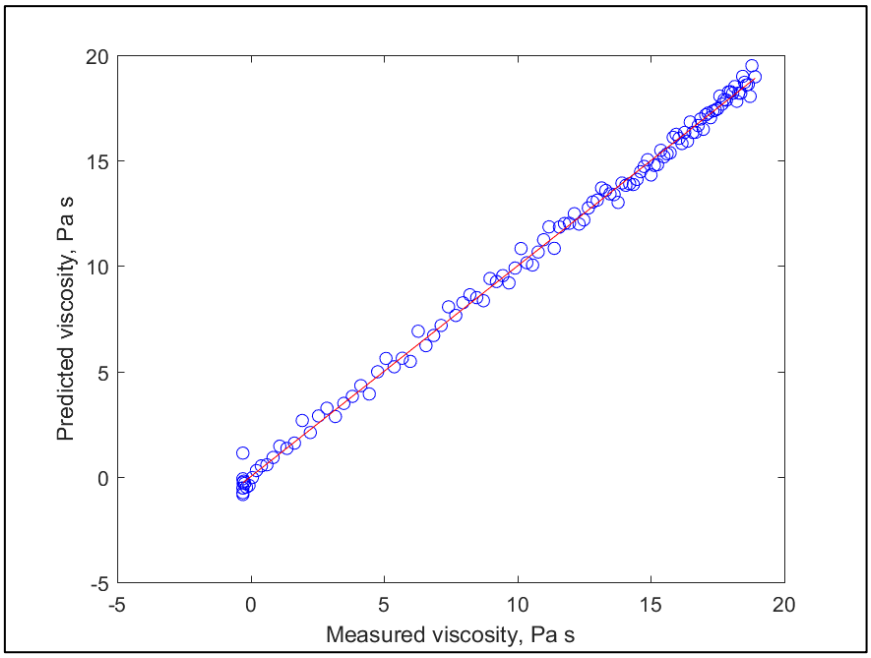

Figure 29. The best prediction for individual modelling (R^2_{adj} = 0.9983 RPD = 14.22)

It is suggested for further estimation models to take into account the probability distribution of energy requirement occurrence for breaking the forming particles, which might also give an insight into the state of fermentation. Even more so, other types of fermentation with a different coagulation mechanism from rennet-induced curdling often do not show a steady, but abrupt change in viscosity, and therefore require a different approach.

For the second estimation set, measurements were clustered by fat content. In order to incorporate all variables that are good descriptors of single measurements, the union of all these values was taken and concatenated in a matrix in the following arrangement:

$$\begin{matrix} a_{11} & a_{12} & \dots & a_{1n} \\ a_{21} & a_{22} & \cdots & a_{2n} \\ \vdots & \vdots & \ddots & \vdots \\ a_{m1} & a_{m2} & \dots & a_{mn} \end{matrix}$$

, where a_{mn} denotes a submatrix, containing coefficients of the *m*-th measurement corresponding to the indices from the model building process of the *n*-th run of experiment. For example, a_{35} consists of 120 rows for all measurements of the third run and contains such a number of columns that equals the number of variables used in the estimation for the fifth run.

Such an arrangement allows coefficients to appear multiple times, belonging to the same, or very close peaks, but PLS regression creates LV based on their covariances, therefore their effect on the prediction will not possess a higher weight.

GOF and accuracy statistics of the second set of models is shown in table 5.

Table 5. Coefficients of determination and Residual Prediction Deviation values at the lowest mean squared error values for prediction

fat content (m/m%)	**R^2_{adj}**	**RPD**
1.5	0.8929	2.72
2.8	0.9464	2.73
3.5	0.8606	2.51

This time estimation did not yield as high values, but they are still satisfactory at the lowest MSE. There is an obvious tradeoff between the fit and prediction accuracy, but if the MSE is not changing monotonously, one might find a good bargain between the prediction power and GOF statistics. The models were tested for successively increasing number of LV to see if a reasonable balance becomes apparent (figure 30.):

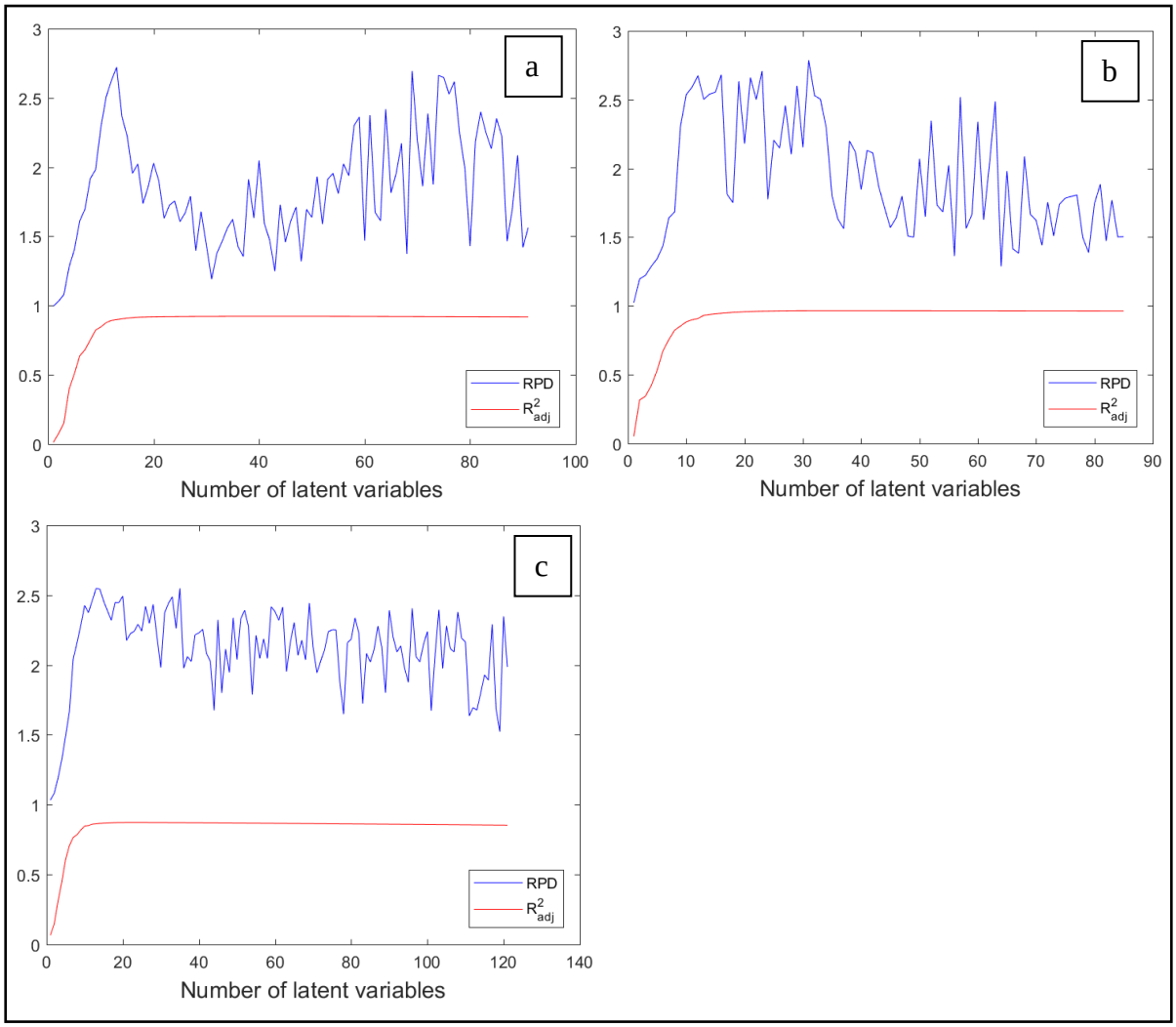

Figure 30. R^2_{adj} and RPD statistics as a function of the number of latent variables for predictions of viscosity in case of milk samples with 1.5% (a), 2.8% (b) and 3.5% (c) fat content.

Although there are certain peaks with higher values of RPD, at higher R^2_{adj}, they are not considerably greater, therefore –for the sake of parsimony– the lower number of LV was preferred, keeping in mind that due to cross-validation, there might be a small amount of variation in these statistics. Estimates of the models are shown in figure 31.

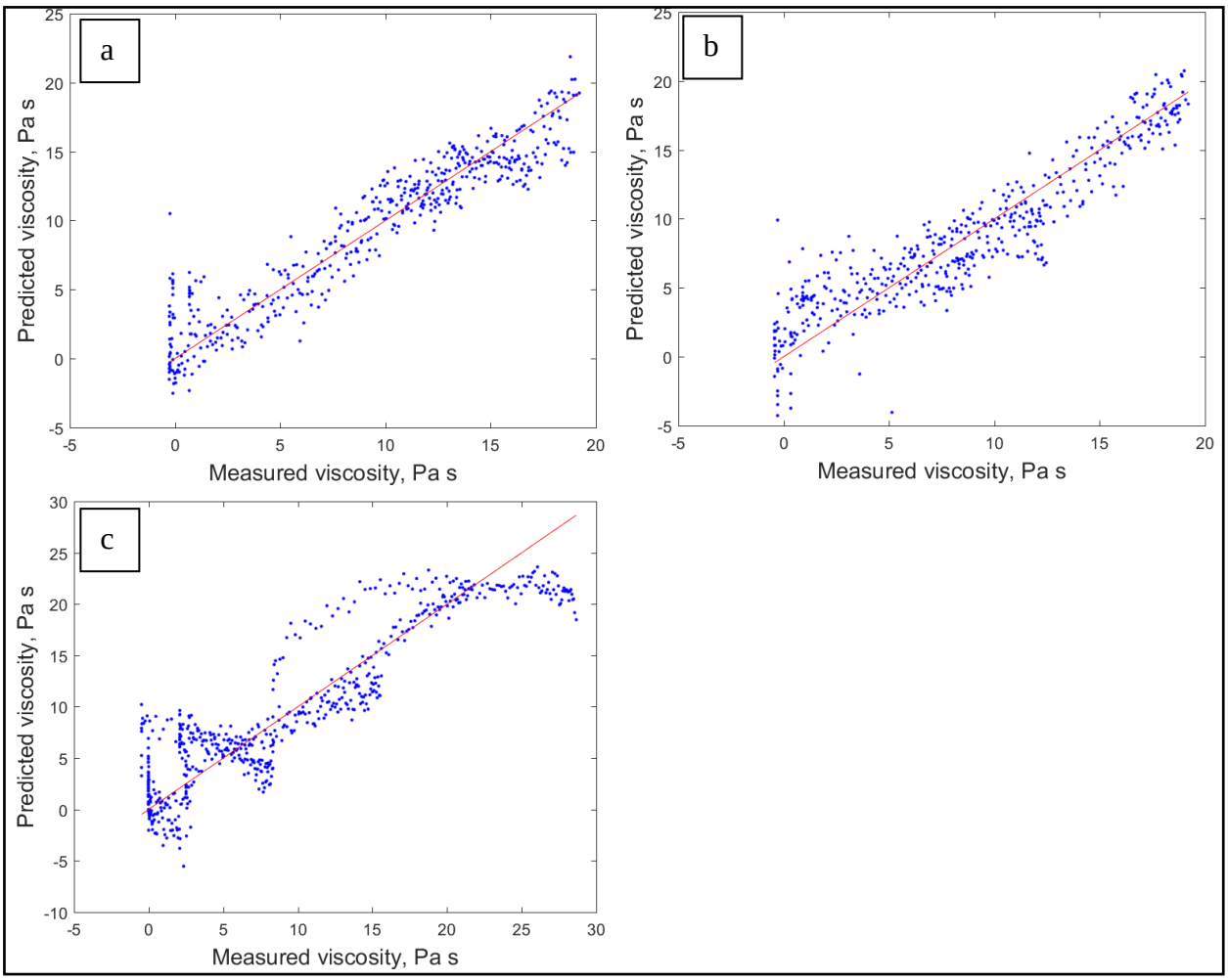

Figure 31. Predictions of viscosity in case of milk samples with 1.5% (a), 2.8% (b) and 3.5% (c) fat content with a limited number of latent variables.

It can be seen from the diagrams of prediction that the model for 3.5% fat content leaves a high level of heteroscedasticity in the residuals. Some level of autocorrelation is also witnessed in the other two estimates' residuals, all verified by Durbin-Watson statistics with $p<0.001$. This concludes that there is still room for development of the proposed method, but it also might be caused by a common trend in the viscosity measurements that the exponential estimation did not describe effectively.

For the last, third set, all measurements were concatenated in a matrix for estimation of the corresponding viscosities. This altogether means $13 \cdot 120 = 1560$ rows to include all observations.

The input variables were chosen the same way as in the previous estimation setup also, this time fat content was added as well, yielding altogether 298 variables. The second loop of PLS regression found the minimum of MSE at the 135rd latent variable, which is a high, but perfectly realistic number taking into account the number of observations and that the estimator variables are already collected from a pool of 135168 (!) variables, which was reduced by keeping representation of common behavior in mind; also overfitting was avoided by cross-validation (this time for extra certainty, the number of folds was increased to 25).

135 LV returned an R^2_{adj} of 0.9708 and an RPD of 5.85, which means a very good, highly explanatory model with a high prediction accuracy. Following the principle of parsimony, a minimum number of LV was searched for, that still satisfies the requirements of a well-fitting model. The minimum required RPD was set to 4.00, and for R^2_{adj}, a threshold of 0.95 was assigned, which for the former one was achieved at the 26th, for the latter one at the 35th latent variable with 0.9514 at which the RPD value was 4.75, their trend is shown in figure 32.

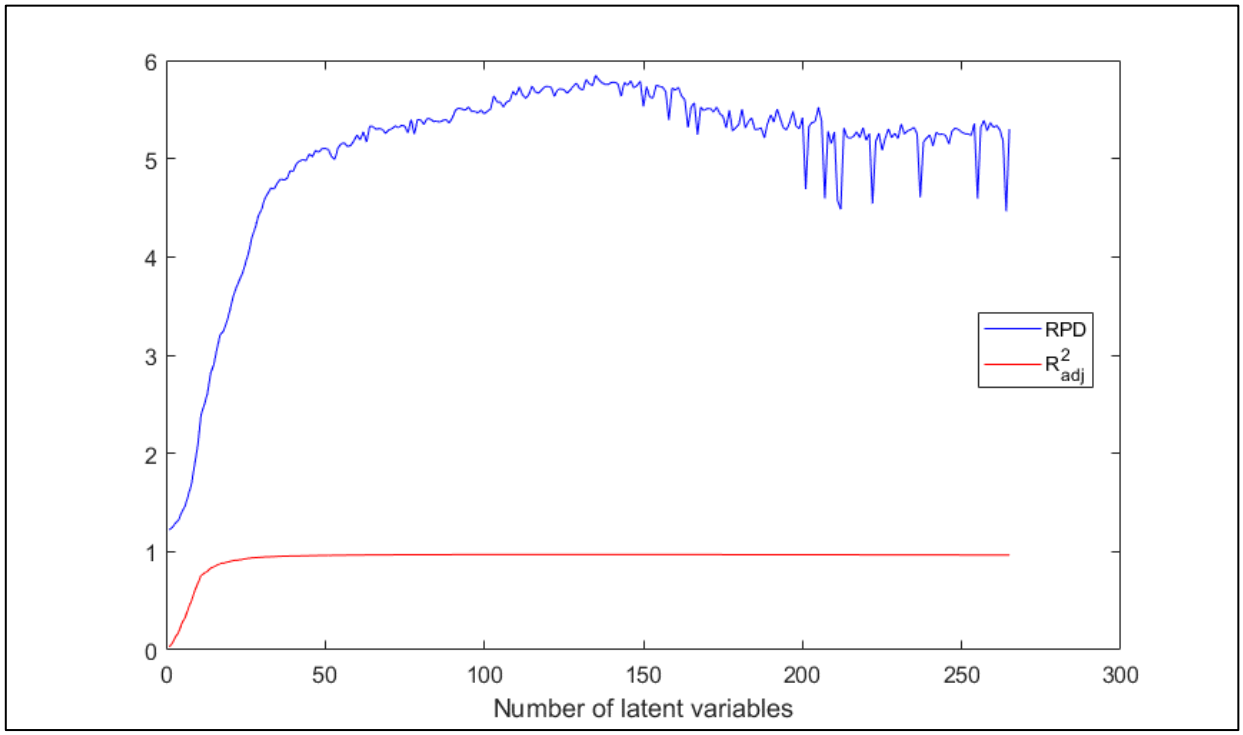

Figure 32. RPD and R^2_{adj} values of prediction of all samples in the function of number of latent variables

It is visible that the two statistics increase rapidly in the beginning, but for goodness of fit does not improve substantially, therefore the focus should rather be on the accuracy.

Estimations with 135 and 35 LV is shown in figures 33. and 34. respectively.

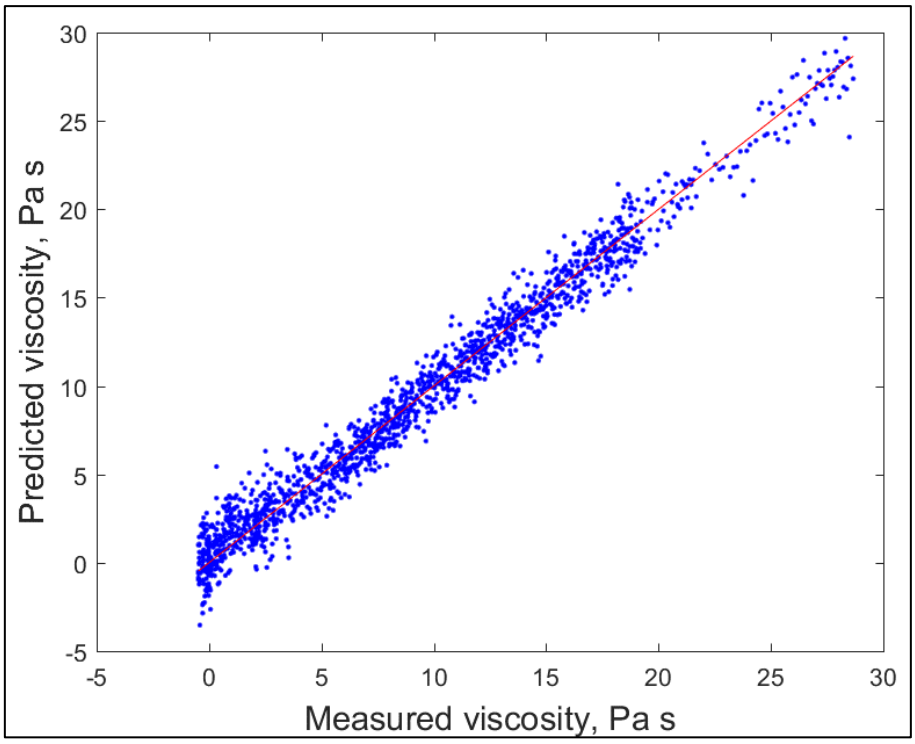

Figure 33. Model prediction with 135 latent variables

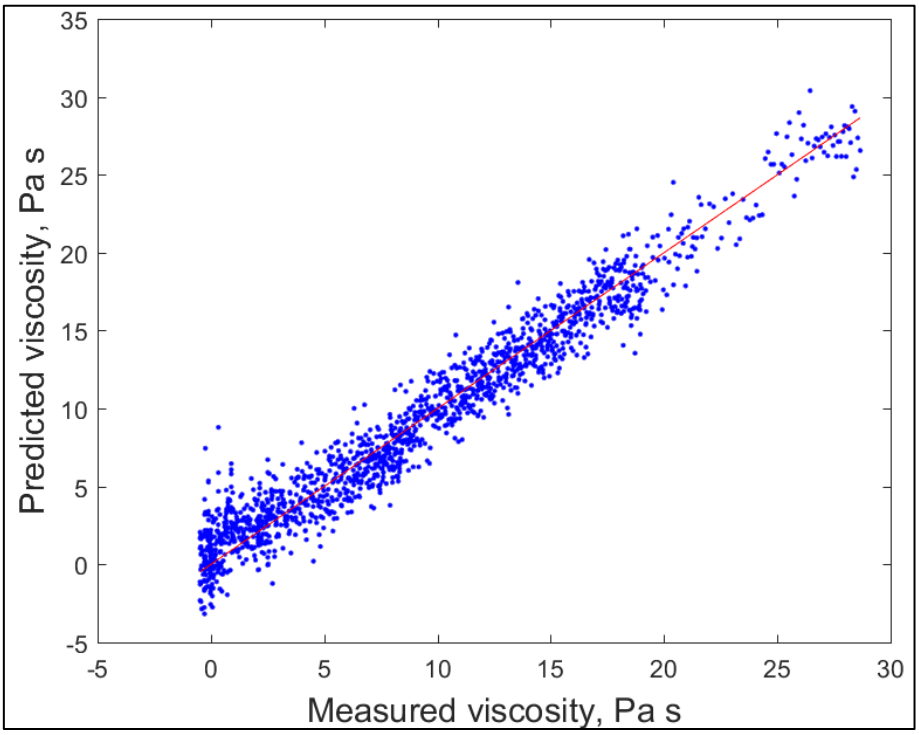

Figure 34. Model prediction with 35 latent variables

Diagrams show a similarly good fit, but slightly worse prediction performance for less LV, thus (being rigorously validated) higher numbers of LV are suggested for use in further experiments.

As a conclusion, it can be asserted that all three runs were successful in terms of prediction applicability, especially for the first and third run. It has been proven, that by choosing a limited number of the wavelet-transform coefficients of the ultrasonic response signal, calibration can be carried out for viscosity and therefore clotting stage estimation. Also, there is evidence that the proposed post-processing method is applicable in general for predictor variable extraction for multidomain measurements.

4.2. Cheese classification

4.2.1. TOF estimation I.

In figure 35. the distribution for the TOF gathered with the XC method is shown, but this resulted in two groups for both the untreated and smoked samples.

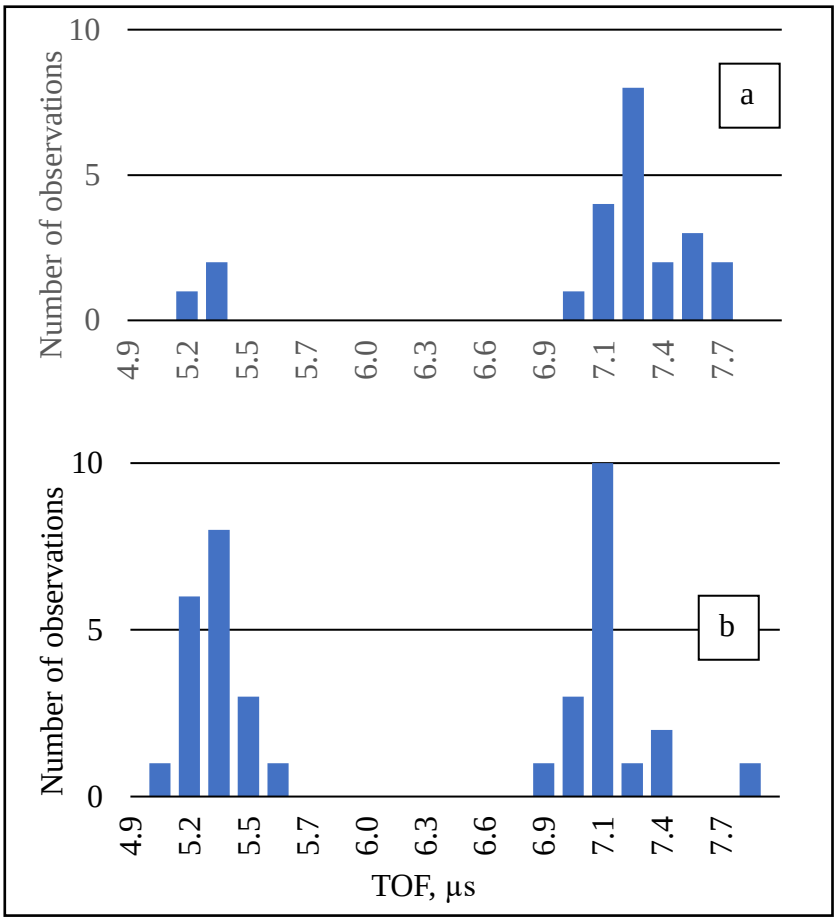

Figure 35. Distribution of Time-of-Flight values from the cross-correlation method for untreated (a) and smoked (b) samples

This is theorized to be because of the wave-like shape of the XC curve, which is similar to the original signals with different peaks showing different heights, and therefore the global maximum

is moving to some extent. This means that the method in itself is not sufficient to be used as a basis for TOF calculation, however having the change of the signal caused by disruption by the media embedded in the data, it is possible that other means can extract this information in a more consistent way. It is noteworthy that the difference between the average of the two groups is approximately the same, meaning the difference between them is the distance between the two peaks in the XC curve, but this could not be corrected for, since it is not self-explanatory that the change is systematically caused by this and other peaks would not take over the value of the TOF.

Several adjustments for the window sizes and weights were tested for the STA/LTA method, but results were inconsistent, in many cases they showed negative values. The inconsistency is probably due to the visible ridges of the two resulting curves (figure 36.), the ratio of which gives the final value of the STA/LTA metric.

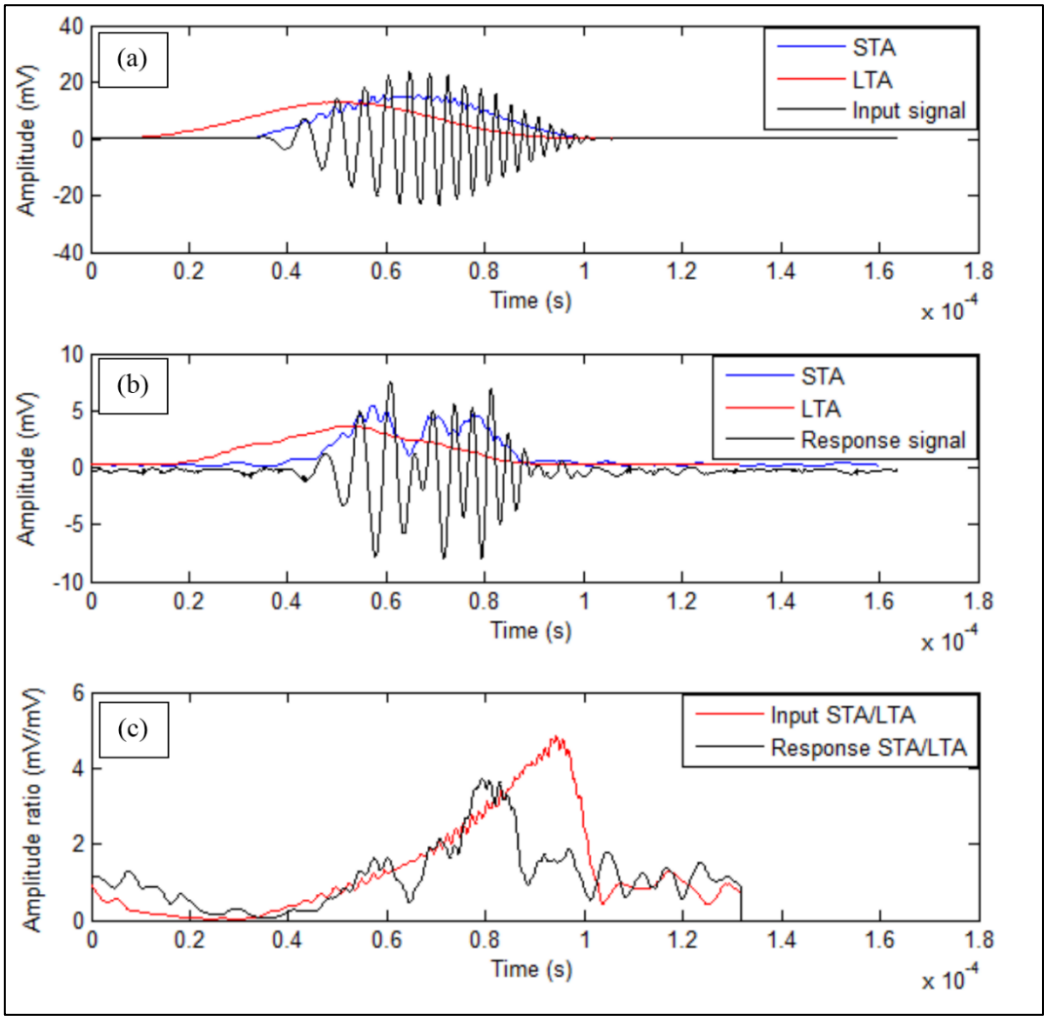

Figure 36. Original signals, their STA and LTA functions (window sizes: 50 and 400 points respectively) for the input signal (a) and the response signal (b). The final STA/LTA functions of the signals (c) (Kertesz & Felföldi, 2016)

The AIC method served the most consistent results for the estimation of TOF, as shown in figure 37.

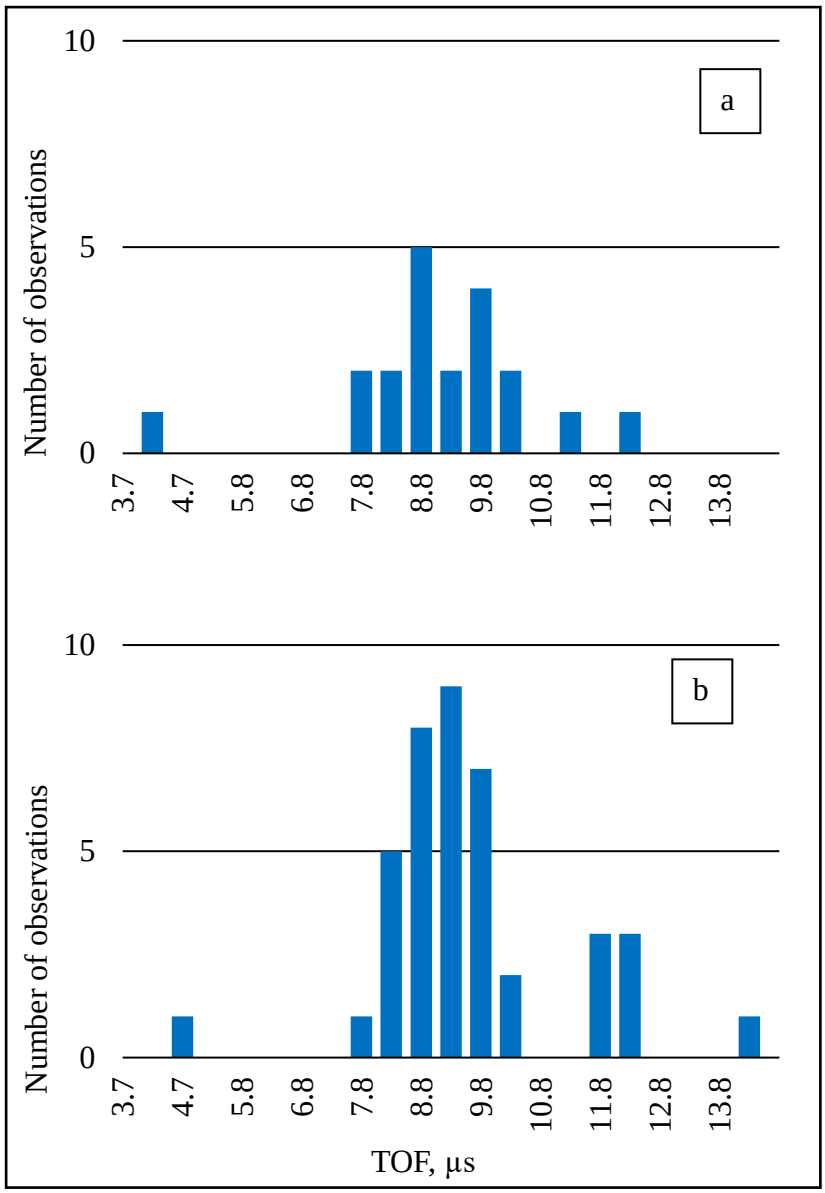

Figure 37. Distribution of Time-of-Flight values from the AR-AIC method for smoked (a) and untreated (b) samples

It is worth mentioning that there is a considerable difference in the mean of the results of the XC and AR-AIC method numerically. As it was shown, the XC method showed a more uncertain result, and at the same time, if there was a third group for the next peak in the XC curve, it would have the mean value matching that of the AR-AIC results' distribution mean. This suggests that the XC method probably misses to capture the actual arrival of the second signal.

Also, it might be of importance for further measurements to note the problem of low signal to noise ratio (SNR), as Espinoza et al. (2018) found that AR-AIC was, in general, a very robust

method, it was less reliable in the presence of noise, estimating a reliability threshold for SNR of 10 dB. They also concluded that the XC method is the most consistent, and specifically chirp-XC combination as opposed to several other signal forms in terms of low variation, and this contradicts the findings of this experiment (although they used a five times amplitude input signal on wood). The tendency of the STA/LTA method for error in presence of noise is even higher for the types of signals used in the investigation described, and the XC method needs further adjustments and post-processing to be used with chirp signals. Two of such methods are presented further as in calculation of the FFT coefficients and CWT coefficients from the XC curve, capitalizing on the wave-like shape and behavior of it.

4.2.2. Classification methods I.

The curve of the cross-correlated input and response signals capture the prominence of the different frequencies present in both signals at a certain point in time. In this sense, it is similar to a joint signal of the two without the interference. Based on this property, one can assume the difference can be revealed by the Fourier-transform of the signal and operating further with the magnitude values taken from the frequency domain. This basically means that the spectral response of the material is used, in this case for classification. All spectra had been normalized again to ensure only their relative shapes are taken into account and not the absolute values, which would defeat the purpose of testing internal patterns of the spectra. The average of the two types was calculated for both types of cheese, to see if there is an apparent trend, as shown in figure 38.

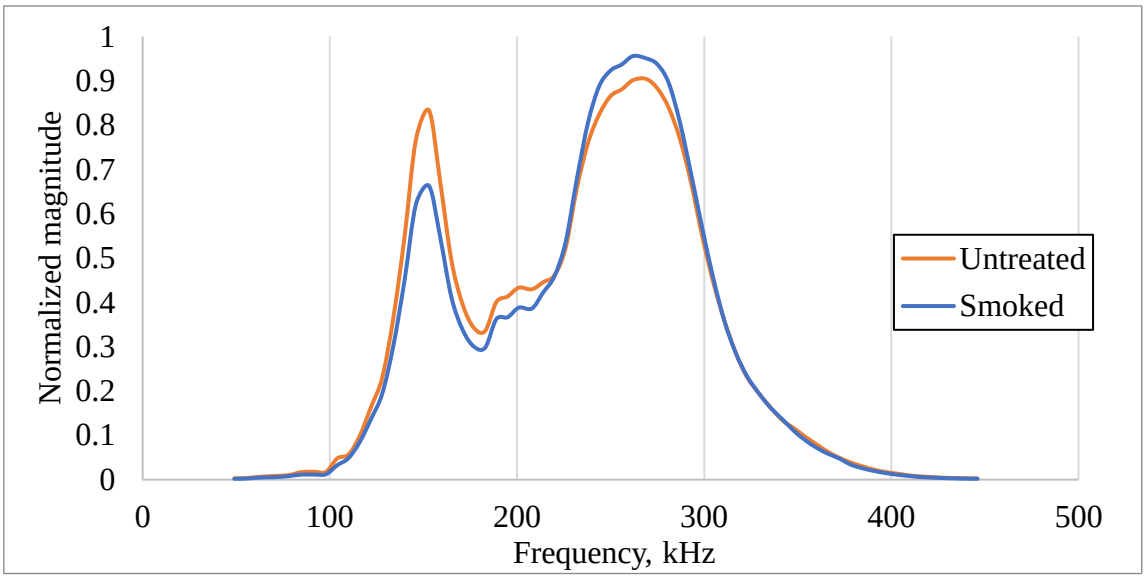

Figure 38. Average Fast Fourier Transform spectra of the two sample types

There seems to be a pronounced difference at 150 kHz and 250 kHz, but it needs to be addressed, that there are natural peaks occurring from the instruments' sensitivity, which are located at approximately 140 kHz and 250 kHz. Another issue is that the averages of the spectra do not give information on the distribution of individual measurements, calculating the standard deviations, their average is comparable to that of the measurements (0.029 and 0.033 for untreated and smoked samples respectively), for their confidence intervals for ±2σ across the spectra are shown in figure 39. and 40.

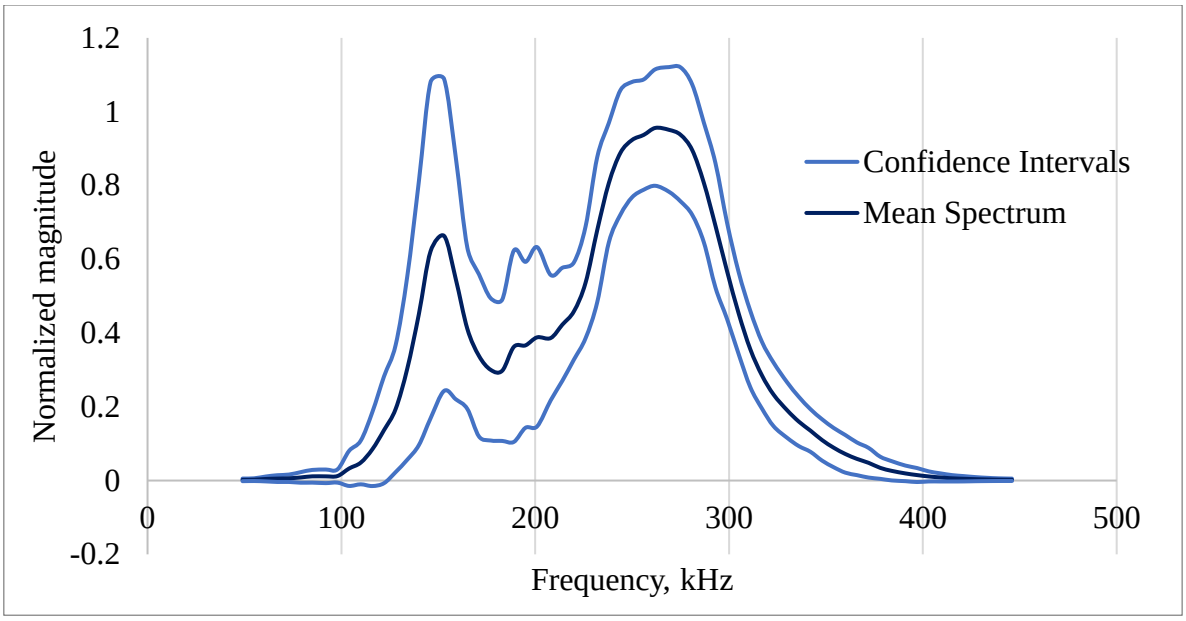

Figure 39. Average Fast Fourier Transform spectrum with ±2σ intervals for the untreated samples

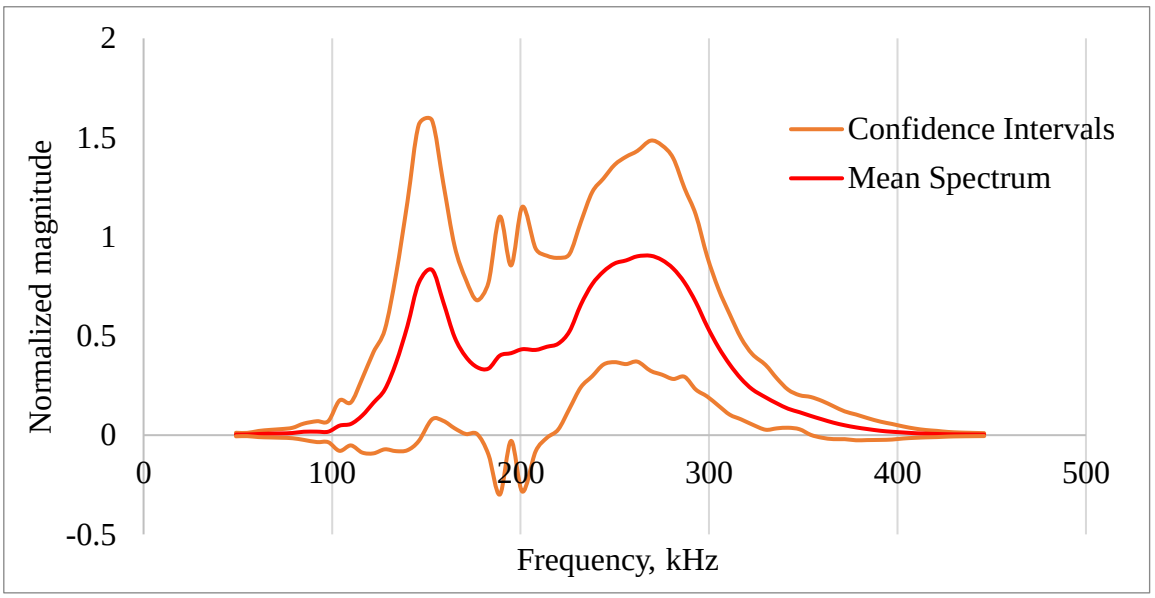

Figure 40. Average Fast Fourier Transform spectrum with ±2σ intervals for the smoked samples

The figures show a very high amount of variation in the spectra, meaning that the difference in the averaged spectra is not caused by systematic differences. In spite of this, the classification performed quite well as shown in table 6. (compared to the random 50% head-or-tale chance), and it suggests that the spectrum explains some of the variance in the observations. For the CWT coefficients, again, the chance of the resulting validated prediction of over the 50% level being caused by luck is very low, and therefore encourages further inspection.

4.2.3. Classification summary I.

The results of the LDA classification are shown only because of the reasons explained in Section 3.6.3. The essence of this classification test is to see whether the two types of samples, sharing features that affect ultrasonic through-transmission response to a great degree can be distinguished. For classification purposes, the TOF from the AR-AIC picker and sample thickness were considered as the most reliable method to extract TOF and used as a reference for comparison with classifications based on the FFT coefficients and CWT coefficients. Table 6. contains the classification matrix for the prediction by sample thickness and TOF.

Table 6. Classification matrix using sample thickness and the AR-AIC picker Time-of-Flight as variables

			Predicted Group Membership		
			untreated	smoked	Total
Original Group Membership	Count	untreated	33	7	40
		smoked	10	10	20
	%	untreated	82.5	17.5	100.0
		smoked	50.0	50.0	100.0

The total misclassification error is quite high, 29.3% (CV: 33.3%), which is reasonable, since we are trying to classify chemically almost identical samples.

On the contrary, the 66 FFT coefficients resulted in a correct classification of 96.7% (CV: 66.7%) instead of 71.7%, which is encouraging, since it only includes partial, hidden information on the delay or spread of the energy in the signal at different frequencies. The misclassification matrix is shown in table 7.

Table 7. Classification matrix using 66 FFT coefficients of the cross-correlated signals as variables

			Predicted Group Membership		
			untreated	smoked	Total
Original Group Membership	Count	untreated	40	0	40
		smoked	0	20	20
	%	untreated	100.0	0.0	100.0
		smoked	0.0	100.0	100.0

The CWT coefficients of the cross-correlated signals showed the best basis for the prediction of classes with a 100% correct classification (CV: 70.0%) as shown in table 8.

Table 8. Classification matrix using 65 wavelet coefficients of the cross-correlated signals as variables

			Predicted Group Membership		
			untreated	smoked	Total
Original Group Membership	Count	untreated	39	1	40
		smoked	1	19	20
	%	untreated	97.5	2.5	100.0
		smoked	5.0	95.0	100.0

The low number of samples contributed largely to the error levels for 10-fold CV, suggesting overfitting, and therefore a similar experiment should be carried out with a higher number of samples. Nevertheless, 70% validated accuracy is still an acceptable value in the face of the level of scrutiny the method was put under with such similar and high variance groups of samples. However, the goal of the assay was to put the algorithm to test (in an industrially not meaningful way, only to see which method performs better), and hence were not deemed satisfactory. This led to conduction of the above experiment and analysis with a refined algorithm in 2019, detailed in the next sections.

4.2.4. TOF estimation II.

The XC and the AR-AIC estimations showed the same trends as in the previous experiment: the XC method caused two groups to form, around 5.2 and 7.3 and around the value 9.2 for AR-AIC, as shown in figures 41. and 42. for easier comparison, the horizontal axes are matching in range.

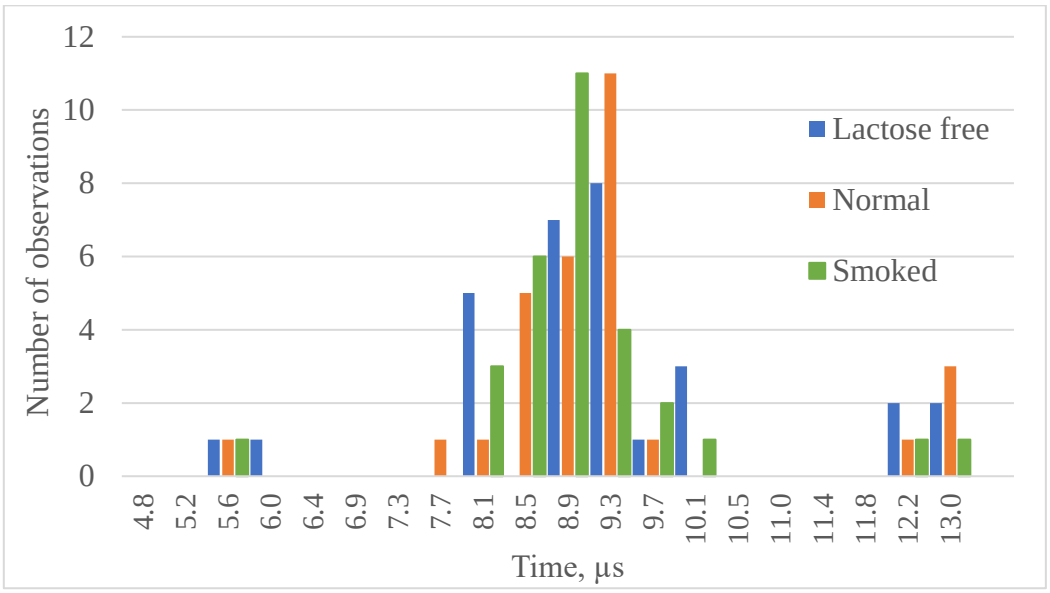

Figure 41. Distribution of Time-of-Flight values from the cross-correlation method for the three sample types

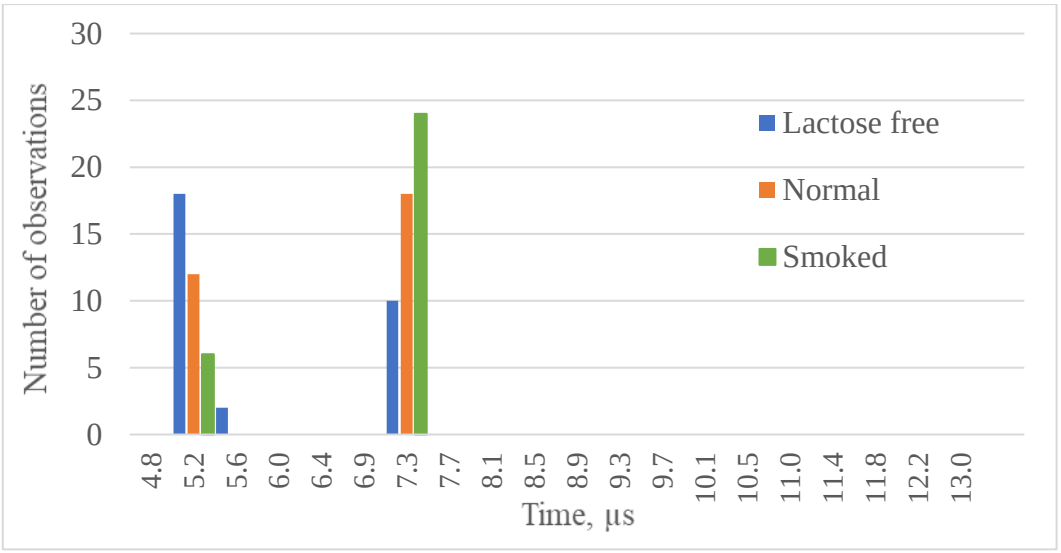

Figure 42. Distribution of Time-of-Flight values from the AR-AIC method for the three sample types

The difference in clustering of the data is clearly visible, with the XC producing two distinct groups with small variances, whereas AIC TOF values are more spread across a wider range with two

smaller groups forming on the extremes. Clustering in both cases is suspected to be caused by such the signal form and probably would be mitigated or completely absent with an impulse signal.

4.2.5. Classification methods II.

The prediction using the reciprocal of the AIC TOF and thickness resulted in 52.2% correct classification with LDA, and 47.8% with SVM, the best performing classifiers in later tests showing some degree of true explanation of variance. This (as expected by the result of the thickness comparisons) can be attributed to thickness rather than the TOF because for estimation only using the reciprocal of the TOF yielded 33.3% and 30.0% respectively for these classifiers. Therefore, from further classification runs –as in the original experiment–, thickness and TOF was omitted altogether, using only FFT coefficients and selected CWT coefficients in the respective runs.

CRW were calculated, and this time all FFT coefficients were used in the process, 2048 altogether for the original signal and 4095 coefficients for XC. The dramatic increase in the number of explanatory variables was motivated by the fact, that this time PCA was applied (to 99% variance explanation) and validation was also taken care of (limited to 5 folds CV, because a higher number would tax the number of observations used for prediction in CV significantly), and therefore there would have been no benefit of reduction of resolution voluntarily. CWT was calculated from the XC curves and this time the original response signals also, using a Morse mother wavelet, and the extraction of the relevant coefficient values was done by the procedure described in detail in 3.6.2. –this step has had a very important implication, which will be discussed later. This led to the use of 92 variables extracted from the original signal and 282 extracted from XC. An example of the original input and output signals and XC curve with their scalograms beneath them are shown in figures 43. and 44. Scalograms show a representation of the original input and response signals on a time-frequency graph. This allows us to compare the spread of the signals in time and frequency, but for the cross-correlated signal, it shows the similarity between the energy distributions of the signals in these two domains.

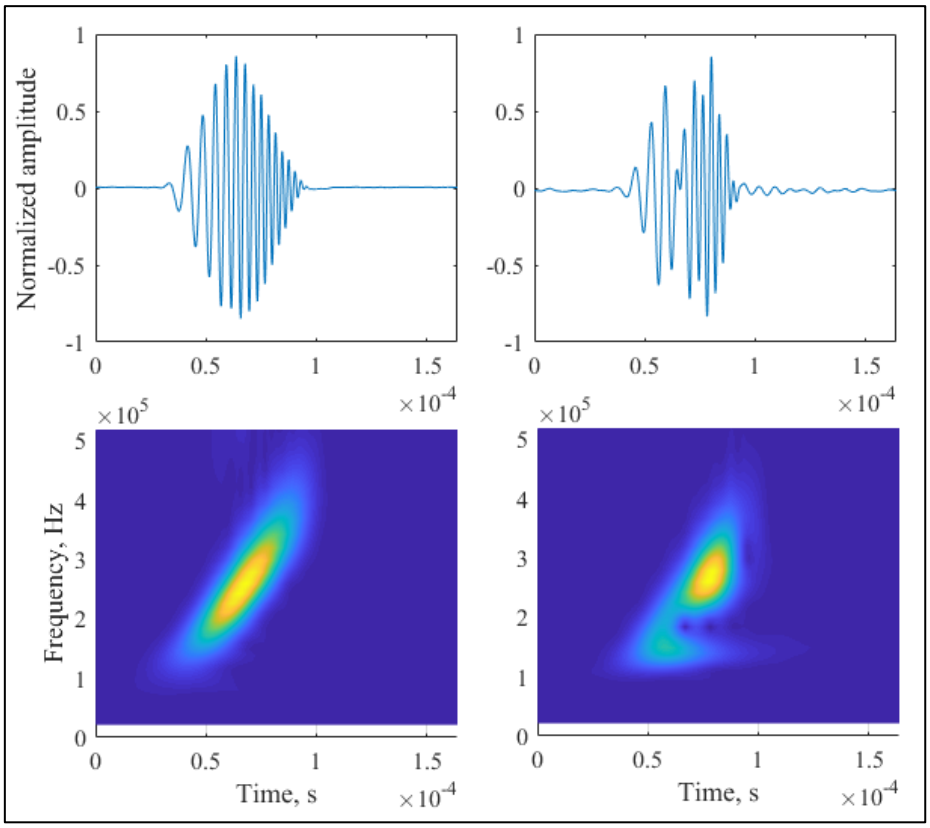

Figure 43. Time domain graphs and scalograms of the input and response signals

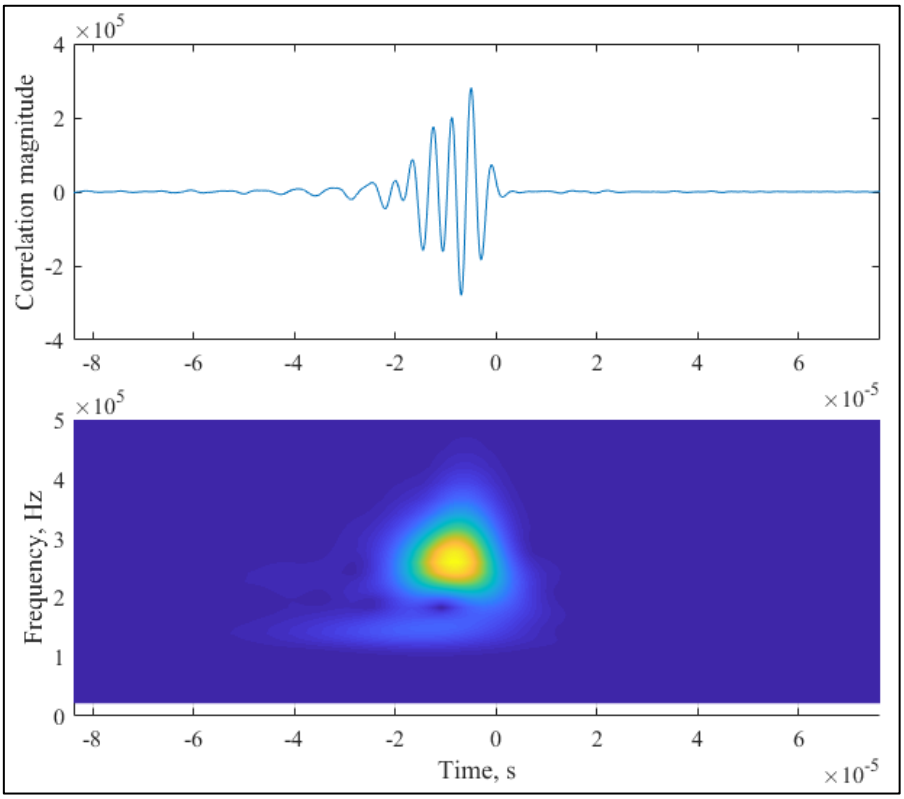

Figure 44. Time domain graph and scalograms of the of the cross-correlation curve

As it is apparent from the scalogram, XC automatically takes up the frequencies of the input and output signals, because of this, it represents not only the similarities in time, but the spectrum as well, introducing a concoction of highly useful variables for prediction.

4.2.6. Classification summary II.

The processing methods to generate explanatory variables performed quite well: for one of the classifiers, the lowest correct classification rate (in terms of predictor variable source) was 61.1% for the XC-FFT process, well above the random rate. Table 9. shows the maximum correct classification rates for the different post-processing algorithms (all validated results).

Table 9. Correct classification rates for different post-processing methods

	response-FFT	**XC-FFT**	**response-CWT**	**XC-CWT**
Tree	97.8%	55.6%	97.8%	95.6%
LDA	96.7%	54.4%	98.9%	96.7%
QDA	84.4%	52.2%	98.9%	97.8%
SVM	96.7%	61.1%	98.9%	97.8%
KNN	97.8%	56.7%	100.0%	97.8%
Ensemble	97.8%	55.6%	100.0%	97.8%

For each of them, confusion matrices of the best classifier methods are reported in tables 10. 11. 12. 13., for being concise only number of observations are shown.

Table 10. Confusion matrix for the response signal & Fast Fourier Transform method predictions by KNN classifier

		Predicted group		
True group		30	0	0
		0	29	1
		0	1	29

Table 11. Confusion matrix for the cross-correlate & Fast Fourier Transform method predictions by SVM classifier

		Predicted group		
True group		14	11	5
		8	19	3
		3	5	22

Table 12. Confusion matrix for the response signal & Continuous Wavelet Transform method predictions by KNN classifier

		Predicted group		
True group		30	0	0
		0	30	0
		0	0	30

Table 13. Confusion matrix for the cross-correlate Continuous Wavelet Transform method predictions by SVM classifier

		Predicted group		
True group		29	1	0
		0	30	0
		0	1	29

As it is clearly shown, this experiment has yielded far better results, although in trends, it shows similarities. The use of more estimators and processing them before classification helped to achieve higher correct classification rates. The use of the CWT extraction method helped with both the response and XC curves in lowering error rates, for the response-FFT by 2.2% (to 100.0%!) and for XC-FFT 36.7%, which is approximately the random chance rate. An important takeaway from this experiment is that although the XC-FFT performed badly compared to only the response used for FFT coefficients, suggesting the delay incorporated in the signal does not affect the outcome, the CWT-based algorithm decreased the disparity in performance, which is the main goal of the study: to extract as much valuable information from multidomain data as possible.

Concluding the experiment, the cross-correlation of the input and response signals and the AIC method for TOF estimation both produced unwanted multiple peaks, but the AIC estimation showed one major culmination of values and was deemed more credible in the present analysis.

The classification by type of cheese resulted in the best validated prediction (100%) with the use of selected coefficients from the original response signals' wavelet-transform and either by using KNN or ensemble classifiers. The Fourier-coefficients of the same response signals used as explanatory variables showed slightly less reliable predictions. The cross-correlate process with either FFT or CWT algorithms produced worse predictions than those calculated from the response

signals. On the other hand, the procedure proposed, based on the selection of the most meaningful wavelet-transform coefficients for predictor variables, increased the prediction accuracy dramatically. The empirical evidence shows that the XC curve is able to describe much of the variance and this is theorized (but not proven) to be due to retaining information on either composition as within-signal patterns and/or lag times at different frequencies.

4.3. Eggshell crack detection

In all cases, the spectrum was first processed with PCA to ensure the independence of the variables, which is a pivotal assumption for some of the classifiers tested. Principal components were calculated of up 99% of described variance in the original data (*i.e.* the spectrum magnitudes). This reduced the number of variables substantially, with an overall bigger effect for multiplier value (from 2^1 to 2^3), with an average of 3.7-fold reduction, compared to a reduction depending on window (from 2^{12} to 2^{14}), the average variable reduction for which was 2.9, suggesting the higher resolution due to multiplication has a smaller effect compared to resolution increase due to window size. Variable reduction factors are shown in table 14. (including EW position to show effect).

Table 14. Reduction factor in number of variables by Principal Component Analysis

Position		**Upright (NS) position**			**Laid down (EW) position**		
Multiplier		**2^1**	**2^2**	**2^3**	**2^1**	**2^2**	**2^3**
Window size	**2^{12}**	15.1	28.4	56.8	12.2	23.3	44.4
	2^{13}	20.5	51.3	97.1	27.0	39.4	75.8
	2^{14}	46.5	85.5	163.9	35.3	66.2	128.2

For classification, a range of techniques were tested including linear and nonlinear prediction methods as well: KNN, SVM, Decision trees, Ensemble methods, LDA and QDA. Among metrics for performance were the total number of misclassifications, number of false positives for cracked eggs (as the most important aspect in the industry) and speed of classification for new independent samples, which obviously depends greatly on the computer used for estimation but is a good basis for comparison between different methods.

All classification techniques were tested on spectra gained with window sizes of 2^{12}, 2^{13}, 2^{14} and multipliers of 2^1, 2^2, 2^3 giving nine results per performance indicator per classifier per position (a total of 270), but the result for the NS positions were subpar, therefore they were omitted from further analysis. In all cases, K-fold cross-validation with 25 folds was applied to avoid underestimation of falsely classified samples.

First, a general prediction was done with all the settings to get an overall picture of which methods should be taken into consideration for later calculations. Results for the three performance indicators are shown in tables 15., 16. and 17. (no decimal precision was provided by the built-in application of Matlab for false positives).

Table 15. Group prediction accuracy (%) of different classification methods. Intensity of the color corresponds to better prediction accuracy

	Multiplier	2^1	2^2	2^3	2^1	2^2	2^3	2^1	2^2	2^3
	Window size		2^{12}			2^{13}			2^{14}	
Classifier	LDA	94.8	94.2	94.5	94.0	94.6	94.6	94.6	95.0	94.7
	QDA	95.5	95.0	94.3	96.3	95.6	95.6	97.2	96.2	97.0
	SVM	95.2	95.9	95.2	95.9	95.3	95.6	96.3	96.3	96.0
	KNN	93.2	92.8	93.3	94.7	94.2	94.9	94.9	94.9	94.7
	Ensemble	94.5	92.5	94.5	94.6	94.6	94.5	94.5	95.0	94.7

Table 16. False positives for crack presence (%) of different classification methods. Intensity of the color corresponds to better prediction accuracy

	Multiplier	2^1	2^2	2^3	2^1	2^2	2^3	2^1	2^2	2^3
	Window size		2^{12}			2^{13}			2^{14}	
Classifier	LDA	6	6	6	6	6	6	6	5	6
	QDA	3	3	3	3	3	3	2	3	2
	SVM	5	4	5	3	5	4	3	3	3
	KNN	6	6	6	5	5	4	4	5	5
	Ensemble	4	5	6	5	6	6	6	5	6

Table 17. Speed of classification (s^{-1}) of different classification methods. Intensity of the color corresponds to higher classification speed

	Multiplier	**2^1**	**2^2**	**2^3**	**2^1**	**2^2**	**2^3**	**2^1**	**2^2**	**2^3**
	Window size		**2^{12}**			**2^{13}**			**2^{14}**	
Classifier	LDA	610	450	130	430	250	220	170	160	91
	QDA	610	500	270	410	210	230	210	100	92
	SVM	780	270	140	480	220	270	260	150	95
	KNN	750	380	140	470	270	260	260	100	91
	Ensemble	460	490	180	300	200	220	120	88	63

It is clear that window size contributed to the classification performance, but the multiplier value did not. On the other hand, -although this still cannot be confirmed undoubtedly,- it is suggested that a multiplier be used upon further calculations for the effect it might have as described earlier, which balances out the small burden it puts on estimation speed (which is still very high). Speed of classification shows very high values, but they decline rapidly with multiplier and window size as well. This indicator, although being important on an industrial scale, can be boosted easily by using the right hardware and firmware, and therefore was evaluated as less relevant than the other two.

The tested classification methods were compared by SRD in terms of being fair. The protocol in Héberger and Kollár-Hunek (2011) was followed. Different model settings and output parameters were assigned to rows and the classification methods to columns: tables 15-17 were transposed and concatenated. Ranks were assigned to each of the 9 model setup results for all parameters, and then the differences between the methods' rankings and the average of all methods were calculated. Following the calculations in the article, the sum of ranking differences for each method were divided by the maximum total ranking error, resulting in values between 0-100%, called the normal sum of ranking differences or SRD_{nor}. The results are shown in table 18.

Table 18. Normal sum of ranking differences for all output parameters of the classification methods

LDA	QDA	SVM	KNN	Ensemble
6.51	4.44	4.73	4.29	4.73

All classifiers resulted in a relatively low total ranking error, and the difference between the two best-performing methods, KNN and QDA, is only 0.15. It is important to mention that the SRD metric is not testing for prediction performance, but fairness, if a choice has to be made. Also, understanding of the original data is necessary for a final decision, and the method does not take importance of the different performance indicators into account; for instance, in some applications, classification speed might be a more important measure than the total classification error..

Summing up the conclusions from the results presented in the tables, QDA and SVM classifiers showed the best performance, values of indicators were not consistent or poor for LDA, KNN and Ensemble methods. The performance difference between QDA and SVM becomes evident when the false positive rates are interpreted correctly: SVM misses the detection of a crack approximately one and a half times more often than QDA. In other words, for two faulty eggs missed by QDA there is a third missed by SVM. This makes it clear, that further only the QDA classifier should be used.

Despite the obvious prevalence of QDA over LDA, it is important to evaluate whether QDA should be applied in the first place instead of the latter one. The difference between LDA and QDA is that for QDA the covariance matrices of variables between groups of observations are different, whereas for LDA they are equal. Inequality is a completely legitimate assumption, so much the more the difference between the spectra of the intact and cracked eggs should be captured in the principal components from the PCA. This can be easily verified by plotting the diagonal (containing the column variances) of the covariance matrix corresponding to the coefficients of the components with the highest variance explanation power (component number one) against the original variables for the two groups: different covariance matrices manifests in different loading (coefficient) patterns as shown in figure 45. (for NS position only).

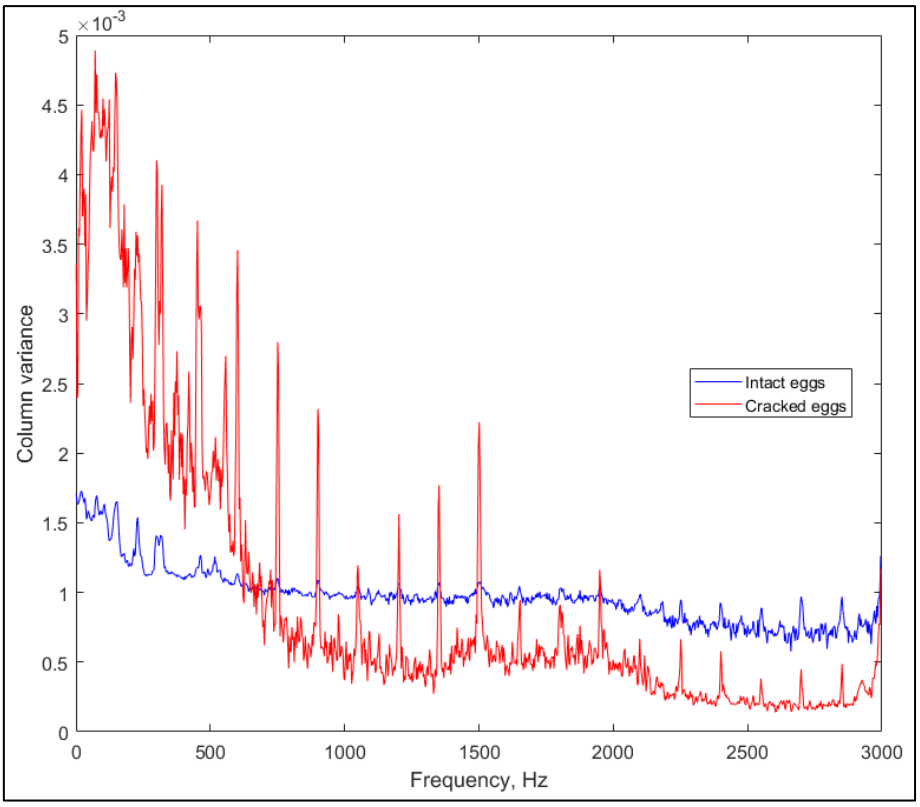

Figure 45. Column variances of the Principal Component Analysis coefficients for the two groups of samples

Also, disparities in covariances of the original variables (*i.e.* the spectra) might give us insights about which frequencies might describe other frequencies well, revealing important regions for differences of the sounds. The main differences in curve shape (not height!) can be found in the interval between 500 and 2000 Hz as seen in figure 46.

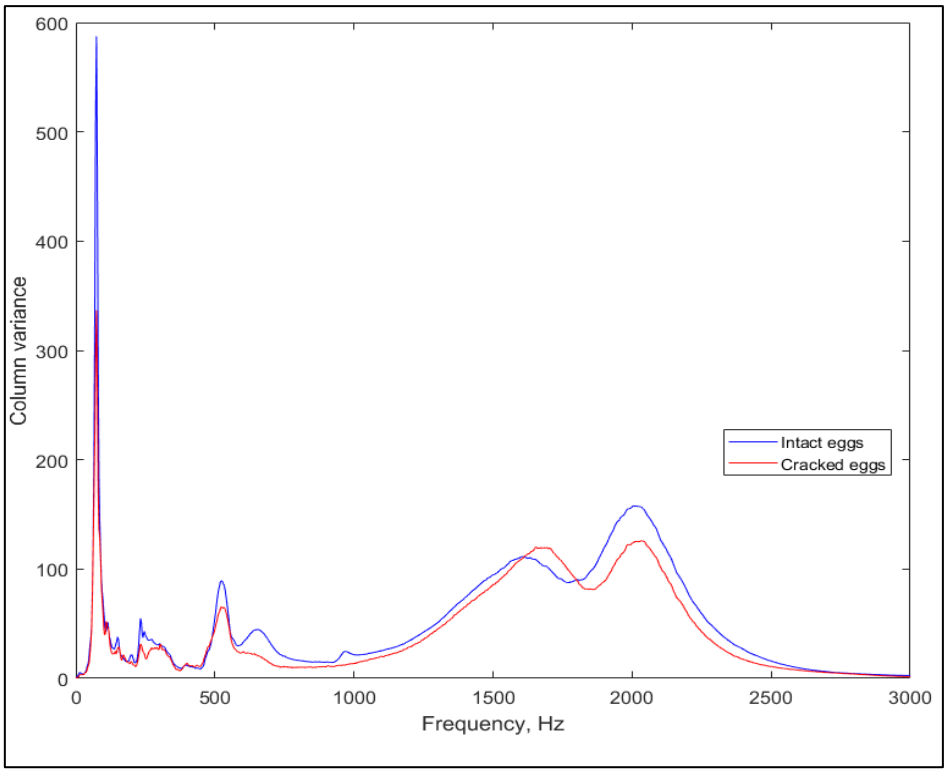

Figure 46. Column variances of the Fast Fourier Transform coefficients for the two groups of samples

After verification of the applicability of QDA, the method should be rigorously tested while pushing the limits of the prediction performance, using the two most important indicators: total classification error and false positive detections of faulty eggs. Shadow of doubt should not be cast on the credibility of the evaluation, therefore a very high fold number for cross-validation was used, 20 to be precise.

The number of LV was calculated by minimizing the total classification error, which corresponded with the false positive error rate. This in the end resulted in 2.1% prediction error for the total number of misclassifications and 0.87% for false positives with 40 LV, which accounted for 99.6% explained variance, as shown in table 18.

Table 18. Classification matrix of the Quadratic Discriminant Analysis algorithm with 40 latent variables.

		true	
		intact	cracked
predicted	intact	566	6
	cracked	9	112

5. Conclusions, recommendations

The developed wavelet-based variable reduction algorithm is now proven to be effective, and not only by a scrutinous classification test, but for estimation of physical change over time of a completely different material. It also raises the question of what domains are explorable with such a method. An interesting test in the future could be to see whether the process works in spatial domains as well as in hypercube images, searching for inhomogeneities and their representative variables in three-dimensional data. Or even ultrasonic imaging, which can provide a 4-D dataset (*i.e.* a tesseract with two spatial, one temporal and one spectral domain). These are questions and possibilities for further testing, and yet to be explored.

It needs to be addressed though, that the algorithm is only a post-processing method for variable extraction, and not an entire model development solution: understanding of the original data and experiment is essential to effectively apply the method. At the same time, the main reason behind the development of the algorithm was to find a way to avoid using other dimension reduction algorithm, which compare variables against each other, because in case of many thousands of variables –as it is the case with the use of continuous wavelet decomposition and spectrogram data as predictors–, it is very difficult if not infeasible to calculate latent variables. If the number of variables do not necessitate the use of this method, there are many other statistical techniques already in use, which can offer less reduction in information content and therefore should be preferred in assays.

Also, an interesting aspect of the proposed method is to inspect how certain corrections would affect the outcome of investigations. The least amount of corrections was applied in the presented experiments in order to prove the robustness of the algorithm itself, but in real applications, accuracy of a highly adapted method is more important than general applicability, and hence corrections are desired. This includes correction with the spectral sensitivity envelope of the instruments, the inclusion of temperature effect on the dynamics of clotting, testing model materials, attenuation correction through the investigated spectrum and zero distance deviation of the TOF.

This suggests that the models developed in this doctoral thesis are not directly transferable, only the principles of model building should be considered as guidance for further experiments. The experimental setup for estimation of the viscosity through enzymatic clotting of milk provides a valuable tool for the industry to follow the state of fermentation with a method that is objective as opposed to the traditional “finger test”. The setup includes a submerged through-transmission

mode pulser-receiver couple, but it might be interesting to test whether a pitch-catch mode setup might be suitable, as the change in viscosity probably affects the waves traveling on the surface of the curdling liquid, and changes in the matrix might affect the signals significantly. Also, pitch-catch mode can be used in a non-contact setup, which is preferred over contact and immersion setups.

The method, as described in Kertész et al., 2021a, is generally suitable for the non-destructive, predictive determination of viscosity and therefore the state of the curdling process in enzymatic milk clotting during coagulation. The proposed novel ultrasonic method is suitable, applicable, and recommended for industrial use in different fields of the food industry with adaptation to the technology at hand.

The end of milk clotting can be determined by matching the specific limit values to the appropriate curd quality that is considered completed. The continuous monitoring of the milk clotting process can lead to technology optimization in small-scale (craft products) and large-scale production as well. Digital data collection and adaptive process control based on the method presented in this thesis leads to quality improvement of the products, capacity and yield increase, loss reduction, and more environmentally friendly production technology in the long term. The principles in the study can also be applied for studies in acidic coagulation in milk. In theory the use of the method can be extended for different products such as yoghurt, sour cream, puddings, *etc.*, to monitor texture properties in phase changing processes.

Egg crack detection resulted in a very high validated accuracy based only on the FFT spectrum magnitude values used as predictor variables. This suggests that it is not only the resonance frequency shift, used in earlier studies that can be reliably used for prediction of faults, but the spectrum magnitudes themselves capture the important variations caused by physical changes in the shell.

In a recently published article, together with my colleagues we have given two recommended setups for industrial application. We have also addressed the possible difficulties that may arise (Kertész et al., 2021b).

In an industrial setting, the most problematic aspects are external sources of noise and automation of a steady excitation process. The problem of noises can be addressed by using a tunnel with quasi-soundproof insulation. This can lower the medium- and high-pitch external noises considerably, and, at the same time, low-frequency vibrations of machines are not of concern, as they appear outside the bandwidth of interest, 500–30,000 Hz. The other important tool for proper

signal extraction is the microphone. The use of a high-sensitivity lobar polar pattern condenser microphone is suggested, as the sensitivity pattern is ideal for focused, unidirectional sound capture, further decreasing the effects of ambient noise. Such microphones are relatively cheap (in the range of a few hundred euros), especially when compared to high-quality industrial cameras used for automated candling. This allows for speeding up of the grading process using multiple grading lines, as the costs of extension are much lower than those of candling. As a side note, the calculation time for individual sample classification is extremely low, does not require high computation power and is completely automatic. This keeps the costs low, and the process will not increase the grading time.

The other condition for a successful automation of the method is either conversion of the steady excitation protocol to a continuously applicable one, or the adaptation of the grading line by adding a stage for the egg coming to a rest. For the latter, as the procedure of excitation and recording requires less than one tenth of a second, they do not create a bottleneck, and a very short stoppage is sufficient. Furthermore, the laid down position favors the automation, since this is the natural rolling and resting position for eggs, and, therefore, no manipulation of the alignment is required. This results in a seemingly continuous procedure, as the whole grading process can be completed in less than one second, which is the lower end of the industry standard. The other option, excitation of rolling samples, can be carried out by stationary obstacles acting as exciters, which allows a completely continuous process. In this case, the time between the successive samples needs to be adjusted to maintain separation of the signals and synchronization of recording, but it opens up the possibility of even faster grading. The supporting pad used in the experiment was made of a relatively stiff polyurethane foam and had an impermeable surface layer; therefore, it is applicable in industrial equipment with the possibility of cleaning and, if necessary, easy replacement. The main purpose of the foam is to minimize the conduction of ambient vibrations, and, therefore, other, nonrigid materials may be suitable for supporting the samples during the excitation if necessary.

An interesting source of theoretical debate is the nature of the cross-correlate of input and response signals as a source of prediction. In the present thesis, the observed effect of wavelet decomposition and Fourier transformation on the XC curve suggests that it can be interpreted as a composite signal carrying characteristics of both waves it originates from, although evidence of this is purely empirical and needs to be verified. The notion of reckoning it as a signal affects what kind of processing algorithms might be suitable and useful for analysis conducted with it.

6. Summary

The trend in present day's strive for high and consistent quality in food production lead to a growing interest in NDT technologies, because they can provide information on the products in a way that does not affect the value, and by testing every manufactured item, requires no sampling, mitigating an important source of bias. The increase in the applications of ultrasonic testing benefited greatly from the research of decades in the medical field, proving the principle to be a very useful tool in estimation of quality attributes of tissues and various matrices, which can be transferred to food product testing. Research in the field mainly focuses on widening the range of application in terms of product types, or refinement of already existing techniques. On the other hand, acoustic testing has a longer history, and has been successfully applied for different fruits and vegetables, and eggs as well. Although in most studies, the method is used for investigation of the resonant frequencies to estimate stiffness, hardness and other textural properties, in experiments focusing on eggs, the most prominent quality parameter to test is cracks of the shell.

Both the acoustic and ultrasonic testing are dealing with sound waves, characteristic to the investigated sample, and therefore can be analyzed with similar methods and principles of signal processing.

In my thesis I have conducted measurements for estimation of viscosity of enzymic curdling of cheese, which is an important attribute for determination of the state of the fermentation process. A piezoelectric transducer-receiver couple with 250 kHz nominal frequency was used in through-transmission mode, submerged in milk fortified with $CaCl_2$. The signal form for testing was a chirp signal, sweeping through the 50-450 kHz range linearly, and enveloped by a Hanning filter, and the input and response signals were recorded with an oscilloscope. After addition of calf stomach rennet enzyme, a small amount of the sample was transferred to a rotational viscometer, and the viscosity was measured over 120 minutes, sampled every 10 seconds at 2 s^{-1} shear rate. The resulting rheogram had several peaks due to the formation of micelle clusters, and therefore a suitable curve fitting protocol was designed with a high level of validated fitting reached with average $R^2 = 0.9618$ (min.: 0.7521, max.: 0.9985). The resulting viscosity estimates were used as dependent variables of a prediction based on PLS regression and a post-processing method developed for analysis of the gathered data, yielding high validated goodness-of-fit (R^2 ranging from 0.9632 to 0.9983) and accuracy (RPD ranging from 4.38 to 14.22).

The algorithm developed consisted of wavelet analysis of the response signals with a Morse wavelet, and systemic extraction of certain coefficients; the standard deviation, as a metric of

variance was calculated for all wavelet coefficients, to ensure a feasible computation time instead of calculation of all of their covariances. Afterwards, peaks in the resulting matrix were searched for, indicating the locations of the highest variance among the time and frequency dependent wavelet coefficients of all signals, and therefore the signals themselves. The coefficient values of the extracted peaks were collected for all signals, and used for estimation, yielding 7-32 variables for individual viscosity estimations, and 298 variables for estimation of all samples at once, the latter resulting in a validated, well-fitted and high accuracy model (R^2 = 0.9708, RPD = 5.85).

A second experiment was conducted, based on an earlier investigation to verify the applicability of the algorithm in a scrutinous setup. 30 slices of three different types of mozzarella cheese (n=90) were measured, smoked, normal and lactose-free; the first two of the groups had the same composition. The TOF parameter from the same ultrasonic setup (250kHz nominal frequency, 50-450 kHz chirp signal), was calculated with cross-correlation (XC) and autoregressive Akaike information criterion picker (AIC) algorithms, and the results of these were evaluated, finding that the XC method yielded smaller variances, but two distinct points where TOF values culminated, whereas AIC gave much bigger variances, but more aligned TOF figures around a single time point. The earlier mentioned algorithm was tested through classification testing with various classifiers. The KNN classifier reached a 100% validated prediction of the samples, with the spectrum of the response signal. Also, high accuracies were reached by processing the response signal with the proposed wavelet coefficient extraction algorithm (97.8%) and by using the FFT coefficients of the cross-correlated signals (97.8%).

An experiment was conducted for eggshell crack detection with 150 samples, altogether which gave 705 measurements altogether. The samples were measured intact and after inducing a hairline crack on the pointy tip in an upright and laid down position on a foam pad equipped with a high sensitivity microphone. Excitation was carried out with a hollow metal rod, and the response signal was recorded with a PC connected to the microphone’s signal analyzer. The spectra of the responses were considered between 0 and 3000 Hz, and different adjustments were applied to increase spectral resolution. The effect of these adjustments, padding the signal with zeros to multiply signal length for more precise FFT calculation and increase of FFT window size were evaluated in the face of the prediction accuracy for fault detection. A total validated classification error rate of 2.1% and a 0.87% false negative were achieved with quadratic discriminant analysis.

7. New scientific results

1. I have developed a novel post-processing method for variable reduction of multidomain signals, and the algorithm has been tested on two distinct, independent materials for estimation and classification purposes.

   The process is based on continuous wavelet transformation of sound signals from time domain to a set of joint time and spectrum domain matrices, using Morse wavelet. These matrices consisting of wavelet coefficients are analyzed across observations for the highest peaks in standard deviation, which thereby represent the coefficients carrying the highest amount of information on the differences between samples. The identified coefficients are extracted from each observation, significantly reducing the number of variables used for further analysis, which would be infeasible with the original matrices due to the vast number of coefficients.

   The proposed post-processing method, in theory, can be applied to other multidomain data, where domains contain continuously changing variables, and therefore peaks can effectively represent nearby data points, such as in spatial or spectral data.

   Kertész, I., Nagy, D., Baranyai, L., Pásztor-Huszár, K., Varsányi, K., Nguyen, L. P. L., Felföldi, J. (2021a): Development of a novel ultrasonic spectroscopy method for estimation of viscosity change during milk clotting. *Molecules.* (accepted for publication)

2. An ultrasonic measurement setup was developed for the determination of viscosity of milk during enzymatic curdling, and therefore the state of the curdling process. The setup consists of an immersed through-transmission mode piezoelectric transducer-receiver couple with 250 kHz nominal frequency and an oscilloscope with $4 \cdot 10^{-8}$ second resolution. The signal form is a linear chirp with a frequency sweep across 50-450 kHz and enveloped with a Hanning filter. A new calibration process was developed for ultrasonic viscosity measurement during clotting of milk. The procedure includes estimation of the viscosity values during enzymatic curdling of cheese by an inverse negative exponential curve (R^2: 0.7251 – 0.9985), and estimation of the modeled values by the proposed algorithm. The ultrasonic signals were normalized, de-noised and put through wavelet-decomposition, relevant peaks in the standard deviation matrix of the wavelet coefficients representing high amount of the information in the signal are extracted from the wavelet transforms of each measurement and used for prediction of viscosity by partial least squares regression. The calibration process yielded high adjusted

coefficient of determination values (0.9632-0.9983) and residual prediction deviation (4.38-14.22), signifying that the process is capable of high accuracy estimation.

A new process was developed for calibration of indirect ultrasonic measurement of viscosity of milk during enzymatic curdling with fat contents between 1.5-3.5%. The calibration was carried out for responses of measurements with a 50-450 kHz linear ultrasonic chirp signal, using a 250kHz immersion through-transmission mode piezoelectric transducer-receiver couple. Analysis of the normalized and denoised signals was done according to the post-processing algorithm proposed and resulted in high prediction ability for viscosity in terms of precision (R^2 = 0.9708) and accuracy (RPD = 5.85).

Kertész, I., Nagy, D., Baranyai, L., Pásztor-Huszár, K., Varsányi, K., Nguyen, L. P. L., Felföldi, J. (2021a): Development of a novel ultrasonic spectroscopy method for estimation of viscosity change during milk clotting. *Molecules.* (accepted for publication)

3. A new setup and acoustic method for eggshell crack detection were developed. The setup consists of a soft foam pad with a built-in high-sensitivity microphone, and a hollow metal rod for a single-hit excitation on a horizontally aligned egg in the equatorial line, in 0° direction from the microphone. The sound of the acoustic response is recorded at 96000 Hz sampling frequency.

   Faulty eggs with hairline cracks were identified by quadratic discriminant analysis at 2.1% total error rate and a 0.87% false negative rate at 40-fold cross-validation. The predictor variables for the discriminant analysis were Fourier coefficients of the acoustic response of eggs to a single hit excitation in a laid down position. The coefficients were obtained using increased precision by padding the sound signals with zeros for double-length and using a window size of 2^{14} points.

   Kertész, I., Zsom-Muha, V., András, R., Horváth, F., Németh, C., Felföldi, J. (2021b): Development of a Novel Acoustic Spectroscopy Method for Detection of Eggshell Cracks. *Molecules,* 26(15), 4693; https://doi.org/10.3390/molecules26154693

4. The proposed new variable reduction method was shown to be applicable with great success for classification in a multiclass classification problem. The applicability was demonstrated on three different types of sliced cheese samples (normal, smoked, lactose free), using only the sound signals of ultrasonic measurements with a chirp signal in through-transmission

configuration. Two of the three groups were identical in composition, all three tested different for thickness and were different in treatment. With 5-fold cross-correlation, the proposed post-processing method applied to the ultrasonic response signals yielded a 100% correct classification using a K-nearest neighbor classifier, compared to 97.8% based on the Fourier coefficients of the signals, providing evidence that the method increases prediction accuracy. Also, the algorithm dramatically increased classification accuracy compared to the predictions based on Fourier coefficients, when the cross-correlate of the input and response signals were processed instead of only the response signals.

Annex I. – References

1. Abbott, J. A., Bachman, G. S., Childers, R. F., Fitzgerald, J. V. & Matusik, F. J. (1968): Sonic techniques for Measuring Texture of Fruits and Vegetables. *Food Technology* 22, p. 101-112.
2. Allen, R. (1982): Automatic phase pickers: Their present use and future prospects. *Bulletin of the Seismological Society of America*, 72. p. 225-242.
3. Amirmazlaghani, M. & Amindavar, H. (2012): Wavelet domain Bayesian processor for speckle removal in medical ultrasound images, *IET Image Processing*, 6. (5) p. 580–588.
4. Aparicio, C., Otero, L., Guignon, B., Molina-Garcia, A. D. & Sanz,P. D. (2008): Ice content and temperature determination from ultrasonic measurements in partially frozen foods. *Journal of Food Engineering*, 88, p. 272-279.
5. Arivazhagan, S., Shebiah, R. N., Sudharsan, H., Kannan, R. R. & Ramesh, R. 2013. External and internal defect detection of egg using machine vision. *Journal of Emerging Trends in Computing and Information Sciences*, 4. (3) p. 257–262.
6. Attar, M. Z. & Fathi, M. M. (2014): Non-Destructive Acoustic Resonance Method for Evaluating Eggshell Strength and Thickness, *International Journal of Biophysics*, 4 (1), p. 9-15.
7. Bain, M. M., Dunn, I. C., Wilson, P. W., Joseph, N., De Ketelaere, B., De Baerdemaeker, J. & Waddington, D. (2006): Probability of an egg cracking during packing can be predicted using a simple non-destructive acoustic test, *British Poultry Science*, 47 (4), p. 462-469.
8. Bamelis, F., De Ketelaere, B., Kemps, B., Mertens, K., Decuypere, E. & De Baerdemaeker, J. (2006): Non invasive methods for egg quality evaluation. [s.n.]
9. Bell, D. D. & Weaver, W. D. (Ed.) (2002): Commercial Chicken Meat and Egg Production. 5. ed. Kluwer Academic Publishers, Massachusetts, USA, 729-730 p.
10. Benedito, J., Cárcel, J., Clemente, G. & Mulet, A. (2000a): Cheese maturity assessment using ultrasonics. *Journal of Dairy Science*, 83. p. 248–254.
11. Benedito, J., Cárcel, J., Sanjuan, N. & Mulet, A. (2000b): Use of ultrasound to assess Cheddar cheese characteristics. *Ultrasonics*, 38. p. 727–730.
12. Benedito, J., Mulet, A., Velasco, J., & Dobarganes M. C. (2002): Ultrasonic assessment of oil quality during frying, *Journal of Agricultural and Food Chemistry*, 50. (16) p. 4531-4536.

13. Benedito, J., Simal, S., Clemente, G. & Mulet, A. (2006): Manchego cheese texture evaluation by ultrasonics and surface probes. *International Dairy Journal*, *16*, p. 431-438.
14. Benguigui, L., Emery, J., Durand, D. & Busnel, J. B. (1994): Ultrasonic study of milk clotting, *Lait*, 74. p. 197-206.
15. Breiman, L., Friedman, J., Olshen R.A., & Stone C. (1984): Classification and Regression Trees. Boca Raton, USA, CRC Press. 246-280. p.
16. Buck, J. R., Daniel, M. M. & Singer, A. C. (2002): Computer Explorations in Signals and Systems Using MATLAB. 2nd Edition, Prentice Hall, Upper Saddle River, USA
17. Campanella, O., Sumali, H., Mert, B. & Patel, B. (2011). The Use of Vibration Principles to Characterize the Mechanical Properties of Biomaterials. *Biomaterials - Physics and Chemistry* p. 299-328.
18. Cho, H. K., Choi, W. K. & Paek, J. H., (2000): Detection of surface cracks in shell eggs by acoustic impulse method, *Transactions of the ASAE,* 43, (6) p. 1921-1926.
19. Cho, B. K. & Irudayaraj, J. M. K. (2003): A noncontact ultrasound approach for mechanical property determination of cheeses. *Journal of Food Science*, 68(7), p. 2243-2247. doi: 10.1111/j.1365-2621.2003.tb05754.x
20. Cristianini, N., and Shawe-Taylor, J. (2000): An Introduction to Support Vector Machines and Other Kernel-based Learning Methods, First Edition, Cambridge University Press, Cambridge, UK, 1-51. p.
21. Clark, H. L. & Mikelson A. K.: Fruit ripeness tester. U.S. Patent US2277037A, 24 March 1942.
22. Cooley, J. W. & Tukey, J. W. (1965): An algorithm for the machine calculation of complex Fourier series, Mathematics of Computation, 19(90), p. 297–301.
23. Coomans, D., & Massart, D. L. (1982): Alternative k-nearest neighbour rules in supervised pattern recognition. *Analytica Chimica Acta*, 136, p. 15–27. doi:10.1016/s0003-2670(01)9535
24. Corredig, M., Alexander, M. & Dalgleish, D. G. (2004): The application of ultrasonic spectroscopy to the study of the gelation of milk components. *Food Research International*, 37, p. 557–565.
25. Coucke, P. (1998)**:** Assessment of some physical egg quality parameters based on vibration analysis. Doctoral thesis. Katholieke University, Leuven.

26. Coucke, P., Room, G. M., Decuypere, E. M. & De Baerdemaeker J. G. (1997): Monitoring embryo development in chicken eggs using acoustic resonance analysis. *Biotechnology Progress.* 13., p. 474-478.
27. Coucke, P., Dewil, E., Decuypere, E. & De Baerdemaeker, J. (1999): Measuring the mechanical stiffness of an eggshell using resonant frequency analysis. *British Poultry Science* 40(2), p. 227-232.
28. Coutts, J. A., Wilson, G. C. & Fernández, S. (2007): Optimum Egg Quality: a Practical Approach. 5M Publishing, Sheffield, UK
29. Daubechies, I. (1994): Ten lectures on wavelets, CBMS, SIAM, 61, p. 194-202.
30. De Belie, N., Schotte, S., Lammertyn, J., Nicolai, B. & De Baerdemaeker, J. (2000a): Firmness changes of pear fruit before and after harvest with the acoustic impulse response technique, *Journal of Agricultural Engineering Research*, 77(2), p. 183-191.
31. De Belie, N., De Smedt, V. & De Baerdemaeker, J. (2000b): Principal component analysis of chewing sounds to detect differences in apple crispness. *Postharvest Biology And Technology* 18(2), p. 109–19.
32. De Belie, N., Tu, K., Jancsók, P. & De Baerdemaeker, J. (1999): Preliminary study on the influence of turgor pressure on body reflectance of red laser light as a ripeness indicator for apples. *Postharvest Biology and Technology*, 16(3), p. 279-284.
33. De Ketelaere, B., Coucke, P. & De Baerdemaeker J. (2000): Eggshell crack detection based on acoustic resonance frequency analysis. *Journal of Agriculture Engineering Research*, 76., p. 157–163.
34. De Ketelaere, B. (2002): Data analysis for the non-destructive quality assessment of agro-products using vibration measurements. Doctoral Thesis, Katholieke Universiteit Leuven, Belgium
35. De Ketelaere, B., H.Vanhoutte, H., De Baerdemaeker, J. (2003): Parameter estimation and multivariable model building for the non-destructive, on-line determination of eggshell strength, *Journal of Sound and Vibration*. 266 (3), p. 699-709. https://doi.org/10.1016/S0022-460X(03)00595-9
36. De Ketelaere, B., Bamelis, F., Kemps, B., Decuypere, E. & De Baerdemaeker, J. (2004a): Non-destructive measurements of the egg quality. *World's Poultry Science Journal.* 60, p. 289-302.
37. De Ketelaere, B., Maertens, K. & De Baerdemaeker, J. (2004b): Noise cancellation in on-line acoustic impulse response measurements for the quality assessment of consumption eggs. *Mathematics and Computers in Simulation.* 65, p. 59-67.

38. Deng, X., Wang, Q., Chen, H. & Xie, H. (2010): Eggshell crack detection using a wavelet-based support vector machine, *Computers and Electronics in Agriculture*, 70 (1) , p. 135-143.
39. Draper, N. R., & Smith, H. (1998): Applied Regression Analysis. Wiley. p. 235-242. doi:10.1002/9781118625590
40. El Kadi, Y. A., Moudden, A., Faiz, B., Gerard Maze, G. & Decultot, D. (2013): Ultrasonic monitoring of fish thawing process optimal time of thawing and effect of freezing/thawing, *Acta Scientiarum Polonorum Technologia Alimentaria*, 12 (3) , p. 273-281.
41. Espinosa, L. Bacca, J., Prieto, F., Lasaygues, P. & Brancheriau, L. (2018): Accuracy on the Time-of-Flight Estimation for Ultrasonic Waves Applied to Non-Destructive Evaluation of Standing Trees: A Comparative Experimental Study. *Acta Acustica*, 104(3), p. 429-439
42. Felföldi, J. & Fekete, A. (2003): Detection of Small Scale Mechanical Changes by Acoustic Measuring System. *ASAE Meeting Presentation.* Paper Number: 036097 1-8.
43. Felföldi, J. & Ignát, T. (1999): Dynamic method for quick and non-destructive measurement of the surface firmness of fruits and vegetables. *Hungarian Agricultural Engineering* 12, p. 29-30.
44. Felföldi, J. (1996): Firmness assessment of fruits and vegetables based on acoustic parameters. *Journal of Food Physics* 58, p. 39-47.
45. Felföldi, J. & Zsom-Muha, V., (2010): Investigation of ripening process of fruit and vegetable samples by acoustic method. *Acta Horticulturae*. 858., p. 393-398.
46. Fourier, J. B. J (1807): Théorie de la propagation de la chaleur dans les solides, Institut de France, 21. Dec. 1807.
47. Friedrich, L. (2008): Ultrahang alkalmazása húskészítmények minősítésében és gyártástechnológiájában, Doctoral thesis, Corvinus University of Budapest, Budapest
48. Gan, T. H., Hutchins, D. A., Billson, D. R., & Schindel, D. W. (2001): The use of broadband acoustic transducers and pulse compression techniques for air-coupled ultrasonic imaging. *Ultrasonics*, 39. (3), p. 181–194.
49. Gan, T. H., Hutchins, D. A., Billson, D. R. (2002): Preliminary studies of a novel air-coupled ultrasonic inspection system for food containers. *Journal of Food Engineering*, 53., p. 315-323.

50. Gómez, A. H., Wang, J. & Pereira, A. G. (2005): Impulse response of pear fruit and its relation to Magness-Taylor firmness during storage. *Postharvest Biology and Technology.* 35, p. 209-215.
51. Gülseren, I. & Coupland, J.N., (2007): Ultrasonic velocity measurements in frozen model food solutions. *Journal of Food Engineering*, 79. (3), p. 1071–1078.
52. Hæggstrom, E. & Luukkala, M. (2001): Ultrasound detection and identification of foreign bodies in food products. *Food Control*, 12. (1), p. 37-45.
53. Hastie, T., Tibshirani, R. & Friedman, J. (2001): The Elements of Statistical Learning. Springer, New York, USA, 2401-248. p.
54. Häupler, M., Peyronel, F., Neeson, I., Weiss, J. & Marangoni, A. G., (2014): In situ ultrasonic characterization of cocoa butter using a chirp. *Food and Bioprocess Technology*, 7. (11), p. 3186–3196.
55. Héberger, K., Klára Kollár-Hunek, K. (2011): Sum of ranking differences for method discrimination and its validation: comparison of ranks with random numbers. *Journal of Chemometrics*, 25(4), p. 151-158. doi: 10.1002/cem.1320
56. Héberger, K., Kollár-Hunek, K. (2019): Comparison of validation variants by sum of ranking differences and ANOVA. *Journal of Chemometrics*, 33(6), 3104. doi: 10.1002/cem.3104.
57. Internet 1 https://www.eggfarmers.org.nz/eating-eggs/buying-quality-eggs Search engine: Google. Keywords: egg farmers candeling downloaded: 09/23/2019
58. Internet 2 https://www.youtube.com/watch?v=HpY-Xlvibpo Search engine: Youtube. Keywords: sanovo egg grading downloaded: 06/22/2019
59. Istella, S. & Felföldi, J. (2003): Measurement of carrot varieties firmness changes with non-destructive acoustic method. *Hajtatás, korai termesztés* 4., p. 24-26.
60. Istella, S., Muha, V. & Terbe, I. (2006): Storage ability and differences of carrot varieties defined by firmness changes measured with new non-destructive acoustic method. *International Journal of Horticultural* Science 12 (1), p. 37-40.
61. Istella S. (2008): Korszerű eljárások a zöldségfélék tárolhatóságának előrejelzésére. Doctoral thesis. Corvinus University of Budapest, Budapest.
62. Izuka, Y. (1998): High signal to noise ratio ultrasonic testing system using chirp pulse compression. *Insight*, 40. (4) , p. 282–285.

63. Jin, Ch., Xie, L. & Ying, Y. (2015): Eggshell crack detection based on the time-domain acoustic signal of rolling eggs on a step-plate, *Journal of Food Engineering*, 157, p. 53-62.
64. Jindal V. K. & Sritham E. (2003): Detecting eggshell cracks by acoustic impulse response and artificial neural networks. In: *ASAE Annual International Meeting*, Las Vegas, Nevada.
65. Kertész, I. & Felföldi, J. (2016): Comparison Of Sound Velocity Estimation And Classification Methods For Ultrasonic Testing Of Cheese *Progress in Agricultural Engineering Sciences,* 12. , p. 51–62.
66. Kertész, I. (2013): Development of a Novel Measurement and Evaluation Method for Ultrasonic Cheese Texture Investigation, Master Thesis, Corvinus University of Budapest
67. Kertész, I., Zsom-Muha, V., Zsom, T., András, R., Nagy, D. & Felföldi, J. (2019): Tojás minőségének és a héj repedésének roncsolásmentes vizsgálata, *Animal welfare, ethology and housing systems* 15. (1) , p. 29-35.
68. Kertész, I., Nagy, D., Baranyai, L., Pásztor-Huszár, K., Varsányi, K., Nguyen, L. P. L., Felföldi, J. (2021a): Development of a novel ultrasonic spectroscopy method for estimation of viscosity change during milk clotting. *Molecules.* (accepted for publication)
69. Kertész, I., Zsom-Muha, V., András, R., Horváth, F., Németh, C., Felföldi, J. (2021b): Development of a Novel Acoustic Spectroscopy Method for Detection of Eggshell Cracks. *Molecules*, 26(15), 4693; https://doi.org/10.3390/molecules26154693
70. Kinsler, L. E., Frey, A. R., Coppens, A. B. & Sanders, J. V. (2000): Fundamentals of Acoustics, 4th Edition, Hoboken, Canada, Wiley
71. Kurz, J., H., Grosse, C. U. & Reinhardt,H., W. (2005) Strategies for reliable automatic onset time picking of acoustic emissions and of ultrasound signals in concrete, *Ultrasonics*, 43 (7) , p. 538-546.
72. Lashgari, M. & Mohammadigol, R. (2018): Comparative study of acoustic signals of rolling eggs on inclined plate and impulse response in eggshell crack detection *Agricultural Engineering International,* 20 (1) , p. 150-156.
73. Lawrence, K. C., Yoon, S. C., Heitchmidt, G. W., Jones, D., Park, B. & Savage, V. A., Egg micro-crack detection systems. US Patent US20090091744A1, 9 April 2009.
74. Leemans, V. & Destain, M.-F. (2009): Ultrasonic internal defect detection in cheese. *Journal of Food Engineering*, 90., p. 333–340.
75. Létang, C., Piau, M., Verdier, C. & Lefebvre, L. (2001): Characterization of wheat-flour–water doughs: a new method using ultrasound. *Ultrasonics*, 39. , p. 133–141.

76. Li, P., Wang, Q., Zhang, Q., Cao, Sh., Liu, Y. & Zhu, T. (2012): Non-destructive Detection on the Egg Crack Based on Wavelet Transform, *International Conference on Future Computer Supported Education, IERI Procedia*, 2, p.372-382.
77. Lin, H., Zhao, J., Chen, Q., Cai, J. & Zhou, P. (2009): Eggshell crack detection based on acoustic response and support vector data description algorithm. *European Food Research and Technology,* 230., p. 95-100.
78. Mizrach, A., Galili, N. & Rosenhouse, G. (1989): Determination of fruit and vegetable properties by ultrasonic excitation, *Transactions of the ASAE,* 32. (6) , p. 2053-2058.
79. Mizrach, A., Galili, N., Gan-Mor, S., Flitsanov, U. & Prigozin, I. (1996): Model of ultrasonic parameters to assess avocado properties and shelf life. *Journal of Agricultural Engineering Research,* 65. , p. 261-267.
80. Mizrach, A., Flitsanov, U., El-Batsri, R. & Degani C. (1999): Determination of avocado maturity by ultrasonic attenuation measurements. *Scientia Horticulturae,* 80. , p. 173-180.
81. Mizrach, A. (2000): Determination of avocado and mango fruit properties by ultrasonic technique, *Ultrasonics*, 38., p. 717-722.
82. Mizrach, A. (2004): Assessing plum fruit quality attributes with an ultrasonic method. *Ultrasonics Sonochemistry,* 18., p. 627-631.
83. Mizrach, A. (2008): Ultrasonic technology for quality evaluation of fresh fruit and vegetables in pre-and postharvest processes, *Postharvest biology and technology*, 48. (3), p. 315-330.
84. Moreau, A., Lévesque, D., Lord, M., Dubois, M., Monchalin, J.-P., Padioleau, C. & Bussière, J. F. (2002): On-line measurement of texture, thickness and plastic strain ratio using laser-ultrasound resonance spectroscopy, *Ultrasonics*, 40., p. 1047-1056.
85. Nerya, O., Ben-Shimol, T., Gizis, A., Zvilling, A., Sharabi-Nov, A. & Ben-Arie, R. (2001). Is the acoustic response of fruits a measure of firmness or of turgor? *Acta Horticulturae,* 553., p. 473–475.
86. Pan, L., Tu, K., Zhao, L. & Pan, X. (2005): Preliminary research of chicken egg crack detection based on acoustic resonance analysis, *Transactions of the Chinese Society of Agricultural Engineering*, 21 (4), p. 11-15.
87. Pan, L., Zhan, G., Tu, K., Tu, S. & Liu, P. (2011): Eggshell crack detection based on computer vision and acoustic response by means of back-propagation artificial neural network. *European Food Research and Technology* 233., p. 457-463.

88. Potter, M. D. G., Dixon, S., Morrison, J. P. & Suliamann A. S. (2006): Development of an advanced multimode automatic ultrasonic texture measurement system for laboratory and production line application, *Ultrasonics*, 44., p. 813-817.
89. Rao, N. A. H. K. (1994): Investigation of a pulse compression technique for medical ultrasound: a simulation study, *Medical and Biological Engineering and Computing*, 32., p. 181–188.
90. Rao, N. A. H. K., Mehra, S., Bridges, J. & Venkatraman, S. (1995): Experimental point spread function of FM pulse imaging scheme. *Ultrasonic Imaging*, 17. (2), p. 14–141.
91. Rokach, L. (2009): Ensemble-based classifiers. *Artificial Intelligence Review*, 33(1), p. 1–39. doi:10.1007/s10462-009-9124-7
92. Rosipal, R., & Kramer, N. (2006): Overview and Recent Advances in Partial Least Squares. In: Saunders, C., Grobelnik, M., Gunn, S. & Shawe-Taylor, J. (In) *Subspace, Latent Structure and Feature Selection*, Springer, Berlin, Germany, 34-51. p. https://doi.org/10.1007/11752790_2
93. Róth, E., Hertog, M. L. A. T. M., Kovács, E. & Bart, N. (2008): Modelling the enzymatic softening of apples in relation to cultivar, growing system, picking date and season. *International Journal of Food Science and Technology* 43., p. 620–628.
94. Santacatalina, J. V., Garcia-Perez, J.V., Corona, E. & Benedito, J. (2011): Ultrasonic monitoring of lard crystallization during storage, *Food Research International*, 44., p. 146–155.
95. Schotte, S. et al., De Belie, N. & De Baerdemaeker, J. (1999): Acoustic impulse-response technique for evaluation and modelling of firmness of tomato fruit. *Postharvest Biology and Technology*. 17., p. 105-115.
96. Seber, G. A. F. (1984): Multivariate Observations. Hoboken, Canada, Wiley. doi: 10.1002/9780470316641
97. Sedlak, P., Hirose, Y., A., Enoki, M. & Sikula J. (2008): Arrival time detection in thin multilayer plates on the basis of Akaike information criterion. European Working Group on Acoustic Emission., Krakow, Poland, p. 166-171.
98. Stoica, P. & Moses, R. (2005): Spectral Analysis of Signals. Prentice Hall, Upper Saddle River, New Jersey
99. Szabo, T. L. (1994): Time domain wave equations for lossy media obeying a frequency power law, *The Journal of the Acoustical Society of America*, 96. (1), p. 491-500.

100. Takanami, T. & Kitagawa, G. (1991): Estimation of the arrival times of seismic waves by multivariate time series model. *Annals of the Institute of Statistical Mathematics*, 43. (3), p. 407-433.
101. Taniwaki, M., Hanadab, T. & Sakurai, N. (2009): Postharvest quality evaluation of "Fuyu" and "Taishuu" persimmons using a nondestructive vibrational method and an acoustic vibration technique. *Postharvest Biology and Technology*, 51., p. 80–85.
102. Tobocman, W., Driscoll D., Shokrollahi, N., Izatt, J. A. (2002): Free of speckle ultrasound images of small tissue structures. *Ultrasonics*, 40., p. 983-996.
103. Trnkoczy, A. (2012): Understanding and parameter setting of STA/LTA trigger algorithm, New Manual of Seismological Observatory Practice 2, Potsdam, Germany, Deutsches GeoForschungsZentrum GFZ, p. 1-20.
104. van de Laar, R. (2014): Memobust Handbook on Methodology of Modern Business Statistics
105. Vanevenhoven, D. W. (2012): A characterization of the rheology of raw milk gouda cheese. Master Thesis, University of Wisconsin-Stout, Menomonie, USA
106. Wang, J., Jiang, R. S. & Yu, Y. (2004): Relationship between dynamic resonance frequency and egg physical properties. *Food Research International.* 37., p. 45-50.
107. Williams, P. C., & Sobering, D. C. (1993): Comparison of Commercial near Infrared Transmittance and Reflectance Instruments for Analysis of Whole Grains and Seeds. *Journal of Near Infrared Spectroscopy*, 1(1), p. 25–32. doi:10.1255/jnirs.3
108. Wold, S., Sjöström, M. & Eriksson, L. (2001): PLS-regression: a basic tool of chemometrics. *Chemometrics and Intelligent Laboratory* Systems 58 (2), p. 109-130. https://doi.org/10.1016/S0169-7439(01)00155-1
109. Wu, L, Wang, Q., Jie, D. Wang, S., Zhu, Z. & Xiong, L., (2018): Detection of Crack Eggs by Image Processing and Soft-margin Support Vector Machine. *Journal of Computational Methods in Sciences and Engineering*, 18 (1), p. 21-31., doi: 10.3233/JCM-170767
110. Zhang, W., Pan, L., Tu, S., Zhan, G. & Tu, K. (2015): Non-destructive internal quality assessment of eggs using a synthesis of hyperspectral imaging and multivariate analysis, *Journal of Food Engineering*, 157, p. 41-48.
111. Zhang, Y., Wu, H., & Cheng, E. (2012). Some new deformation formulas about variance and covariance. In: *Proceedings of 4th International Conference on Modelling, Identification and Control*, p. 987–992.

112. Zhu, Z., Wu, L., Hu, D. & Wen, Y. (2012): Cracked-Shell Detection of Preserved Eggs Based on Bayes Theory in Mechanical Engineering, *2012 International Conference on Mechanical and Electronic Engineering*
113. Zsom, T., Zsom-Muha, V., Dénes, D. L., Baranyai, L. & J. Felföldi (2016): Quality Changes of Pear during Shelf-Life, *Progress in Agricultural Engineering Sciences*, 12., p. 81–106.
114. Zsom-Muha, V. & Felföldi, J., (2007): Vibration Behavior of Long Shape Vegetables, *Progress in Agricultural Engineering Sciences,* 3., p. 21-46.
115. Zsom-Muha, V. (2008): Dinamikus módszerek kertészeti termények jellemzésére. Doctoral Thesis. Corvinus University of Budapest, Budapest

Annex II. – Summary in Hungarian language

A jelenleg tapasztalható törekvés a magas és állandó minőségű élelmiszer-előállításra a roncsolásmentes technológiák iránti érdeklődés növekedéséhez vezetett, mivel úgy képesek információt szolgáltatni a termékről, hogy közben annak értékét nem befolyásolják, és minden egyes legyártott termék vizsgálható, így nem igényel mintavételezést, ami a téves következtetések egyik fő forrása. Az évtizedek során az orvoslásban gyűjtött tapasztalat nagyban hozzájárult az ultrahangos vizsgálatok alkalmazási lehetőséginek bővítéséhez, a mögöttes elv kiemelkedően hasznos tulajdonságbecslési eljárást tett lehetővé szövetek és más mátrixok vizsgálatára, amely átültethető az élelmiszerek vizsgálatának területére is. A kutatások főként a vizsgálható termékek körének tágítására, vagy a már alkalmazott technikák finomítására koncentrálnak. Mindemellett az akusztikus vizsgálat régebbre visszanyúló múlttal rendelkezik, és sikeresen alkalmazták már termények és tojások vizsgálatára is. Habár a legtöbb tanulmány a rezonancia frekvencia mérésére fókuszál, amelyből keménységi és egyéb állománytulajdonságok becsülhetők, a tojások esetén elsődlegesen repedések detektálására alkalmazzák.

Mind az akusztikus, mind az ultrahangos mérési módszerek hanghullámok elemzésén alapul, amely a vizsgált minta jellemzőivel hozhatók összefüggésbe, ezáltal hasonló elemző módszerek alkalmazása lehetséges a jelfeldolgozás során.

Disszertációmban méréseket mutattam be a tej enzimes alvasztása során végbemenő viszkozitás-változás becslésére, amely a fermentáció állapotát jellemző lényeges tulajdonság. Piezoelektromos, 250 kHz névleges frekvenciájú adó-vevő párt alkalmaztam a mintába merítve, átmenő sugárzásos elrendezésben, $CaCl_2$ hozzáadása mellett. A vizsgált jel egy chirp jel volt, amely egy lineárisan, 50-től 450 kHz-ig növekvő frekvenciájú pásztázó jel, Hanning-filterrel burkolva, a jeleket oszcilloszkóppal gyűjtöttem. Borjúgyomor oltóenzim hozzáadása után egy kisebb mennyiséget rotációs viszkoziméterbe mértem, amellyel 120 percen keresztül 10 másodpercenként mértem a viszkozitást 2 s^{-1} nyírási sebesség mellett. A kapott reogramokon csúcsok mutatkoztak, amely a micellák összekapcsolódásának eredménye, ezért görbeillesztést végeztem magas R^2 értékeket kapva (min.: 0,7521, max.: 0,9985). A kapott görbék pontjait a továbbiakban PLS regresszióval becsültem egy általam kidolgozott jelfeldolgozási módszer segítségével, magas R^2 (0,9632 – 0,9983) és RPD (4,38 – 14,22) értékek mellett.

A kidolgozott eljárás a válaszjelek Morse anyawavelettel végrehajtott wavelet-analíziséből, majd egy együttható-kiválasztási folyamatból áll. A variancia leírására kiszámításra kerül a korrigált tapasztalati szórás minden wavelet-együtthatóra, ezzel biztosítva az alacsony számítási időt,

szemben a kovariancia-mátrixok számításával. Ezt követi a kiszámított mátrixban megjelenő csúcsok keresése az idő- és frekvenciafüggő wavelet-együtthatók között. A kinyert együtthatók száma 7 és 32 között változott, ezek felhasználásra kerültek az egyes mérések viszkozitásának becslésére, és az össze mérés egyszerre történő becslésére, jól illeszkedő és jól becslő modellt eredményezve (R^2 = 0,9708, RPD = 5,85).

Egy másik szigorú kísérletet végeztem a módszer alkalmazhatóságának ellenőrzésére, mely egy korábbi vizsgálaton alapult. Összesen 90 szelet mozzarellát vizsgáltam három típusból, mindegyikből 30 mintát, ezek normál, füstölt és laktózmentes típusok voltak, az első két típus összetétele megegyezett. A TOF paraméter számítására, a fentivel megegyező instrumentáció mellett, kereszt-korrelált (XC) és Autoregresszív Akaike Információs Kritérium picker (AIC) algoritmusokat használtam. Az eredmények azt mutatták, hogy a bár az XC megközelítés kisebb teljes varianciát eredményezett, két jól elkülönülő csoportra oszlottak a TOF eredmények, míg az AIC nagyobb varianciát, de összetartóbb eredményeket nyújtott. A korábban említett algoritmus több osztályozó módszerrel kipróbálásra került. KNN osztályozással 100%-os validált helyes osztályozást sikerült elérni a válaszjel alapján. Szintén nagy pontosságot ért el a becslés a kereszt-korrelált a bemutatott feldolgozási módszerrel (97,8%) és a válaszjel FFT-együtthatói alapján (97,8%).

Kísérletet végeztem tojáshéj repedtségének detektálására 150 mintával, összesen 705 méréssel. Magát a mérést a tojás óvatos, üreges fémpálcával történő megütésével végeztem, mely egyetlen ütést jelentett álló és elfektetett pozíciókban, a jeleket egy számítógépre kötött jelanalizátoron keresztül rögzítettem egy stabilizálás és zajcsillapítás céljából habszivacsból készült platformba épített mikrofonnal. A válaszjelek spektrumait 0 és 300 Hz között vizsgáltam, különböző felbontásnövelő eljárások alkalmazása mellett: ezek a nullákkal történő feltöltés és az FFT-ablak méretének növelése voltak, ezeket a becslési pontosságra gyakorolt hatásuk szempontjából vizsgáltam. Végeredményben 2,1%-os teljes becslési hibát és 0,87%-os téves negatív becslést értem el négyzetes diszkriminancia analízis segítségével.

Acknowledgements

I would like to thank my supervisors, Dr. József Felföldi and Dr. László Baranyai for their patience and guidance over the years.

Also, I would like to thank all my colleagues at the Department of Food Measurements and Process Control at the Hungarian University of Agriculture and Life Sciences, friends and family members for their support.